

VTT PUBLICATIONS 391

*Cranfield*  
UNIVERSITY

# **Immobilisation of Biomolecules onto Organised Molecular Assemblies**

Willem M. Albers  
VTT Chemical Technology

*ACADEMIC DISSERTATION*  
*submitted in partial fulfilment of the requirements for the degree of Doctor of  
Philosophy in Biotechnology and defended on April 21st 1999, at 9.30 a.m.*

Cranfield Biotechnology Centre  
**Cranfield University**  
Cranfield, Bedfordshire, England



---

TECHNICAL RESEARCH CENTRE OF FINLAND  
ESPOO 1999

ISBN 951-38-5389-6 (soft back ed.)

ISSN 1235-0621 (soft back ed.)

ISBN 951-38-5390-X (URL: <http://www.inf.vtt.fi/pdf/>)

ISSN 1455-0849 (URL: <http://www.inf.vtt.fi/pdf/>)

Copyright © Valtion teknillinen tutkimuskeskus (VTT) 1999

#### JULKAISIJA – UTGIVARE – PUBLISHER

Valtion teknillinen tutkimuskeskus (VTT), Vuorimiehentie 5, PL 2000, 02044 VTT  
puh. vaihde (09) 4561, faksi (09) 456 4374

Statens tekniska forskningscentral (VTT), Bergsmansvägen 5, PB 2000, 02044 VTT  
tel. växel (09) 4561, fax (09) 456 4374

Technical Research Centre of Finland (VTT), Vuorimiehentie 5, P.O.Box 2000, FIN-02044 VTT, Finland  
phone internat. + 358 9 4561, fax + 358 9 456 4374

VTT Kemiantekniikka, Materiaalitekniikka, Sinitaival 6, PL 1402, 33101 TAMPERE  
puh. vaihde (03) 316 3111, faksi (03) 316 3498

VTT Kemiteknik, Materialteknik, Sinitaival 6, PB 1402, 33101 TAMMERFORS  
tel. växel (03) 316 3111, fax (03) 316 3498

VTT Chemical Technology, Materials Technology,  
Sinitaival 6, P.O.Box 1402, FIN-33101 TAMPERE, Finland  
phone internat. + 358 3 316 3111, fax + 358 3 316 3498

Technical editing Kerttu Tirronen

Libella Painopalvelu Oy, Espoo 1999

*In remembrance of*  
***Hage Albers***

Albers, Willem M. Immobilisation of biomolecules onto organised molecular assemblies. Espoo 1999. Technical Research Centre of Finland, VTT Publications 391. 124 p. +app. 37 p.

**Keywords** immobilisation, molecules, Langmuir-Blodgett films, enzymes, oxidases, biosensors, modelling, bilayers, lipid membranes

## Abstract

This thesis describes immobilisation techniques for biomolecules on solid surfaces via an intermediate self-assembled or Langmuir-Blodgett (LB) film. Such films are advantageous, because the biological activity can be optimised by tailoring the layer composition. Factors like charge density, density of the linking group and composition of the monolayer matrix have particularly large effects on the activity.

In the first part, oxidase enzymes were immobilised on self-assembled, conductive layers of bispyridiniumthiophene oligomers (thienoviologens) on gold substrates. The enzyme was bound by electrostatic interaction of the negatively charged enzyme with the positively charged pyridinium groups. The enzymatic activity of glucose oxidase was dependent on the surface density of the conductor and on the ionic strength during adsorption.

In the second part of the thesis, Fab'-fragments were bound to LB-films of various linker lipids and the immobilisation efficiency (relative amount of binding sites) was optimised by variation of the constitution of the lipid LB-film. The films were deposited onto various substrates by vertical contact transfer of a preformed mixed Langmuir film of the linker lipid and a matrix lipid. The immobilisation efficiency was investigated with radioassay, quartz crystal microbalance (QCM) and surface plasmon resonance (SPR) measurements, while also atomic force microscopy (AFM) was used to image the structure of the films at different stages of binding. The immobilisation efficiency of the LB-films appeared to be much higher as that of more conventional methods for antibody immobilisation. Between 20 and 70% of the binding sites could be preserved, depending on the type of linker and film matrix composition, while that of the conventional methods was less than 10%. Films with dipalmitoylphosphatidylcholine as the matrix lipid and a maleimide derivative of dipalmitoylphosphatidyl-ethanolamine showed the highest sensitivity (and lowest detection limit) in QCM measurements.

# Preface

The modelling and practical realisation of biosensing interfaces has become an important research subject within biosensor research, which comprises: (1) the study of receptor-ligand interactions and structure-function relationships of molecules at solid/liquid interfaces, (2) the development of in situ methods for monitoring binding reactions at these interfaces and (3) the synthesis and utilisation of interfacial molecules with linking, signal transducing and other suitable properties for the attainment of specific sensing properties of the interface.

Because of the multidisciplinary nature of this field, requiring biochemistry, organic synthetic and analytical chemistry, interface chemistry, materials science and electronics expertise, a European joint effort in this research area between various research centres in Europe was very much needed. To this end the ESF programme on “Artificial Biosensing Interfaces” (ESF/ABI) was conducted through the years 1994 to 1998. The ABI workshops and summer schools indeed provided increased awareness of the fundamental research in the interfacial aspects of biosensor development and an increased awareness of cooperation possibilities.

Biosensor development has been supported by VTT at three locations. The group for Sensor Materials at VTT Chemical Technology concentrates primarily on immobilisation chemistry and instrumentation aspects, while VTT Biotechnology and Food Research produces antibodies and is also active in bioelectrochemistry and biospecific interaction analysis. Finally, VTT Electronics has been supplying basic materials and is focusing presently on miniaturisation technology, which could also be used in biosensors.

# Acknowledgements

Financial support from VTT Chemical Technology, the Technology Development Centre (TEKES) and the Finnish Academy is gratefully acknowledged.

I express my thanks to the following persons for their contribution to this work: *Inger Vikholm* (VTT Chemical Technology) for LB-film production and QCM measurements, *Tapani Viitala*, (Åbo Akademi University) for providing AFM pictures. *Aulis Marttinen* (Tampere University Hospital, Biomedical Centre) for radio-labelling services and *Petri Vuoristo* (Tampere University of Technology) for plasma etching.

I also express my thanks to *Jukka Lekkala* (VTT Chemical Technology) for his support through the years and *Jouko Peltonen* for useful discussions. Particularly to *Anthony Turner* I would like to express my gratefulness for giving me the opportunity to study at Cranfield Institute of BioScience & Technology (IBST).

Finally, I would like to thank the members of my family, *Riitta* for her enthusiastic support and *Hanna* and *Timo* for dragging me frequently out of the test tube.

# Contents

ABSTRACT .....	4
PREFACE .....	5
ACKNOWLEDGEMENTS .....	6
LIST OF PUBLICATIONS .....	9
LIST OF TABLES .....	11
LIST OF FIGURES .....	12
LIST OF SYMBOLS AND ABBREVIATIONS .....	14
1. GENERAL INTRODUCTION .....	16
1.1 Biosensor Technology .....	16
1.1.1 The biosensor concept .....	16
1.1.2 The biosensor market .....	20
1.2 Electrode modification techniques .....	23
1.3 Bilayer Lipid Membranes (BLM) .....	25
1.3.1 BLM formation and properties .....	25
1.3.2 BLM-based biosensors .....	30
1.4 Scope of the present thesis .....	32
2. IMMOBILIZATION OF ENZYMES ON CONDUCTING BILAYERS ....	33
2.1 Introduction .....	33
2.2 First and second generation enzyme electrodes .....	34
2.3 Direct electron transfer .....	37
2.4 Enzyme immobilisation onto self-assembled films .....	44
2.5 Cofactor modified “fourth generation” enzyme electrodes .....	47
2.6 Modelling approaches to enzyme electrode design .....	49
2.7 Experimental .....	53
2.7.1 Thienoviologen synthesis .....	53
2.7.2 Electrode coating .....	54
2.7.3 Enzyme immobilisation and activity assay .....	54
2.7.4 Electrochemical and impedance measurements .....	55

2.8	Results and discussion .....	57
2.8.1	Film formation.....	57
2.8.2	Enzyme immobilisation.....	61
2.9	Conclusions.....	65
3.	IMMOBILIZATION OF FAB'-FRAGMENTS ON LIPID LB-FILMS.....	67
3.1	Immunoassays.....	67
3.2	Site-directed immobilisation of antibodies .....	68
3.3	Linker lipids.....	73
3.4	The Quartz Crystal Microbalance.....	74
3.5	Experimental.....	76
3.5.1	Materials.....	76
3.5.2	Preparation of linker lipids .....	77
3.5.3	LB-film formation .....	79
3.5.4	Quartz Crystal Microbalance measurements .....	79
3.5.5	Surface Plasmon Resonance measurements .....	81
3.5.6	Radiometric assay.....	82
3.5.7	Atomic Force Microscopy.....	84
3.6	Results and discussion .....	85
3.6.1	Film formation.....	85
3.6.2	Fab' binding and activity.....	86
3.6.3	Monolayer matrix effects.....	90
3.6.4	Operation of the QCM.....	93
3.6.5	Detection limits for QCM response of hIgG .....	99
3.6.6	Film structure.....	100
3.7	Conclusions.....	105
4.	GENERAL CONCLUSIONS .....	107
	REFERENCES.....	109

APPENDICES (PAPERS I-V)

***Appendices of this publication are not included in the PDF version.  
Please order the printed version to get the complete publication  
(<http://www.inf.vtt.fi/pdf/publications/1999/>)***



# List of publications

The present thesis is based on the following publications:

**I.** Albers, W. M., Canters, G. W. & Reedijk J. (1995). Preparation of extended di(4-pyridyl)thiophene oligomers. *Tetrahedron* **51**, 3895-3904.

**II.** Albers, W. M., Lekkala, J. O., Jeuken, L., Canters, G. W. & Turner, A. P. F. (1997). Design of novel molecular wires for realising long-distance electron transfer. *Bioelectrochem. & Bioenerg.* **42**, 25-33.

**III.** Viitala, T., Albers, W. M., Vikholm, I. & Peltonen, J. (1998). Synthesis and Langmuir film formation of N-( $\epsilon$ -maleimidocaproyl)-dilinoleoylphosphatidyl-ethanolamine. *Langmuir* **14**, 1272-1277.

**IV.** Vikholm, I., Albers, W. M., Välimäki, H. (1998). In situ quartz crystal microbalance monitoring of Fab'-fragment binding to linker lipids in a phosphatidylcholine monolayer matrix. Application to immunosensors. *Thin Solid Films* in press.

**V.** Vikholm, I. & Albers, W. M. (1998). Oriented Immobilisation of Antibodies for Immunosensing. *Langmuir* **14**, 3865-3872.

At certain places also reference has been made to the following closely related work:

**VI.** Airikkala, S. & Albers, W. M. (1990). Immobilisation of anti-hCG on gold and aluminium surfaces. *Prog. Colloid & Polym. Sci.* **82**, 345-348.

**VII.** Albers, W. M., Airikkala, S., Sadowski, J., Vikholm, I., Joki, H. & Lekkala, J. (1989). The application of antibodies in immunosensing. *VTT Research Reports* **670**, Espoo.

**VIII.** Albers W. M. (1996). Electron-conducting molecular preparations. *US Pat. Nr. 5556524*.

**IX.** Albers, W. M. (1997) Design aspects of viologen molecular wires. MSc Thesis, Tampere University of Technology.

**X.** Albers, W. M., Likonen, J., Peltonen, J., Teleman, O. & Lemmetyinen, H. (1998). Structural aspects of self-assembly of thienoviologen molecular conductors on gold substrates. *Thin Solid Films* **330**, 114-119.

In the text these articles will be referred to by their roman numerals. The thesis also presents new unpublished results.

## List of tables

<b>Table 1.1</b> Natural lipid components in weight% of total.....	25
<b>Table 2.1</b> Oxidase enzymes in the Brookhaven data base with FAD cofactor...49	
<b>Table 3.1</b> Measured NMR parameters (600 MHz, CDCl <sub>3</sub> ) for the protons in DLPE-EMCS.....	78
<b>Table 3.2</b> Comparison of immobilisation system performance with radioassay (RIA), QCM and SPR.....	98
<b>Table 3.3</b> Effective noise (N), sensitivity (S) and detection limits (DL) for hIgG detection at different immobilisation matrices.....	99

# List of figures

<b>Figure 1.1</b> The general scheme of a chemical sensor.....	16
<b>Figure 1.2</b> The structures of the most important natural BLM constituents.....	26
<b>Figure 2.1</b> The principle of a first generation enzyme electrode.....	34
<b>Figure 2.2</b> The operation principle of a mediated enzyme electrode. ....	34
<b>Figure 2.3.</b> The principle of a third generation enzyme electrode.....	38
<b>Figure 2.4</b> Structure of a caroviologen (A) and the general structure of the thienoviologens (B). ....	43
<b>Figure 2.5.</b> Photoconversion of SP to MRH <sup>+</sup> .....	46
<b>Figure 2.6</b> Attachment of an FAD analogue to a carbon electrode. ....	48
<b>Figure 2.7</b> The solvent-accessible surface of GOx and the position of the FAD cofactor. ....	50
<b>Figure 2.8</b> Immobilisation sites in GOx .....	51
<b>Figure 2.9</b> Preparation of PT2 and PT3.....	53
<b>Figure 2.10</b> Electrochemical response of copper electrodes towards ODM. ....	59
<b>Figure 2.11</b> Stripping of ODM from copper electrodes. ....	59
<b>Figure 2.12</b> Electrochemical response of copper electrodes towards PT2.. ....	60
<b>Figure 2.13</b> Adsorption isotherms of GOx on Au/DPBT, Au/PT2 and Au/ODM/PT2.....	62
<b>Figure 2.14</b> Enzymatic activity of GOx on Au/ODM/PT2. ....	64
<b>Figure 3.1</b> Binding of human IgG to epoxytated gold and the interaction with anti-human IgG, as monitored with SPR.....	70
<b>Figure 3.2</b> The Fab-fragment against a synthetic peptide, .....	72
<b>Figure 3.3</b> Structures of linker lipids used in this study. ....	74
<b>Figure 3.4</b> The measuring set-up for performing in situ measurements with the QCM of a Langmuir film.....	80
<b>Figure 3.5</b> The SPR set-up used in the present study. ....	82
<b>Figure 3.6</b> The change in resonant frequency upon binding of F(ab') <sub>2</sub> and Fab'.....	87
<b>Figure 3.7</b> The total change in frequency upon binding of Fab'-fragments.....	88
<b>Figure 3.8.</b> The change in frequency upon binding of human IgG to Fab'- fragments bound to a monolayer of DPPC/DPPE-EMCS at various Fab'-fragment concentrations.. ....	89

<b>Figure 3.9.</b> The binding efficiency of Fab'-fragments attached to a monolayer of DPPC/DPPE-EMCS in binding to human IgG .....	90
<b>Figure 3.10</b> The change in frequency upon binding of (A) Fab'-fragments and (B) the subsequent binding of human IgG to a monolayer of DPPC/Chol/DPPE-EMCS. ....	91
<b>Figure 3.11.</b> The binding efficiency of the Fab'-fragments bound to a monolayer of DPPC/Chol/DPPE-EMCS to human IgG. (n=1).....	92
<b>Figure 3.12</b> (A) The total change in frequency in liquid and air after binding of Fab'-fragments, 0.1 mg/ml BSA and 0.1 mg/ml human IgG to a monolayer of DPPC/DPPE-EMCS vs. Fab'-fragment concentration .....	94
<b>Figure 3.13.</b> Binding curves of Fab' and F(ab') <sub>2</sub> to derivatised polystyrene via PPL and EMCS.....	95
<b>Figure 3.14.</b> Binding curves of Fab' to various linker lipid films. ....	96
<b>Figure 3.15 (A-B)</b> AFM images (area: 1024 x 1024 nm) of anti-hIgG Fab', BSA and hIgG on DPPC/DPPE-EMCS (9:1). (A) the monolayer matrix DPPC/DPPE-EMCS, (B) after Fab'-attachment. ....	101
<b>Figure 3.15 (C-D)</b> AFM images (area: 1024 x 1024 nm) of anti-hIgG Fab', BSA and hIgG on DPPC/DPPE-EMCS (9:1). (C) after BSA adsorption (blocking) (D) after reaction with the antigen human IgG. ....	102
<b>Figure 3.16 (A-B)</b> AFM images (area: 1024 x 1024 nm) of anti-hIgG Fab', BSA and hIgG on DPPC/CHOL/DPPE-SPDP (4:5:1). (A) the monolayer matrix (B) after Fab'-attachment.....	103
<b>Figure 3.16 (C-D)</b> AFM images (area: 1024 x 1024 nm) of anti-hIgG Fab', BSA and hIgG on DPPC/CHOL/DPPE-SPDP (4:5:1). (C) after BSA adsorption (blocking) (D) after reaction with the antigen human IgG .....	104

## List of symbols and abbreviations

$R$	resistance, $V.A^{-1}$ ( $\Omega$ )
$C$	capacitance, $C.V^{-1}$ (F)
CPM	counts per minute
$Z$	impedance, $V.A^{-1}$
$B$	bound analyte concentration, $mol.l^{-1}$
$F$	free analyte concentration, $mol.l^{-1}$
$T$	total analyte concentration, $mol.l^{-1}$
$c$	cooperativity constant
$\Gamma$	surface density, $ng.cm^{-2}$
$\Theta$	total coverage, ng
$\theta$	relative surface density
$K_a$	(apparent) affinity constant, $mol^{-1}.l$
$Q$	capacity constant, $mol.l^{-1}$
$\eta_a$	immobilisation efficiency, %
$U$	International unit for enzymatic conversion rate, $\mu mol.min^{-1}$
ABTS	2,2'-Azino-bis(3-ethylbenzothiazole-6-sulphonic acid)
APTES	3-aminopropyltriethoxysilane
ATP	adenosine triphosphate
BLM	bilayer lipid membrane
BSA	bovine serum albumin
CEA	carcinoembryonic antigen
CHOL	Cholesterol
ChOx	choline oxidase
CRP	C-Reactive Protein
DLPE	1,2-dilinoleoyl- <i>sn</i> -glycero-3-phosphatidylethanolamine
DMPE	1,2-dimyristoyl- <i>sn</i> -glycero-3-phosphatidylethanolamine
DPPC	1,2-dipalmitoyl- <i>sn</i> -glycero-3-phosphatidylcholine
DPPE	1,2-dipalmitoyl- <i>sn</i> -glycero-3-phosphatidylethanolamine
EMCS	N-( $\epsilon$ -maleimidylcaproyloxy)succinimide
FAD/FADH <sub>2</sub>	flavin adenine dinucleotide
FIA	flow injection analysis
GOx	glucose oxidase

hCG	human chorionic gonadotropin
HEPES	N-(2-hydroxyethyl)-piperazine-N'-(2-ethanesulfonic acid)
LB	Langmuir-Blodgett
NAD <sup>+</sup> /NADH	nicotinamide adenine dinucleotide
ODIA	o-Dianisidine, 3,3-dimethoxybenzidine
ODM	octadecylmercaptan
ODTCS	octadecyltrichlorosilane
PCR	polymerase chain reaction
PMS	phenazine methosulphate
PPy	polypyrrole
QCM	quartz crystal microbalance
SAM	self-assembled monolayer
SPDP	N-succinimidyl-3-(2-pyridyldithio)propionate
SPR	surface plasmon resonance
TCNQ	tetracyanoquinodimethane
TTF	tetrathiafulvalene

# 1. GENERAL INTRODUCTION

## 1.1 Biosensor Technology

### 1.1.1 The biosensor concept

Biosensors are measuring devices in which a component of biological origin is introduced for the reagentless quantitation of a chemical species in a complex mixture<sup>1</sup>. Over the past 13 years the development of biosensors has become an established research field. Although now a comprehensive review series is available<sup>2</sup>, the academic literature on biosensors has expanded gradually to huge proportions (more than 10 000 basic science references and patents), which complicates the task of reviewing even for the various biosensor subfields.

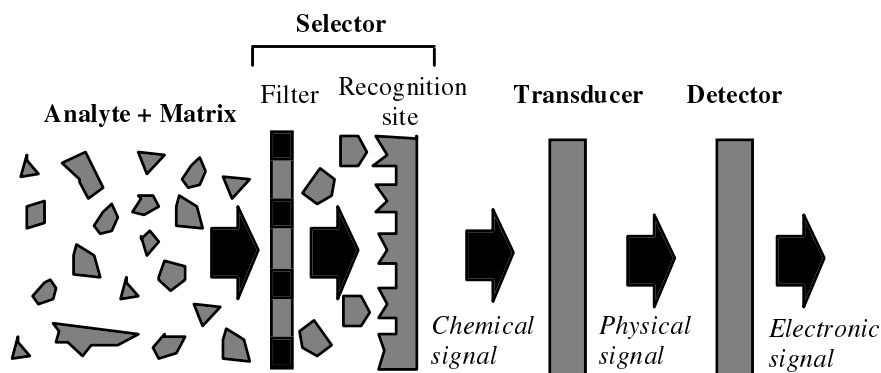


**Figure 1.1** *The general scheme of a chemical sensor.*

The operation scheme of a chemical sensor is schematically illustrated in Figure 1.1. In its most general form, a chemical sensor consists of a selector, a transducer and a detector linked together in an appropriate way. The selector imparts selectivity to the sensor and is commonly a filter followed by a recognition site. If this site is from a biomolecule (such as an enzyme, receptor, antibody or DNA preparation) the device may be called a biosensor. The recognition site must be designed to generate a chemical signal (changes in



chemical bonding) upon binding with the analyte and the function of the transducer is to convert this event into a physically measurable signal (electrical, thermal, mechanical, optical or magnetic) and pass this signal to a detector, which produces the desired electrical output. The selector and the transducer together form a “molecular device”, which exhibits a specific interaction with the analyte and transforms this interaction into a measurable signal. The recognition site can, in fact, be a synthetic molecular preparation. With the advent of ever increasing computing power and further development of molecular modelling methods, the possibilities for designing fully synthetic receptors, combining the selector and the transducer into a single molecule, is nowadays quite feasible. Such an approach has, for instance, been successfully demonstrated for creatinine<sup>3</sup>. In many applications the chemical complexity of the analyte molecule, particularly when it is a protein, is high and ample selectivity can only be attained via a biological molecule. In principle all analytes that are important in clinical medicine can be recognised by antibodies, enzymes or receptors. The real power of a biosensor results from the possibility of integration of the biomolecular recognition with optics or electronics and accounts for its commercial potential. In some cases, however, a true difficulty may arise in the design of the transducer. To extract or induce a measurable physical signal exclusively from the biological recognition reaction and not from other chemical processes occurring simultaneously may be a difficult task in particular cases.

When the selector is a molecule of biological origin, the transducer is usually an additional chemical compound which needs to be engineered into the system as a "mediator" or "reporter". Additionally, the mode of generation of the signal will be important in the attainment of the desired analytical characteristics of the sensor (selectivity, sensitivity, detection limit, measuring range, linearity, reversibility, response time, environmental and thermal stability). In this respect chemical amplification, by catalysis and cycling of reagents, is a crucial factor in obtaining the required high selectivity and sensitivity<sup>4</sup>. In many cases, however, there is a clear trade-off between some analytical parameters. For instance, the need for high reversibility may preclude a high sensitivity, and an increase in sensitivity (for instance by including cycling reactions) may lower the selectivity or accuracy of the device. These are ultimately all related to the basic properties of the biomolecules and the way the biomolecule is integrated in the biosensor device. The most persistent problem with biosensors is their vulnerability to

long-term use, which is again ordained by the biomolecule and how the biomolecule is incorporated into the sensor. Thus it will not be surprising that the *in-vivo* or *in-line* monitoring capabilities of biosensors are a problematic research area today.

The most direct approach for biosensing is electrochemical detection using redox enzymes (an oxidase, reductase or dehydrogenase). Here the detection is based on direct measurement of the oxidation (or reduction) current associated with the enzymatic reaction (“enzyme electrodes” or “amperometric biosensors”). Today many purified enzymes are commercially available. Also the structural details and reaction mechanisms of quite a number of enzymes have been elucidated. Although the latter knowledge may be of fundamental importance in the design of an enzyme-based sensor, empirical approaches for immobilisation have still prevailed and have generated a considerable amount of literature. Nowadays, the immobilisation of enzymes onto non-covalently associated molecular layers, in which the film properties and constitution can be well controlled, is actively investigated. This subject will be covered in Chapter 2 of this thesis.

Immunosensors form a second mainstream within biosensor research, aimed at the direct detection of immunological reactions, i.e. the reaction between an antigen and an antibody. Antibodies of various types are present in animals and humans as a line of defence against intruding substances, such as viruses and bacteria. Presently there are three main techniques for production of antibodies and with these techniques antibodies may be obtained to any analyte desired. Initially, antibodies could be obtained by immunising animals or humans with the antigen and purifying the antibodies directly from blood serum. The resulting antibodies in this preparation have various specificities, because the antibodies are produced by different cell lines (polyclonal).

With the advent of the hybridoma technique, described first by Georges Köhler in 1981<sup>5</sup>, it became possible to transfer antibody production to a new level, that of the monoclonal antibody, which has a single specificity. Such antibodies were produced by fusing the spleen cells of immunised mice with mouse myeloma cells, which yields hybrid cells (hybridoma cells), which have an antibody production typical for the spleen cells. These cells also proliferate rapidly, a feature that is inherited from the mouse myeloma cells, which are a particular

type of cancer cells. Monoclonal antibodies can nowadays also be obtained by recombinant methods<sup>6</sup>. The method also starts from the spleen cells of immunised animals, from which the B-lymphocyte mRNA is isolated. cDNA is then synthesised from the mRNA and the desired sequences from the cDNA amplified by PCR and cloned into a vector, which is then expressed in a suitable organism (e.g. E-coli). The recombinant methods offer besides the advantages of in-vitro production also the possibility for production of fusion proteins.

Presently, sub-picomolar concentrations may be easily reached with immunoassays based on labelling techniques<sup>7,8</sup> and below-attomolar detection strategies have also been devised<sup>9</sup>. Some earlier immunosensing strategies relied on “homogeneous labelling” techniques, of which two approaches have been introduced by Edwin Ullman. A first method was based on the “channelling” of enzymatic reactions at the solid-liquid interface<sup>10</sup> and a second on fluorescence energy transfer between two fluorophore-labelled biochemical binding partners<sup>11</sup>. Most immunosensing strategies devised today do not rely on labels and are based on direct monitoring of protein surface concentrations. Due to the fact that proteins usually have a high molecular weight, they perturb some interfacial properties much more strongly than small organic molecules. Measurable surface parameters are optical (refractive index, absorption), electronic/dielectric (charge, capacitance, resistance), or mechanical (mass of the surface layer, viscosity/elasticity and frictional forces). With surface plasmon resonance (SPR) the refractive index and optical absorption changes of surface layers can be measured and with quartz crystal microbalances (QCM) the mass and other mechanical forces of antibody/antigen layers at a solid surface may be measured. The rules of the game, however, become quite different when disposing of a specific label, because in this case also the non-specific binding of all other proteins to the surface must be taken into account. In principle the detection limits in direct immunosensors reaches down to nanomolar concentrations<sup>12</sup>, although in practice lower detection limits may be found. Bataillard<sup>13</sup> achieved a 16 pM detection limit for alpha-fetoprotein in a 10% goat serum matrix with capacitance measurements. With high molecular weight proteins, however, the use of molar units may give a much too positive picture about detection limits. Antibody immobilisation techniques are crucial in the optimisation of performance of immunoassays and particularly in direct immunosensing methods, since here the density of the available binding sites has to be maximal to give a sensitive response. Methods for the preparation of

homogeneous and well-orientated antibody layers are presented in this thesis in Chapter 3 enabling the determination of IgG concentrations down to down to 0.12 ppm (0.8 nM).

### **1.1.2 The biosensor market**

Biosensor research has now effectively progressed from the feasibility assessment phase to a stage of commercialisation. Most of the biosensors commercialised today work on the systems that were devised, roughly, in the years 1962-1985 (although the basic principles may be much older). The largest market segment for biosensors undoubtedly lies in home glucose testing, but new markets are still emerging for more specialised biosensors, e.g. in environmental monitoring and food analysis. European biosensor projects have been conducted particularly in the field of in-vivo glucose monitoring and environmental analysis, e.g. for pesticide residue detection.

In the clinical diagnostics field the most important small molecule analytes are glucose, lactate, cholesterol, alcohol and creatinine, while protein analytes are the infection indicator CRP, the pregnancy hormone hCG and the cancer marker CEA. The market for lactate testing is, however, much smaller than that of glucose. In the environmental monitoring field the most important analytes include oxygen, phosphate, nitrate, ATP and various metal ions (Pb, Hg, As). In the environmental sphere, however, there is also a large need for quantitation of classes of compounds, such as pesticide residues or more global parameters, such as degree of eutrophication, the chemical/biological oxygen demand (COD/BOD) or toxicity index. The primary issue is the usability of a biosensor, i.e. the ability of untrained persons to measure the analyte reliably and diagnose their own state on basis of the measured result. Biosensors also offer the possibility for increased accuracy for analytes where such accuracy is needed or increased selectivity in cases where interferences are present in the chemical tests.

Many new biosensor products have been launched during the last twelve years, predominantly in the clinical area. The first important commercial biosensor device was the ExacTech<sup>®</sup> pen- or card-sized glucose sensor, which was invented jointly by Cranfield and Oxford Universities and developed at Cranfield University and is based on a redox enzyme immobilised onto a

chemically modified electrode. The device was commercialised in 1987 by MediSense and is used world-wide for glucose testing by diabetics. Presently, this device is sold by Abbott Diagnostics as the *Precision Q.I.D.* A number of companies, such as Bayer, Boehringer-Mannheim, Lifescan and Johnson & Johnson, have released their own versions of the device and are now strong competitors.

A second significant commercial device utilising the biosensor concept is the BIAcore<sup>®</sup>. The device was originally developed by Pharmacia AB, Sweden, in a special project and launched in 1990 by Pharmacia Biosensor. Presently, the BIAcore is marketed and sold by Biacore AB. The BIAcore<sup>®</sup> is (still) an expensive research instrument, targeted for the research laboratory and has found by now widespread use in major life-science research centres all over the world. The original BIAcore<sup>®</sup> instrument used three technological innovations in one device: SPR for the direct detection of biochemical interactions, a carboxydextran-coated gold substrate as a generic immobilisation matrix for biomolecules and microfluidics for reagent and sample handling. The newest instrument, the BIAcore<sup>®</sup>Probe, is conceptually already much closer to a real biosensor, omitting the microfluidics part and utilising SPR in an optical fibre. The SPR detection principle has by now also been utilised in quite a number of devices competitive to the BIAcore. E.g. a cheaper Dutch SPR device, the IBIS, has also been launched recently by Intersens Instruments. The system exploits the resonant mirror concept, as originally developed at Twente University. The IBIS is available in a manual, a single channel FIA and a dual channel FIA configuration. The newest instrument in the range of SPR-based devices, announced for release, is the KI1 (BioTul Instruments GmbH, Munich, Germany), which is based on dual wavelength SPR detection. Other devices based on evanescent wave optical measuring principles are the BIOS1 by ASI (Switzerland) and the IAsys by Afinity Sensors (UK).

An other interesting example of a chemical sensor device is the electronic nose, initially developed by the University of Manchester's Institute of Science & Technology (UMIST). The electronic nose was commercialised in 1994 by the British company AromaScan. The device is based on a conducting polymer array and is capable of classifying smells. The device is targeted for the food, drink and perfume industries. Electronic noses can be based on conductometric, MOSFET, resonant quartz crystal or optical technologies and may utilise also

bioreceptors in the future. A modular electronic nose (the 'MOSES II') is presently being developed by Lennartz Electronics in cooperation with the University of Tübingen, which can utilise different detection principles in the same device.

When thinking of commercialisation, careful targeting of any new biosensor product has to be performed already at an early stage. A persistent problem in the commercialisation of biosensors has been the severe competition from more conventional, cheaper dry-chemistry test kits and test strips (Boehringer Mannheim, Johnson & Johnson Lifescan, Merck, Orion). An example of a highly competitive instrument is the Reflotron<sup>®</sup>, which was introduced in 1985 by Boehringer Mannheim and is still widely used in doctor's offices and health care centres for the determination of various analytes directly in blood serum or plasma. The Reflotron<sup>®</sup> is a portable diffuse reflectance photometer.

## 1.2 Electrode modification techniques

Many processes utilised in biosensors are based on reactions that take place at the solid/liquid interface and such processes are influenced profoundly by chemical modification of the interface<sup>14</sup>. Coating of a metal electrode with a single molecular layer has a large influence on the wetting, friction and adsorption properties of the electrode, while the electrochemical reactions at the electrode are significantly modified. Electrode coating methods now play a major role in electroanalytical chemistry<sup>15</sup>. Besides the design of electrochemical sensors, electrode modification can be applied to the construction of rechargeable batteries and fuel cells, electrosynthesis, the study of electron transfer mechanisms, corrosion protection and the design of electrochromic and electroluminescent displays. With the present knowledge it is indeed possible to design the electrode interface more rationally than before (“molecular electrochemistry”) and eventually this knowledge may be used to construct molecular electronic components and devices (“supramolecular electrochemistry”). An interesting trend is that the size of electronic circuit components has continuously decreased and that of individual synthetic molecules has increased, such that by now there is only a gap of a single order of magnitude left (from 10 to 100 nm).

Earlier methods for electrode modification included electrochemical pretreatment (e.g. of glassy carbon)<sup>16</sup> and chemical derivatisation of the electrode surface<sup>17,18</sup>. Other film techniques for electrode modification comprise electrochemical polymerisation of monomers, resulting in either conductive or isolating (permselective) polymer layers, and deposition of preformed polymers by spin-coating. For instance, perfluorinated ion-conductive materials of Nafion have been used much in sensor and fuel cell applications due to their good chemical stability<sup>19</sup>. Bulk polymeric electrodes are also attractive. Here organic compounds, and possibly biocomponents, are directly cast together with carbon paste, graphite or metal particles into a polymer (epoxy, acrylate, PVC) to form a robust electrode body. The surface properties can be controlled by the formulation of the polymer. Inorganic materials are also used much for electrode modification and include metal oxides, silicates, clays (e.g. bentonite) and zeolites, which can be deposited onto the electrode by spin-coating or sol-gel techniques. From the many surface modification techniques offered by surface

science, especially those used in the electronics industry (evaporation, sputtering, photolithography and etching) many are useful for biosensor development. Also other methods that allow mass production have been used, such as screen-printing and ink-jet printing.

In the present study two molecular thin film techniques have been utilised: the Langmuir-Blodgett (LB) film technique and self-assembly. LB-films are presently regarded as ideal for sensor construction and in future molecular electronics applications<sup>20</sup>. The advantages of the LB-technique are that highly uniform mono- or multi-molecular films can be produced, in which orientation and packing can be controlled by an externally applied surface pressure. Additionally, different components can be included in the molecular film in a predefined ratio. A disadvantage of the LB-film technique is that strict control of the environmental and experimental conditions is required and that the film deposition may be time-consuming. Although there are presently no LB-film-based biosensor or bioelectronics products on the market and the instrumentation is rather costly, automated LB-methods for mass production may be devised. The method also consumes very small amounts of purified compounds. Self-assembly is a special case of chemisorption in which the molecules form a monomolecular layer with a high degree of ordering on the solid surface through a terminal functional group<sup>21</sup>. The ordering process is usually controlled by lateral interactions of the main chain. Self-assembled molecular layers (SAM's) may exhibit a varying degree of ordering and fluidity, depending on the structure of the molecule and the nature of the surface and they are usually very stable<sup>22,23</sup>. Compounds capable of forming SAM's are very similar to surfactants. As a model surface for SAM-formation gold has been very much used in conjunction with alkylmercaptans, alkylpyridines, alkylpyridiniums and phosphines, while self-assembly on silicon and glass is much performed with alkylsilanes. Self-assembled layers without biocomponents are already used as such in the sensing of low molecular weight compounds of biological and medicinal importance<sup>24</sup>. Coupling of biological compounds to self-assembled films for the realisation of biosensors has been pioneered by Kinnear & Monbouquette<sup>25</sup> and Itamar Willner and co-workers<sup>26</sup>. Monolayers of lipids can also be self-assembled on mercury and these layers can be studied conveniently with polarography<sup>27</sup>. The self-assembly of lipid bilayers onto platinum has been put forward as a most promising technique for biosensor construction as will be discussed further below.



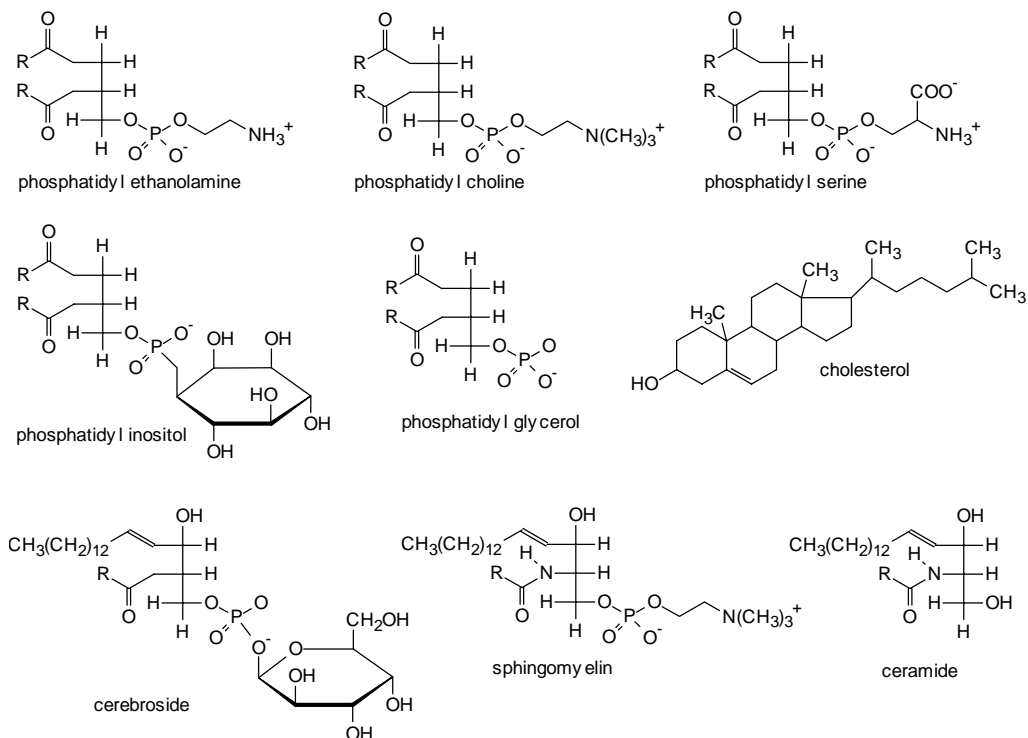
## 1.3 Bilayer Lipid Membranes (BLM)

### 1.3.1 BLM formation and properties

A bilayer lipid membrane (BLM) is a thin bimolecular membrane formed from lipids<sup>28</sup>. Lipids are amphiphilic compounds consisting of a hydrophilic head group connected via a glycerol unit to a pair of hydrophobic hydrocarbon chains and are as a whole water-insoluble. Other amphiphiles can also form BLM-like structures or can be used as additives to the BLM. They include cholesterol, fatty acids and hydrocarbons with quaternary ammonium, sulphonate, phosphate or sulphate terminal groups. Figure 1.2 displays some important structures and their abbreviations as used in the present work. The lipid content of a number of natural membranes is presented in Table 1.1. As can be observed, the membranes of simple bacteria contain only a single lipid component, while those of the higher organisms are complicated mixtures.

**Table 1.1** *Natural lipid components in weight% of total. (from ref. 29)*

<b>Lipid component</b>	<b>myelin sheath of nerve fibre</b>	<b>Erythro- cyte</b>	<b>Mitochon- drion</b>	<b>Azobacter Agilis</b>	<b>E-coli</b>
Phosphatidyl ethanolamine	14	20	28	100	100
Phosphatidyl serine	7	11			
Phosphatidyl choline	11	23	48		
Phosphatidyl inositol		2	8		
Phosphatidyl glycerol			1		
Cholesterol	25	25	5		
Sphingomyelin	6	18			
Cerebroside	25				
Ceramide	1				
Others	12	2	11		



DPPE=dipalmitoyl phosphatidyl ethanolamine ( $R=CH_3(CH_2)_{14}$ )

DLPE=dilinoleoyl phosphatidyl ethanolamine ( $R=CH_3(CH_2)_4-C=C-CH_2-C=C-(CH_2)_7$ )

DPPC=dipalmitoyl phosphatidyl choline ( $R=CH_3(CH_2)_{14}$ )

DLPC=dilinoleoyl phosphatidyl choline ( $R=CH_3(CH_2)_4-C=C-CH_2-C=C-(CH_2)_7$ )

**Figure 1.2** The structures of the most important natural BLM constituents.

BLM's may be considered as ideal model systems for cell membranes. Cell membranes have many functions in living systems: they provide permeability barriers for ions and organic compounds, are involved in the accumulation and transport of biologically active compounds and play an important role in photosynthesis, protein synthesis and vision. Furthermore, many types of immunological reactions take place at the cell membrane. BLM's can be formed spontaneously in buffer solutions as liposomes by sonification or extrusion. They can also form free-standing planar membranes within small hydrophobic apertures in plastic<sup>30</sup> or silanised glass ("patch clamp methods")<sup>31,32</sup>. Moreover, the LB-film deposition and self-assembly of BLM's on electrode surfaces is generally practised.

The physical properties of a BLM compare favourably with those of natural membranes. They have a thickness ranging from 4–15 nm, a resistance of  $10^3$ – $10^9 \Omega \cdot \text{cm}^2$ , a capacitance of 0.3–1.3  $\mu\text{F}/\text{cm}^2$  and a refractive index of around 1.60. The typical value for the membrane capacitance is around 1  $\mu\text{F}/\text{cm}^2$  and is roughly a factor 10 to 100 lower as that of the normal electrode double layer capacitance. Natural and synthetic BLM's may also display electronic/photonic excitation, ion- and electron-conduction and ion selectivity<sup>28,43,47</sup>. Various theoretical studies on bilayer membranes have been conducted. The earliest questions were related to the molecular basis of the stability of the BLM and the origin and nature of the transmembrane potential. The physical properties of a BLM critically depend on the membrane constituents used. The phase behaviour of mixed Langmuir layers of lipids has been studied by Albrecht et al.<sup>33</sup>, while the optimization of experimental conditions for LB films has been recently studied by Sellström et al.<sup>34</sup>.

Lipid bilayers of pure dipalmitoyl phosphatidyl choline (DPPC) display two distinct phases in the physiological temperature range: the lower temperature  $L_\beta$  and the higher temperature  $L_\alpha$  phase. The  $L_\beta$  phase is highly ordered, while the  $L_\alpha$  phase is a partially disordered liquid crystalline phase, which is important for biological activity. The fluidity of the membrane increases and the thickness decreases when going from the  $L_\beta$  to the  $L_\alpha$  phase. At neutral pH the net charge on a DPPC membrane is zero. The negative charge of the phosphate group is fully compensated by the positively charged trimethylammonium group. There is a considerable electrostatic interaction between the phosphate and choline groups, an interaction that has a stabilising effect on the membrane. DPPC membranes have the great advantage of having very low non-specific binding to proteins<sup>35</sup>. Tien and co-workers initially investigated the influence of cholesterol on the stability of BLM's. Especially oxidised cholesterol, obtained by an ageing process from cholesterol, seemed to be highly effective for obtaining stable free-standing BLM's<sup>28</sup>. Cholesterol is a major constituent in the cell membranes of higher organisms (Table 1.1) and has a stabilising effect on the liquid-crystalline state of DPPC<sup>36</sup>. Cholesterol has also been used in the present study in the formation of lipid LB-films.

The theory of membrane electrochemistry has been most elegantly presented in the textbook of Koryta and Dvorak (1987)<sup>29</sup>. Membrane potential theories were developed, among others, by Shinpei Ohki, who showed the contribution of

surface potentials and diffusion potentials to the observed transmembrane potentials of phosphatidyl choline and phosphatidyl serine membranes<sup>37</sup>. The transmembrane potential is considered as the sum of the *adsorption* (or *Gouy*) potentials ( $\psi_G$ ) and the *diffusion* potential ( $\phi_d$ ). The first of these describes the component of interfacial charge adsorption at the aqueous membrane face, while the second is related to the membrane permeability for a particular ion. Lately, theories have been developed for describing the passive ion conductivity of single pores in bilayer membranes<sup>38</sup>, while molecular dynamics studies on DPPC have been reported by the group of Karplus<sup>39</sup>.

The introduction of suitable lipophilic additives to a BLM can drastically modify its physicochemical properties. The most important modifications are those that enhance the ion or electron-conductivity of the membrane. These processes may be based on passive or active transport, the latter relying on enzymes or coupled chemical reactions to transport ions to a higher electrochemical potential. There are numerous studies on the modification of BLM's with ion channels. These comprise *transport antibiotics* (e.g. valinomycins and gramicidins), *neurotransmitters* (e.g. the nicotine and acetylcholine receptors) and various *toxins* (e.g. delta-endotoxins and neurotoxins). Also synthetic compounds designed for ion-selective electrodes may be used in BLM's for enhancement of selective ion-conductivity<sup>40</sup>. Conductive (or photoconductive) properties may be introduced into BLM's through the incorporation of redox compounds and conducting polymers as initially studied intensively by Tien and co-workers. Tetracyanoquinodimethane (TCNQ) was the first modifier that was investigated for producing conducting BLM's<sup>41</sup>. Many common redox-active dyes, such as crystal violet, appeared to produce characteristic cyclic voltammograms<sup>42</sup>. BLM's were also modified with liquid crystals and TCNQ, which resulted in BLM's with a photoelectric response<sup>43</sup>. Lecithin membranes containing Polypyrrole (PPy) appeared to be conductive and quite stable<sup>44</sup>. Tien's group was also the first to discuss the spontaneous self-assembly of lipids onto nascent platinum surfaces<sup>45</sup>, a technique that can be utilised in the design of various types of biosensors<sup>46-48</sup>.

The synthetic aspects of lipid synthesis has been recently reviewed by Paltauf & Hermetter<sup>49</sup>. Chemical modification of lipids is much needed for a number of purposes: (1) the lipid may be modified to introduce a transducing function (e.g. ion or electronic conductivity), (2) polymerisable or cross-linked lipids may be

used for improving the stability of the bilayers, and (3) groups may be introduced which enable binding to a solid surface, or covalent attachment to a (bio)molecule of interest. All these modifications can be combined, if needed, in a single molecule. Polymerisable lipid linkers are also introduced in the present study in Chapter 3.

### 1.3.2 BLM-based biosensors

As protein functions are highly specific and are always influenced by their environment, the use of natural materials is highly favourable for retention of protein functionality. In nature many proteins are associated with cell membranes. They may be bound at the ionically charged interface or may be incorporated in the hydrophobic phase of the membrane. In the latter case the hydrophobic phase of the membrane provides a part of the folding environment of the protein and the transfer to a solid-state device will be more difficult. Proteins that are not normally associated with biomembranes may also be bound to BLM's. Functional groups may be introduced on the surface of the BLM to enable covalent binding, electrostatic interactions, hydrogen bonding or ligand binding to the protein. The conjugation of Fab'-fragments to vesicles is already an established technique for obtaining labels for immunoassay or reagents for drug targeting.

The binding of biomolecules to solid-phase BLM's is nowadays considered as a main research topic for design of biosensors and will be further discussed below. The advantages of BLM's as an immobilisation support for biomolecules has been discussed by a number of authors: Tien, et al. (1988)<sup>50</sup>; Thompson & Krull (1991)<sup>51</sup>, Valleton, (1990)<sup>52</sup> and Tedesco et al. (1989)<sup>53</sup>. Firstly, through chemical modification and variation of membrane components, the binding for proteins may be engineered. Secondly, functional BLM's may be deposited on solid supports, by self-assembly or LB-film techniques, as mentioned earlier. Thirdly, many chemical processes can be directly converted into an electronic response by using a bilayer membrane. Finally, and most significantly, due to the high electronic isolation<sup>54,55</sup> and the low permeability for ions<sup>56</sup>, undesired electrochemical processes can be effectively suppressed. The high isolation of BLM's is particularly needed in biosensors based on ion-channel systems, but is also desired in amperometric biosensors. With ion-channel systems the demands on isolation are crucial to the performance of the sensor<sup>57</sup>. In an early study by Michael Thompson's group, BLM's could be deposited successfully on nylon<sup>58</sup>. Later, a polyacrylamide gel deposited onto a Ag/AgCl electrode was used as a support for a BLM, using epoxy resin as an encapsulation material<sup>59</sup>. The BLM was deposited by the LB technique within an aperture of the epoxy resin. A number of bottlenecks of the method were, however, found: there was poor adhesion of the polyacrylamide gel to the Ag/AgCl electrode, insufficient

control of the gel properties for optimal lipid adhesion (surface morphology, hydration of the gel, hydrophobicity) and large leakage currents. It is well-known that small imperfections at the boundary location readily give leakage currents with the LB-film technique, since here no proper Plateau-Gibbs border can be formed (lipid/solvent reservoir around the BLM, which seals the aperture).

An example of an amperometric biosensor based on a free-standing BLM was presented in a study of Kotowski et al.<sup>60</sup>. Glucose oxidase was immobilised onto a free-standing BLM, either by electrostatic interaction with the membrane via didodecyldimethylammonium bromide or covalent cross-linking with glutaraldehyde. PPy was generated in the membrane by chemical oxidation of pyrrole, which yielded a membrane responsive to glucose. The self-assembly of lipid bilayers onto platinum, earlier mentioned as a most promising method for biosensor construction, proceeds extremely well when the lipid solution is brought in contact with a freshly-cut (nascent) metal surface<sup>61</sup>. Salamon and Tollin have reported the direct electron transfer of cytochrome c at such lipid membranes and discussed the importance of electrostatic interactions between lipid and protein in the electron transfer process<sup>62</sup>.

The immobilisation of enzymes on lipid bilayer supports gives also possibilities for the time-dependent processes in the enzyme layer to be studied. With GOx typical conductance fluctuations related to the enzymatic oxidation cycle can be observed, which are clearly resolvable from the thermal background<sup>63</sup>. The noise spectral density curves and amplitude of the membrane current were clearly dependent on glucose concentration, particularly at concentrations below 10 mM.

## 1.4 Scope of the present thesis

The objectives of the present thesis is to evaluate some novel immobilisation methods for biological compounds (oxidase enzymes and Fab' fragments) on ordered molecular thin film assemblies, the main focus lying on the functionality of the biological compound in relation to surface chemistry and properties. Functionality of the biological compound has been assessed by *in situ* monitoring and standardised methods and has been related to the amount of biomolecule immobilised. In the first part of the thesis, enzymes are immobilised onto self-assembled layers of octadecylmercaptan (ODM) and thienoviologens, the latter compounds representing a novel class of molecular wires. In the second part of the thesis antibodies are immobilised onto lipid bilayers, which were produced by the LB-film technique. Both enzyme- and immunosensors are discussed, the common theme being the immobilisation of both types of biomolecules on molecular monolayers. It is the purpose of the present work to demonstrate that: (1) the surface constitution and properties greatly influence the specific activity of immobilised biomolecules and the sensitivity of the produced biosensor; (2) biomolecule performance can be optimised by changing surface chemistry in a predefined manner; (3) very low concentrations and surface densities of biologically active compounds are needed to form functionally active and stable mono-molecular films.



## 2. Immobilization of enzymes on conducting bilayers

### 2.1 Introduction

Since the pioneering article by Clark & Lyons in 1962<sup>64</sup> a considerable body of literature on the design and practical application of amperometric enzyme electrodes has accumulated, while also numerous reviews have been devoted to this subject: Guilbault & Kauffmann (1987)<sup>65</sup>, Frew & Hill (1987)<sup>66</sup>, Nagy & Pungor (1988)<sup>67</sup>, Mascini & Paleschi (1989)<sup>68</sup>, Gorton et al. (1991)<sup>69</sup>, Campanella & Tomassetti (1992)<sup>70</sup>, Bartlett & Cooper (1993)<sup>71</sup>, Wang (1994)<sup>72</sup>, and Ikeda (1995)<sup>73</sup>. In the laboratory many systems have proven their feasibility as well as in the commercial field. The academic literature on the subject amounts presently to about 3500 basic science articles, while the conceptual evolution of enzyme electrodes can be measured in three distinct generations.

In most of the studies on amperometric biosensors glucose oxidase (GOx) from *Aspergillus niger* species has been used as the model compound, since GOx has many useful properties<sup>74</sup>. The first important advantage is the presence of a tightly bound FAD-cofactor ( $K_a=10^{10}$ ), which eliminates the necessity to add a soluble cofactor. Secondly, due to its high negative charge at physiological pH, GOx has a high solubility and is not easily precipitated (e.g. by trichloroacetic acid). Thirdly, the enzyme is highly stable in crystalline form and is in solution very resistant to proteolysis and non-ionic detergents. One drawback of GOx that can be mentioned is its low thermal stability. Also ionic detergents inactivate the enzyme easily, SDS at low and alkyltrimethylammonium ions at high pH. GOx does not have many inhibitors that interfere in *in vitro* studies. At low micromolar concentrations GOx is inhibited by polyamines, mercury, lead and silver ions, and at millimolar concentrations by hydrazines, hydroxylamine, nitrate and semicarbazide. In *in vivo* studies, however, a reversible loss of sensor sensitivity has been observed, which could be caused, among other things, by inhibition of GOx<sup>75</sup>. PQQ-dependent dehydrogenases are presently also actively investigated, because of their high catalytic activity (turnover number) and because they also have a firmly attached cofactor<sup>76,81</sup>.

## 2.2 First and second generation enzyme electrodes

The first generation enzyme electrode is defined as a device in which the electrochemical current is generated by a product of the enzymatic reaction or its co-substrate (Figure 2.1). With oxidase-type enzymes this is usually the oxygen substrate or hydrogen peroxide product, which both can be detected at a membrane-covered platinum electrode (the “Clark-electrode”). The first generation electrode could be improved in response time by immobilisation of the enzyme directly onto the electrode surface<sup>77,78</sup>.

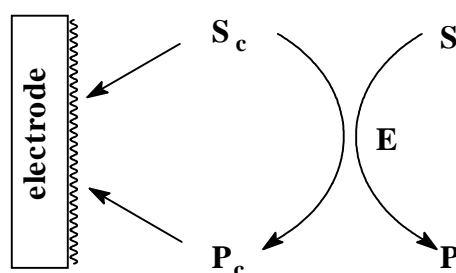


**Figure 2.1** The principle of a first generation enzyme electrode.  $S$ =substrate,  $E$ =enzyme,  $P$ =product,  $S_c$ =cosubstrate,  $P_c$ =coproduct.

The second generation of enzyme sensors, which appeared around 1985, utilised electroactive mediators for electron transfer between the enzyme and the electrode. This is basically a mediated coulometric titration principle (Figure 2.2).

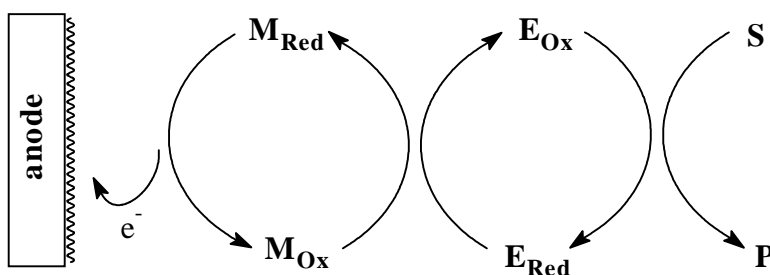


**Figure 2.2** The operation principle of a mediated enzyme electrode.  $M$ =mediator,  $E$ =enzyme,  $S$ =substrate.

With mediated electrochemistry the detection is faster, more sensitive and less prone to interference from other redox compounds due to a lowered potential for detection. Suitable mediators were found for oxidase enzymes<sup>79</sup> and dehydrogenase type redox enzymes<sup>80</sup>. Especially ferrocene derivatives have been studied most intensively in conjunction with GOx from *Aspergillus niger* (EC 1.1.3.4.). As a mediator ferrocene has many advantages: (1) it displays a high standard reaction rate constant ( $k_{sh}$ ) at a variety of electrodes ( $10^5$ - $10^6$  M<sup>-1</sup>.s<sup>-1</sup>), (2) it has a favourable formal redox potential which does not provoke interfering electrochemical reactions (depending on the derivative used, 100-400 mV vs. Ag/AgCl), and (3) ferrocene has a high insensitivity of its electrochemical parameters towards pH and ionic strength. The ultimate advantage of the ferrocene mediator system is its general applicability with various redox enzymes. Two ferrocene derivatives also enabled mediated electron transfer from a PQQ-dependent aldose dehydrogenase as reported by Smolander in 1992<sup>81</sup>.

Disadvantages of the ferrocene derivatives are that the ferrocinium ion slowly dissociates and is highly water-soluble, which yields a decrease of the sensor response upon repeated use, the former by loss of activity and the latter because of leakage of the mediator from the sensor. On the other hand, the efficacy of ferrocene and dimethylferrocene for mediation may well lie in the difference in solubility between the oxidised and reduced form. Although alkyl ferrocene derivatives have a low toxicity<sup>82</sup>, the solubility of ferrocene may seriously limit the *in vivo* application of ferrocene-based glucose sensors. Other types of organometallic complexes have been investigated systematically by Zakeeruddin and coworkers<sup>83</sup>, while hexacyanoferrate ions were used, for instance, by Abu Nader in a sensor for sulphite<sup>84</sup>. Many types of organic mediators have also been used as mediators, including TTF, TCNQ, and various phenothiazine dye compounds. The electrocatalytic reoxidation of NADH by phenazines, (benzo)phenoxazines (e.g. Meldola Blue) and phenothiazines has been intensively studied by Gorton and coworkers<sup>69</sup>. The enzyme cofactor FAD has been used as a soluble mediator for the reduction of cytochrome c, GOx and methemoglobin and the oxidation of ferredoxin<sup>85</sup>.

A number of strategies to confine the mediator within the sensor have been devised. For instance, anionic mediators, such as hexacyanoferrate, can be trapped behind an anionic ion exchange membrane or within a cationic ion

exchange membrane<sup>86</sup>. Wang and Varughese reported the interesting possibility for obtaining very robust enzyme electrodes by casting the GOx and 1,1'-dimethylferrocene directly in a graphite-epoxy electrode<sup>87</sup>. Such electrodes could be regenerated simply by polishing.

A major improvement on the mediation scheme is to use redox polymers. A redox polymer provides faster electron transport, because the diffusion-controlled transport of the mediator between electrode and enzyme can be eliminated (although this diffusion distance can be quite small, when the enzyme is immobilised on the electrode). The final electron transfer rate in a redox polymer is, however, still critically dependent on the distance between the redox centres, the rate constant of electron self-exchange of the redox centre ( $k_{se}$ ) and the type of the polymer medium, as follows from normal electron transfer theory<sup>88</sup>. A large density of redox sites and high electron exchange rate will usually be required to obtain sufficiently fast electron transfer.

Various redox polymers have shown their efficacy as electronic conductors in enzyme electrodes. Initially, Foulds and Lowe prepared GOx films entrapped in ferrocene-modified PPy, which yielded an electrode with a response to glucose at 0.30 V vs. Ag/AgCl<sup>89</sup>. The electrodes, however, were not very stable, activity being lost within two days, and sensitivity to oxygen was observed. Other types of polyferrocenes have been reported, which yielded functional enzyme electrodes, but the sensitivity was lower in comparison with monomeric (soluble) ferrocene, TTF and TCNQ<sup>90,91</sup>. More successful was the performance of a TTF-containing redox-polymer in carbon paste, giving limiting current densities in excess of 250  $\mu\text{A}/\text{cm}^2$  with GOx at a potential of 0.2 V vs. SCE<sup>92</sup>.

Heller and co-workers have extensively studied the high efficiency of Osmium-2,2'-bipyridyl complexes of polyvinylpyridine for electron transfer from various enzymes<sup>93</sup>. In later studies similar complexes based on poly(1-vinylimidazole) were used<sup>94</sup>. The obtained current densities rank among the highest in the literature. In a study by Ye et al.<sup>95</sup> GOx gave a limiting current of 1.7  $\text{mA}/\text{cm}^2$  and PQQ-dependent glucose dehydrogenase a limiting current of 0.5  $\text{mA}/\text{cm}^2$ . The high current densities are probably the combined result of the favourable properties of the Osmium redox polymer (high  $k_{se}$ ) and very high enzyme loadings. This type of linking, however, cannot be truly called "electronic wiring", since it is still a mediated electron transfer principle, in which the

electrochemical response is fully determined by the properties of the redox gel and the enzymatic reaction rate is still controlled by the reaction of the redox groups with the (reduced) enzyme. Also, in spite of the impressive results, these polymers appear to be less versatile in comparison with the ferrocenes. For instance Smolander and co-workers observed that the Osmium polymer showed much less activity with the PQQ-dependent aldose dehydrogenase compared to soluble dimethylferrocene and phenazine methosulphate mediators<sup>96</sup>.

Other interesting approaches include the linking of the mediator covalently to the electrode or to the enzyme. Linking of ferrocenes via an organic spacer chain and a terminal polycyclic hydrocarbon to carbon electrodes was initially attempted by Lo Gorton's group<sup>69</sup>. Bartlett et al. have recently reported on the covalent attachment of a TTF derivative to GOx and could obtain good response characteristics at 0.35 V vs. SCE<sup>97</sup>. Itamar Willner initially described a covalently cross-linked multilayer structure of GOx with N-(2-methylferrocene)caproic acid linked to the enzyme, which gave a good response at 0.4 V vs. Ag/AgCl<sup>26</sup>. In a more recent study Willner coupled the ferrocene or the PQQ unit to FAD and obtained an electrocatalytic response for glucose using apo-GOx reconstituted with both diads<sup>98</sup>. Moreover, Kinnear et al. have recently described an interesting way to mediate the electron transfer from fructose dehydrogenase, using the lipophilic mediator ubiquinone-6 within a self-assembled monolayer of ODM and lipids<sup>99</sup>.

## 2.3 Direct electron transfer

Much scientific effort has been devoted to the third generation of enzyme sensors in which direct electron transfer or "electronic wiring" of enzymes to electrodes is pursued. Direct electron transfer can be obtained by immobilisation of the enzyme in an orientation suitable for electron transfer ("promotion") or, alternatively, when the active site is too deeply buried in the protein, by linking of the enzyme via a conducting spacer to the electrode. This basically gives the scheme in which the enzyme is directly reoxidised at the electrode (Figure 2.3).

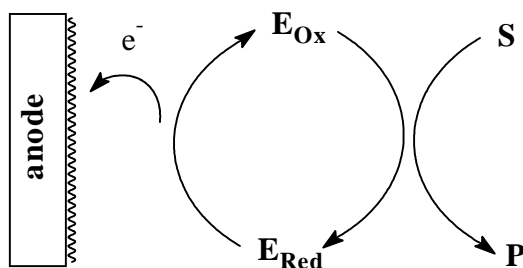


**Figure 2.3** The principle of a third generation enzyme electrode. *E*=enzyme, *S*=substrate, *P*=product.

In the former case the enzyme should be immobilised at a site close to the active centre of the enzyme or at a site which has a strong electronic coupling with the electroactive centre. In the latter case the conductive spacer must be designed so that one of the termini of the spacer can approach the enzymes' active site close enough for direct tunnelling ( $<5\text{\AA}$ ). Different approaches to direct electron transfer have been followed, utilising either conducting polymers, charge transfer salts or thin films of organic conductors, which can all form intrinsic, metal-like conductors which may enable unmediated electron transfer to the electrode. The possibility for obtaining direct electron transfer from the enzyme will in first instance depend on the possibility to retain the structural integrity of the enzyme on the electrode surface. In 1994 Alvarez-Icaza described the mild immobilisation of GOx on carbon using aminophenylboronic acid, through which direct electron transfer could be achieved<sup>100</sup>.

A first approach to direct electron transfer involves the entrapment of the enzyme in a conducting polymer by electropolymerisation of heteroaromatic compounds in the presence of the enzyme. Electropolymerisation has the advantage that relatively thick conductive layers can be produced which have high enzyme loadings<sup>71,101-103</sup>. Furthermore, the film can be neatly patterned onto the electrode and the physicochemical properties of the conductive polymer can be controlled by the applied potential or current and the type of solvent from which the polymer is deposited (protic/aprotic, polar/apolar, pH, ionic strength). Electropolymerised films may already show useful properties for sensing without incorporated enzymes<sup>104</sup>. The intrinsic nature of conduction through conducting polymers should, in principle, give much higher electron transfer

rates than mediated electron transfer. The entrapment of GOx into PPy was initially studied by Foulds and Lowe<sup>105</sup> and Umana & Waller in 1986<sup>106</sup>, and the entrapment of GOx in poly(N-methylpyrrole) was investigated by Bartlett & Whitaker<sup>107,108</sup>. In these initial studies, however, evidence against a direct electrochemical mechanism has been found. The potential for glucose measurement was generally larger than 0.6 V vs. SCE<sup>109</sup>. Bartlett and Whitaker investigated the effect of enzyme loading and film thickness on the amperometric response for the GOx/poly(N-methylpyrrole) system and found that the response was caused by oxidation of H<sub>2</sub>O<sub>2</sub> at the platinum electrode and not by direct reoxidation of the enzyme in the polymer. Soluble mediators were supplemented to the system to lower the oxidation potential. Kitani et al. found that GOx/PPy films were electroinactive, but showed a good response when including additional FAD in the polymerisation medium<sup>110</sup>. The potential used for measurement was, however, also quite high in this study (0.6 V vs. SCE) and the response was dependent on oxygen, indicating that hydrogen peroxide was involved in the detection. In the earlier mentioned BLM study of Kotowski et al.<sup>60</sup> with GOx and PPy inconclusive evidence was also presented in describing the role of the PPy, as control measurements were not made in the absence of PPy. Moreover, ferric ions were present in one BLM-electrode compartment during measurement, which could give rise to a mediation mechanism. Furthermore, in a study of Cooper and Bloor with electrochemically deposited PPy/GOx films the authors observed that the addition of catalase to the film inhibited the glucose response, implying the presence of enzymatically formed H<sub>2</sub>O<sub>2</sub><sup>111</sup>. Interference of the applied mediator and hydrogen peroxide with the conductivity of the PPy film was also observed. Bélanger et al.<sup>112</sup> noticed that hydrogen peroxide degrades the conductivity of the PPy film, and Bartlett & Birkin<sup>103</sup> observed the same effect for poly(N-methylpyrrole).

There were also more positive reports on the GOx/PPy system, however. Almeida et al.<sup>113</sup>, studied the influence of the polymerisation conditions and film thickness on the activity and stability of GOx in PPy films. It was found that the electrochemical entrapment produced excellent reproducibility. The activity of GOx (as measured spectrophotometrically with the o-dianisidine/horseradish peroxidase system) was increasing with film thickness up to 1.6 µm, but showed a non-linear curve due to morphology changes in the PPy film. The optimal conditions for enzyme deposition were found at an enzyme concentration of 0.15

mg/ml at pH 7.0 using a pyrrole concentration of 0.25 M. The activity appeared to be critically dependent on the enzyme concentration.

A number of reports have appeared, suggesting that direct reoxidation of GOx may occur to PPy under certain conditions. In the first, Taxis du Poet entrapped GOx within poly(N-methylpyrrole) at 50 °C and found evidence for direct reoxidation of the enzyme, although the enzyme was here partially denatured<sup>114</sup>. A second system was described by Koopal and Nolte, who immobilised GOx within microtubular PPy<sup>115</sup>. Pyrrole, when chemically polymerised in the nanoscale pores of track-etch membranes with ferric chloride, gains intrinsic conductivity, due to the increased parallel orientation of the PPy chains<sup>116</sup>. When immobilised onto the microtubular PPy, GOx afforded a sensitive glucose sensor. Koopal et al. claimed to have established direct electron transfer between GOx and the polymer, for which substantial evidence was provided. Firstly, the glucose response was not affected by oxygen (although the authors presented no direct measurements illustrating this fact). Most reported measurements were conducted under anaerobic conditions in the presence of catalase<sup>117-119</sup>, but no significant loss of membrane sensitivity upon continuous operation of the enzyme membrane under oxygen atmosphere without added catalase was observed<sup>117</sup>. Secondly, glucose could be measured at much lower oxidation potentials, much below that of hydrogen peroxide. In most experiments 0.35 V vs. Ag/AgCl was used, but glucose could be detected at potentials down to 0.1 mV vs. Ag/AgCl<sup>119</sup>. At this potential hydrogen peroxide effectively gave a reduction current. Bartlett, in his review on the PPy/GOx system<sup>71</sup>, raised some doubts about the absence of peroxide interference in Koopal's studies, possibly because this had been demonstrated in the literature (*vide supra*) and no explicit data was presented. Koopal, however, reported the reduction current at 0.1 V vs. Ag/AgCl for added hydrogen peroxide in his PhD thesis (ref. 118, pp. 67). In a later study, similar behaviour for peroxide was observed with GOx/PPy electrochemically deposited in a matrix of latex particles<sup>119</sup>. The binding of GOx to PPy was proposed to be predominantly of electrostatic nature, as evidenced by the modulation of glucose response by ionic strength. This effect may, however, also be explained as a reversible partial inhibition of the enzyme activity, particularly when considering that the chemical environment of the enzyme is on the acidic side within a cationic PPy membrane, which yields a larger sensitivity for halide ion concentration changes<sup>120</sup>. Kuwabata et al. questioned the findings of Koopal and Nolte, by showing that the response to glucose was also present



when the GOx and PPy were removed<sup>121</sup>. According to the authors, the response was due to a direct catalytic conversion of glucose at the platinum electrode, which was sputtered at the backside of the membrane for electrical contact. This data is, however, in strong disagreement with the observations in the PhD thesis of Koopal, by which PPy membranes without GOx had no glucose response at the used potential (ref. 118, page 64). It will be anyhow clear that direct electrocatalytic conversion of enzymes within nanoscopic void materials (such as track-etch membranes and latex membranes) deserves further attention. The approach of Koopal and Nolte may hold some potential for commercial applications of enzyme sensors. The possible mediating role of small iron residues in the chemically polymerised PPy should, however, also be investigated.

Other oxidase enzymes have been entrapped within PPy. For instance, whole banana cells, containing polyphenol oxidase, were entrapped in PPy by potentiostatic deposition at 0.91 V vs. SCE from a 0.1 M monomer concentration in a neutral phosphate buffer<sup>122</sup>. The polymer/enzyme film showed favourable selectivity and response time in the detection of catecholamines at 0.7 V vs. SCE. Cosnier and colleagues immobilised tyrosinase at N-substituted amphiphilic PPys, which were deposited at 0.75 V vs. SCE. A sensor for different phenols, operating at -0.2 V vs. SCE was the result<sup>123</sup>. A similar system was described by the same author for the detection of glutamate, using glutamate oxidase<sup>124</sup>. Finally, cholesterol oxidase has been immobilised in PPy. Here, however, ferrocenecarboxylic acid needed to be added as a mediator<sup>125</sup>. Other conducting polymers have been reported, which initially were not very successful for functional enzyme electrodes. In most cases high potentials (0.65-0.7 V vs. SCE) were used for the detection of hydrogen peroxide<sup>126,127</sup>.

Many conducting polymers are presently known with more complicated topology and functionality and these could offer substantial advantages in the design of enzyme sensors. References 128 to 138 give a representative selection of substances which may be particularly useful. Much recent work proceeds in the direction of viologen-containing polymers as illustrated by works of Sariciftci et al. (1992)<sup>139</sup>, Bauerle & Gaudl (1990)<sup>140</sup> and Saika et al. (1993)<sup>141</sup>. Viologen polymers may be successfully used in conjunction with reductase enzymes because of their reversible electrochemistry at low redox potentials<sup>142</sup>. Serge Cosnier and co-workers recently described the reduction of nitrite reductase on

electrodes modified with viologen derivatives of PPy<sup>143,144</sup>, while also a system was described for the iron-sulphur enzyme hydrogenase by Eng et al.<sup>145</sup>.

Yet another approach for direct electron transfer involves the use of conducting organic charge transfer salts. The mixing of aromatic electron donors with electron acceptors may yield charge transfer salts with nearly metallic conductivity, the most well-known example being the TTF/TCNQ couple. Such salts have been investigated initially by Kulys as immobilisation matrices for redox enzymes and they proved to be effective oxidisers of NADH<sup>146</sup>. Recently, Khan and Wernet reported the immobilisation of GOx in a dendritic type of TTF/TCNQ<sup>147</sup>, which gave comparable current densities as the systems based on Osmium-polyvinylpyridine redox polymers ( $> 1 \text{ mA/cm}^2$ ). This is probably also due to the enhanced surface area of the organic salt electrode, allowing high enzyme loadings. As, however, both TCNQ and TTF have been used separately as mediators, the mechanism of conduction might still contain an electron mediation step via dissolved TCNQ or TTF.

The linkage of enzymes to electrodes via the biotin-avidin pair is another important innovation. The high affinity of biotin for avidin and streptavidin has been used successfully in immunological methods, but may also serve as a means of immobilisation of enzymes in a more orientated fashion on solid substrates<sup>148</sup>. The aspect of how to establish electronic contact with the enzyme is, however, in this case not yet properly addressed. In at least one study ferrocene derivatives were included in the system<sup>149</sup>. Possibly, conductive streptavidin modifications could be useful in further work.

The LB-film method has already featured in many biosensor studies as a means to get ordered film structures of biomolecules<sup>150</sup>. The first LB-film studies with GOx were performed by Moriizumi in 1985, who studied the adsorption of GOx to lipid films<sup>151</sup>. More recent studies have been conducted by Nakagawa et al.<sup>152</sup>, Lee et al.<sup>153</sup> and Arisawa et al.<sup>154</sup>. LB films of amphiphilic molecules with a  $\pi$ -donor or  $\pi$ -acceptor head group are another class of compounds that can be used for the design of enzyme electrodes<sup>155,156</sup>. Such form  $\pi$ -stacked layers with intrinsic conductivity.

Molecular wires comprise the most interesting group of materials for the construction of amperometric enzyme electrodes. In principle, molecular wires

can provide the fastest electron transfer by delocalisation of electrons over macromolecular distances ( $>2$  nm). The principle of molecular “rectifiers” (diodes) had already been assessed at a theoretical level by Aviram & Ratner in 1974<sup>157</sup>, while the practical realisation of the concept of molecular wires was demonstrated in 1986 by Thomas Arrhenius et al. with the “caroviologens”<sup>158</sup>. Molecular wires of precise length and constitution are presently extensively investigated and have been subject of a recent review by James Tour<sup>159</sup>.

Organic molecular wires have been described in the literature with overall  $\pi$ -acceptor (A- $\pi$ -A)<sup>160,161</sup>,  $\pi$ -donor (D- $\pi$ -D)<sup>162-168</sup> or  $\pi$ -donor-acceptor function (D- $\pi$ -A, “push-pull”-type molecular wires or “molecular rectifiers”)<sup>157,169,170</sup>. Also various molecular wires with terminal metal complexes have been described<sup>171-174</sup>. The caroviologens described by Arrhenius and co-workers have been highly cited, because at the time they were the longest A- $\pi$ -A type wires ever reported, their molecular length ranging from 19 to 36 Å (Figure 2.4.A). Originally they were designed to operate in biomembranes. In the present work molecular wires, consisting of an oligothiophene conducting spacer of variable length, terminated by pyridine or pyridinium substituents have been utilised (“thienoviologens”, Figure 2.4.B). They are molecular wires of the acceptor-donor-acceptor (A-D-A) type, the oligothiophenyl unit acting as a  $\pi$ -donor with respect to the pyridine groups<sup>IX</sup>.

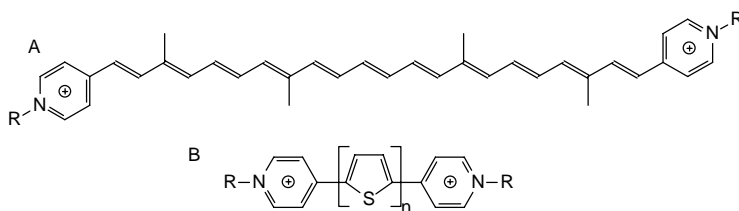


**Figure 2.4** Structure of a caroviologen (A) and the general structure of the thienoviologens (B).

The shortest thienoviologen (with one central thiophene) has previously been described by Takahashi as a compound capable of forming stable radical monocations with a strong absorption in the near-infrared region<sup>175</sup>. Indeed the formation of stable radical monocations is general for the viologens. Thienoviologens with two thiophene units have been synthesised by Nakajima et al. in 1990 and were found to be highly fluorescent<sup>176</sup>. Longer bipyridylthio-

phene oligomers were also prepared by Nakajima, showing the effect of insertion of additional thiophene units in the chain on the optical absorption and fluorescence spectra<sup>177</sup>. Thienoviologens are also known for their electrochromic properties<sup>178</sup> and thus may prove to have great utility as opto-electronic transducing materials. The insertion of thienoviologens in electronically insulating monomolecular layers provides a convenient method to prepare thienoviologen-modified electrode surfaces. Such a surface may be subsequently used as an immobilisation matrix for redox enzymes.

Besides self-assembled films, LB films from molecular wires have already been produced by various research groups. These studies are particularly concerned with  $\pi$ -donor-acceptor molecules, because these have the desired degree of amphiphilicity and display interesting optical properties. Examples are films from aminostyrylpyridinium dyes<sup>179</sup> and BEDTTF-pyridinium dyes<sup>180</sup>. Such films hold also high potentiality in enzyme electrode construction.

## 2.4 Enzyme immobilisation onto self-assembled films

The association of redox proteins with self-assembled organic layers has been subject of intensive study since the discovery by Eddowes and Hill in 1977 that 4,4'-bipyridyl, self-assembled on gold electrodes, enabled efficient electron transfer from cytochrome *c*<sup>181</sup>. Many types of surface modifiers for gold, including several  $\pi$ -bridged 4,4'-bipyridyls, were described as effective promoters for cytochrome *c* electrochemistry<sup>182</sup>. The proposed prerequisites for successful electron transfer with this system was the possibility to form weak, reversible binding between the protein and the surface via complementary electrostatic bonds. In detailed studies of Sagara et al. the weak interaction of cytochrome *c* with 4,4'-bipyridyl on gold could be confirmed, although the actual situation appeared to be more complex<sup>183,184</sup>. The choice of bipyridine and the strength of binding of the bipyridine to the gold surface appears to greatly determine the cytochrome *c* adsorption: 4-mercaptopyridine and bis(4-pyridyl)disulfide attached most tightly to gold, enabling strong binding with cytochrome *c* without denaturation of the protein. 4,4'-bipyridyl was less strongly bound to gold and showed competitive binding with cytochrome *c*. The co-adsorption of 4,4'-bipyridyl with cytochrome *c* partially prevents the denaturation of the protein. 1,2-bis(4-pyridyl)ethylene did not adsorb to gold

strongly enough to compete with cytochrome c and bare protein adsorbed to the gold surface in a denatured state. 4,4'-bipyridyl co-adsorbes with the cytochrome c which gives rise to electrochemical processes from two species on the gold electrode: cytochrome c in direct contact with gold (at -165 mV vs. NHE) and cytochrome loosely adsorbed to the bipyridyl (at +60 mV vs. NHE). The latter species is responsible for the reversible electrochemistry.

GOx has already been immobilised onto various self-assembled films. Jiang et al. immobilised GOx covalently onto a self-assembled layer of the homobifunctional crosslinking reagent 3,3'-dithiobis-succinimidylpropionate and found evidence for direct electron transfer<sup>185</sup>. A reversible reduction of FAD within GOx was observed at -283 mV vs. Ag/AgCl and glucose could be oxidised at potentials larger than -200 mV vs. Ag/AgCl. The method has the advantage that GOx is bound covalently to an anionic surface, which allows for mild immobilisation conditions. Recently the immobilisation of GOx onto different types of self-assembled layers has also been studied by Dong et al.<sup>186</sup>. The most active layers of GOx could be formed by passive adsorption onto hydrophobic alkylthiols on platinum and by passive adsorption of GOx covalently modified with lipoic acid onto gold or platinum. In a recent study on the attachment of GOx to self-assembled layers of bis(4-pyridyl)disulfide it was observed that the electrochemical currents of oxygen, hydrogen peroxide and ascorbic acid were decreased by the bispyridyldisulfide layer, while the mediator ferrocene carboxylic acid could still function as a mediator between GOx and the electrode<sup>187</sup>. Willner et al. has recently studied the adsorption of GOx onto self-assembled 1-(4-mercaptobutyl)-3,3-dimethyl-6'-nitrospiro[indolin-2,2'-[1-2*H*]-benzo-pyran] (SP) on gold<sup>188</sup>. SP is a photo-switchable dye compound, which can be reversibly converted into a positively charged nitromerocyanine dye (MRH<sup>+</sup>) by UV light irradiation (Fig. 2.5). It was observed that GOx adsorbed more strongly to the thin film in the MRH<sup>+</sup> state, as evidenced by QCM measurements. This may indicate a reinforcement of the electrostatic interaction between the photochemically introduced positive charge in the film with the negatively charged GOx.

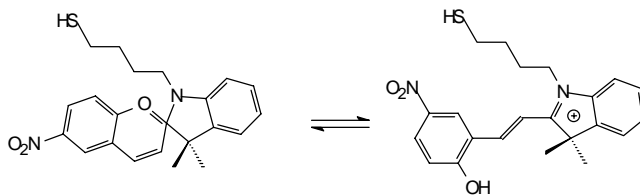


**Figure 2.5.** *Photoconversion of SP to MRH<sup>+</sup>*

Electron transfer rates, in the presence of the mediator ferrocene carboxylic acid, appeared to decrease from  $4.7 \times 10^{-2}$  to  $5.6 \times 10^{-3}$   $\text{cm}\cdot\text{s}^{-1}$ . This may be primarily due to electrostatic repulsion between the ferrocene carboxylic acid and the MRH<sup>+</sup> film. Conversely, the electron transfer rate of GOx covalently modified with ferrocene showed an almost 2-fold increase when the film was switched from SP to MRH<sup>+</sup>.

As illustrated by these studies, more basic understanding of how redox proteins and redox enzymes are attached to self-assembled layers as a function of various surface parameters is crucial in the design of enzyme electrodes. One important factor is the control of the density of positive surface charges, through which it is possible to optimise the activity of the bound enzyme. Besides a wiring function also the shielding of extraneous electrochemical reactions is an important task of the self-assembled layer.

## 2.5 Cofactor modified “fourth generation” enzyme electrodes

The linking of a modified cofactor directly to the electrode and recombining this cofactor with the apoenzyme is a good strategy to attain direct electron transfer, because the distance between the electrode and enzyme's active site is minimised and the protein is properly orientated on the electrode<sup>189</sup>. Elimination of the final electron transfer step between the enzyme (cofactor) and the electrode would yet comprise significant progress in enzyme electrode development and could lead to a “fourth generation” enzyme electrode, in which the electronic coupling between electrode and cofactor becomes sufficiently strong for direct electrochemical control (*acceleration* or *reversal*) of the enzymatic reaction. This can possibly be attained by direct chemical linking via a conjugated  $\pi$ -system or via  $\pi$ -stacking interactions to the prosthetic group (FAD, PQQ or NAD<sup>+</sup>). The observation of electrochemical control of the enzyme activity by the electrode potential would be a good indication that a fourth generation enzyme sensor has been attained. Aizawa reported in 1988 that the forward rate of the enzymatic reaction of PPy-bound GOx and alcohol dehydrogenase could be electrochemically regulated<sup>190</sup>. However, such fully-linked systems are at present highly speculative and have not yet been demonstrated in practice.

Research on cofactor-engineered enzyme electrodes was initiated in the early 80's by Lemuel B. Wingard and co-workers<sup>191</sup>, although they were not successful in linking the apoenzyme to the FAD-modified electrode. In 1988, however, an Indian group reported a successful linking of GOx apoenzyme to graphite electrodes via an electrode-linked FAD analogue<sup>192</sup>. Here the FAD cofactor was bound to the electrode via different lengths of conjugated spacers. The reconstitution of GOx apoenzyme with the electrode-immobilised FAD was most effective (in terms of enzymatic activity) by using a sufficiently long spacer.

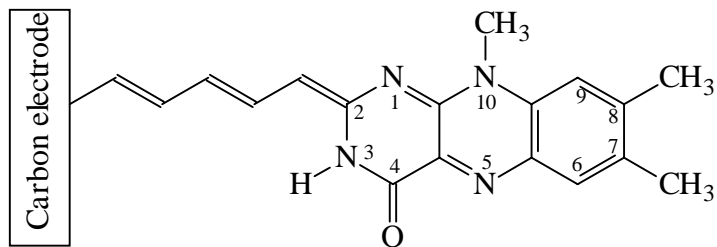


**Figure 2.6** Attachment of an FAD analogue to a carbon electrode.

The FAD was linked to the electrode via the carboxyl group on position 2 of the isoalloxazine ring system (Fig. 2.6) and displayed a characteristic cyclic voltammogram, indicating that the electrons could be transferred from the FAD to the electrode by an electrochemical step.

Recently electrochemically deposited rubidium Prussian Blue has been described as a substrate for the attachment of  $\text{NAD}^+$  to gold electrodes<sup>193</sup>. Such electrodes could be useful for the design of enzyme sensors based on various dehydrogenase enzymes. Also the attachment of PQQ-enzymes to the electrode via PQQ-analogues has been attempted. A PQQ-dependent glucose dehydrogenase could be linked via PQQ to a gold electrode with a thiol spacer<sup>194</sup>. Although the immobilised PQQ showed a reversible response and also the reconstituted enzyme was active, an electrochemical link was not established and a mediator (DCIP) was used to obtain the electrochemical response to glucose. Recently, Schlereth and Kooyman reported on the immobilisation of lactate dehydrogenase to layers of triazine dyes which were attached to mixed self-assembled alkanethiol layers<sup>195</sup>. The enzyme attachment was detected with SPR, and the enzymatic activity was optimised for various types of mixed self-assembled layers. Although an optimum was found for enzymatic activity, using a suitable ligand, short enzyme immobilisation times and a high enzyme immobilisation concentration, direct electrochemistry could not be demonstrated for the dye systems used. In the electrochemical activity measurements  $\text{NAD}^+$  or both  $\text{NAD}^+$  and PMS were used as mediators.



## 2.6 Modelling approaches to enzyme electrode design

Knowledge of the enzyme structure and reaction mechanisms, as well as new theories of electron transfer would clearly enable a more rational design of enzyme electrodes, both with respect to the immobilisation strategy and the possibility of forming an electronic link. The crystal structures of quite a number of oxidase enzymes are presently known and methods for mapping electron pathways in proteins have been recently developed<sup>196</sup>. Table 2.1 lists some FAD-dependent oxidase enzymes that can be found in the Brookhaven protein bank.

**Table 2.1** *Oxidase enzymes in the Brookhaven data base with FAD cofactor.*

PDB code	Enzyme	E.C. nr.	Species
1AA8	D-Amino Acid Oxidase	1.4.3.3.	porcine kidney
1AOZ	Ascorbate Oxidase	1.10.3.3	Zucchini
1COX	Cholesterol oxidase	1.1.3.6	Brevibacterium Sterolicum
1GAL	Glucose oxidase	1.1.3.4	Aspergillus Niger
1POW	Pyruvate oxidase	1.2.3.3	Lactobacillus Plantarum

The structure of GOx was published by Hecht et al. in 1993<sup>197</sup> and the earlier attempts to immobilise GOx may be reviewed shortly in the light of the published crystal structure. Figure 2.7 shows the solvent-accessible surface of a GOx monomeric unit, with the surface coloured according to charge. The surface charge of the protein is predominantly negative. In the centre a small tunnel leading to the flavin group can be discerned. This small cavity is only accessible for small molecules like glucose, ferrocene and oxygen, but cannot accommodate a larger electron relay<sup>198</sup>. The FAD cofactor, represented as a CPK-model coloured according to atom-type, can be seen lying within the cleft. The oxygen at the 2-position of the isoalloxazine ring (not visible in the figure) has an unfavourable orientation for external linking to a spacer, which argues against the results of Phadke et al. On the other hand, the favourable orientation and slight protrusion of the oxygen at the 4-position suggests that making external contact via this group is more realistic. On basis of the structure it can also be observed that the orientation of the enzyme cannot be easily controlled by electrostatic binding to negative groups.

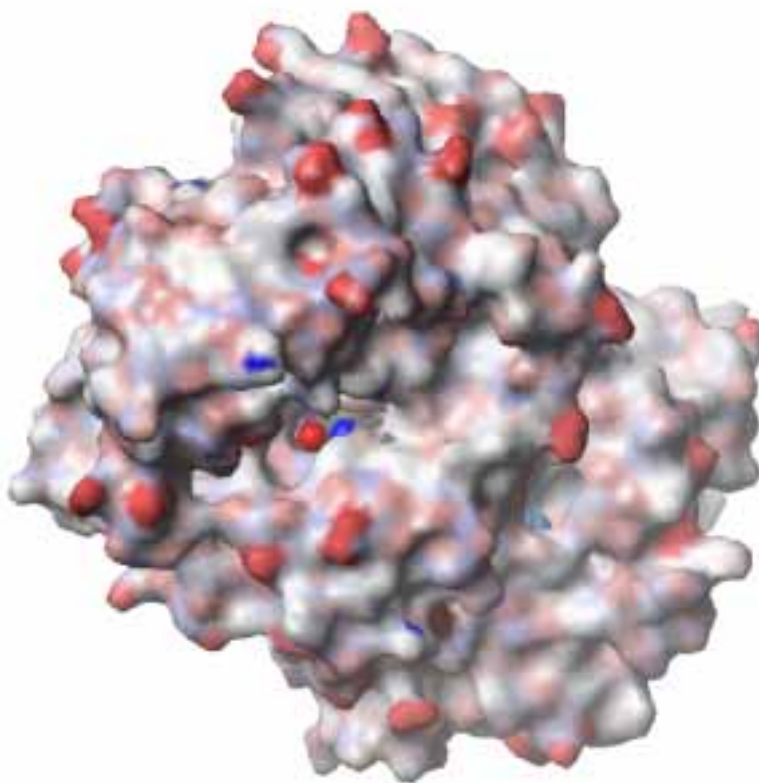


**Figure 2.7** *The solvent-accessible surface of GOx and the position of the FAD cofactor.*

Figure 2.8 shows the positions of some common aminoacid residues, used for covalent attachment. Since lysines are distributed in the protein at all sides, orientated immobilisation will not be warranted by immobilisation via lysine residues. Thiol groups are clearly more favourable, especially the well-exposed Cys164-Cys206 pair. Three possible electron pathways from the active centre to the protein surface were mapped by Alvarez-Icaza et al.<sup>198</sup>. One of more

promising sites was considered to be Cys164. Attempts to immobilise the GOx via the disulphide, by using dithiotreitol splitting and binding to a pyridyldithiopropionate linking group, however, did not give satisfactory results. Denaturation of the enzyme at the electrode surface was suspected. Another problem was the lack of means to check whether the immobilisation had proceeded in the desired way.

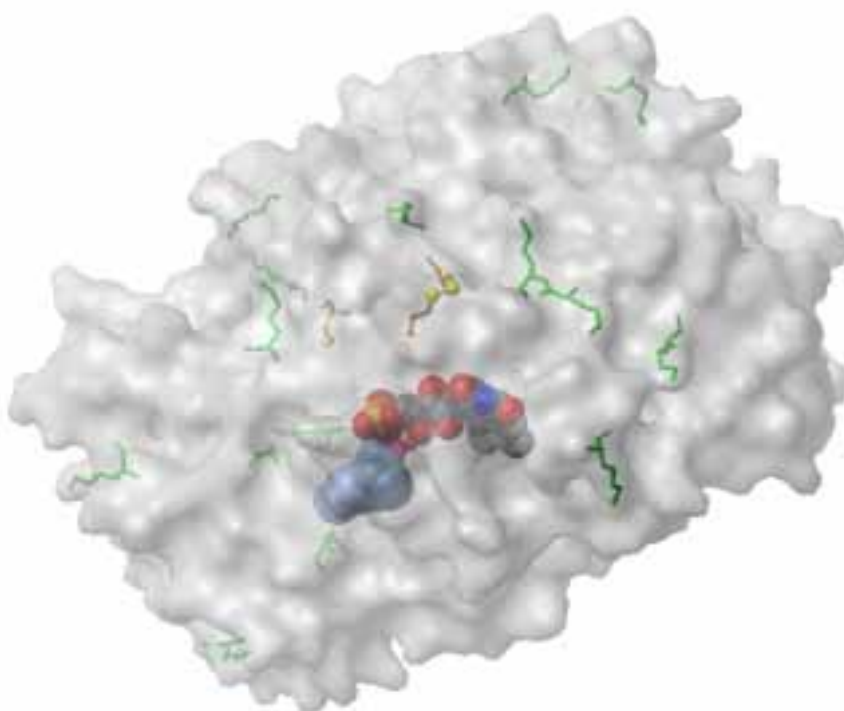


**Figure 2.8** Immobilisation sites in GOx. Lysines (green) and cysteines (yellow/orange).

The modelling of electron transfer in proteins by mapping electron pathways must be presently considered as highly approximate. The PATHWAYS II program, moreover, uses no quantum chemical calculations, but only maps minima in the coupling decay between different points in the protein via constant parametrised decay functions. There are separate types of decay functions for covalent, hydrogen bonding and through-space connections<sup>199</sup>. The decay parameters are difficult to compute reliably and verify experimentally, but the method has worked remarkably well for many cases of biological interest. In reality the decay parameters depend on the protein structure and should be calculated at a suitable quantum chemical level<sup>200</sup>. Semi-empirical methods may offer some relief in the near future. The practical size limit for molecular systems presently lies in the range of 4 000 to 10 000 atoms on large supercomputers, using the MOZYME program<sup>201</sup>. This brings small protein molecules already within reach of quantum chemical calculations, which are more accurate than earlier quantum chemical methods for proteins.

The aim of the present chapter is: (1) to investigate the possibility to obtain stable and conductive self-assembled layers of thienoviologens on gold substrates, (2) to partly elucidate the mechanism of binding of glucose oxidase to the self-assembled thienoviologen layers and (3) to assess the activity of the produced enzyme layer.

## 2.7 Experimental

### 2.7.1 Thienoviologen synthesis

Cross-coupling of Grignard, organotin or organozinc reagents with haloarenes, in the presence of Nickel or Palladium phosphine catalysts is generally used for the efficient preparation of heteroarene oligomers<sup>202,203</sup>. In the present study these methods were used for the preparation of 5-(4-pyridyl)-5'-[4-(N-methyl)pyridinio]-2,2'-bithiophene iodide (PT2) and 5,5''-bis[4-(N-methyl)pyridinio]-2,2':5',2''-terthiophene di-iodide (PT3) as shown in Figure 2.9<sup>I, VIII</sup>.

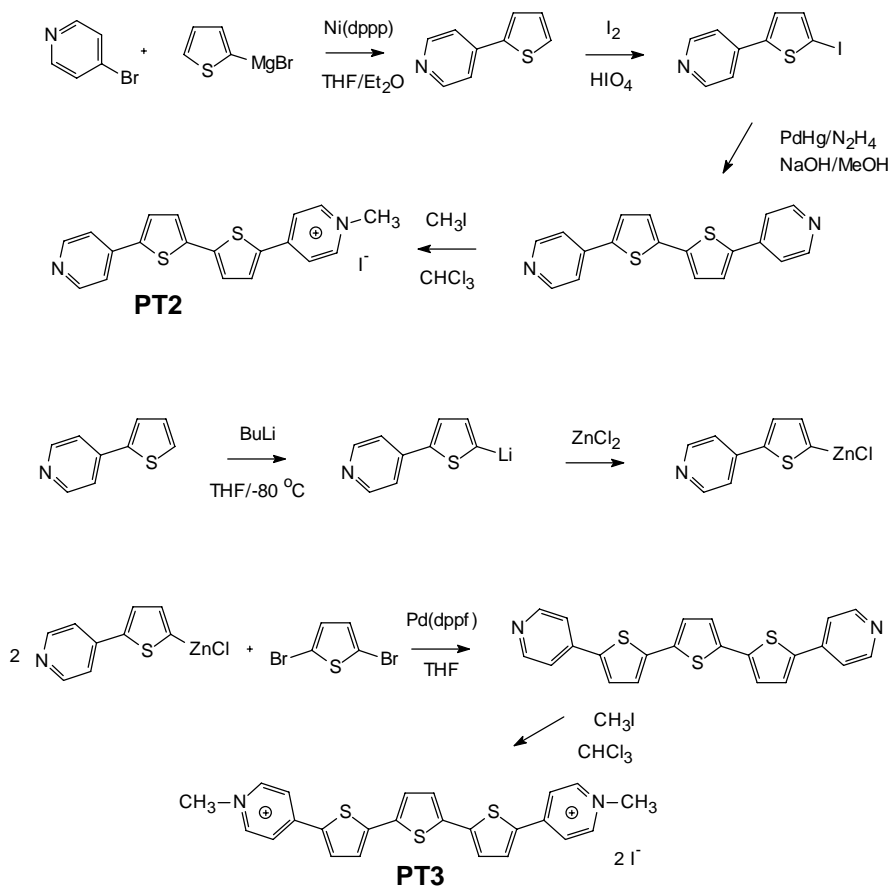


Figure 2.9 Preparation of PT2 and PT3.

## 2.7.2 Electrode coating

Miniature three-electrode systems, containing a gold working electrode, a silver reference electrode and a platinum counter electrode were patterned on glass or silicon dioxide substrates by a sputtering/lift-off technique (VTT Electronics, Otaniemi, Finland). The working electrode (Au) had a geometric surface area of 9 mm<sup>2</sup>. In other types of coating studies, where no electrochemical tests were required, gold was sputtered on silicon wafers, which were subsequently cut into rectangular pieces of 6 x 9 mm<sup>2</sup>. In all cases the adhesion of the gold to the substrate was enhanced by a 10 nm intermediate layer of chromium or titanium.

The gold substrates were cleaned by an RF argon plasma for 10–20 seconds at 0.8 kV and a pressure of 1,33 Pa (10 mTorr), and immediately transferred to a coating solution containing 1 mM ODM (Aldrich Prod. Nr. O-185-8) in ethanol. The electrodes were left in the solution for 18 hours, thoroughly rinsed with ethanol and generally kept at least one night in ethanol before use in subsequent experiments. PT2 or PT3 were adsorbed for about 18 hours from dilute solutions, also in ethanol, onto the Au/ODM, at concentrations ranging from 5 to 200 µM. In this care must be taken to use very clean glassware. All glassware was been treated with piranha (30% hydrogen peroxide/concentrated sulphuric acid 1:4 v/v) at 80–100°C, rinsed with water (MilliQ-grade) and dried in the oven at 105°C. During adsorption (overnight) tubes were covered with aluminium foil. Glassware and silicon slides were generally cleaned by boiling first in a mixture of 30 % H<sub>2</sub>O<sub>2</sub>, 25% ammonia and water (1:1:5 v/v) and thereafter in a mixture of 30 % H<sub>2</sub>O<sub>2</sub>, 12 N HCl and water (1:1:5 v/v) for 1–2 hours.

## 2.7.3 Enzyme immobilisation and activity assay

### *Radioassay*

The enzymes, GOx, [EC 1.1.3.4] 149 U/mg (Fluka 49182) and choline oxidase, (ChOx), [EC 1.1.3.17], 10.6 U/mg (Fluka 26986), were labelled, using "BioBeads", with <sup>125</sup>I. The specific activities of the enzymes varied between 10<sup>7</sup>–10<sup>8</sup> CPM/mg. Enzymes were immobilised by passive adsorption by placing the gold chip or electrode with the gold face down on an acrylic block with a 0.5 mm gap. 30 µl of enzyme solution, of appropriate concentration, was then

injected in the gap between the electrode and the acrylic block with a Hamilton syringe. The enzymes were allowed to adsorb at room temperature for 3 hours. Hereafter the substrates were transferred to glass test tubes and rinsed with PBS buffer three times, taking care not to allow the surface to dry. The substrates were then left in buffer and the radioactivity was measured, if needed correcting the CPM values for a 61 day decay time. Comparison of the residual radioactivity on the chips with the value of the specific activity (in CPM/ $\mu\text{g}$ ) yielded the amount of immobilised enzyme.

#### *Enzymatic activity*

The activity of the enzymes was determined with methods similar as described in the enzyme handbook of Bergmeyer<sup>204</sup>. The additional reagents used were horse radish peroxidase (POx) (EC 1.11.1.7, Fluka 77336, 727 U/mg), choline chloride (Sigma) and D-glucose (BDH). As the chromophore 2,2'-Azino-bis(3-ethylbenzothiazole-6-sulphonic acid (ABTS, Fluka 11557) or 3,3'-dimethoxybenzidine (o-Dianisidine, ODIA, Fluka 33430) was used. The enzymatic activity of the slides was recorded in 1 cm cuvettes on the spectrophotometer at 405 nm, using the ABTS dye (ref. II) or in microtiter plates as absorbance values at 436 nm using the ODIA dye (this thesis). The microtiter plates were shaken for 1 hour at 25°C prior to reading the absorbance values. For ODIA the conversion factor from absorbance units to microunits was 0,88 mU per absorbance unit (assay volume=300  $\mu\text{l}$ , effective path length=6,83 mm).

### **2.7.4 Electrochemical and impedance measurements**

To evaluate the passive electrical properties and the AC conductivity of the gold electrodes, impedance measurements were carried out with an a Hewlett Packard 4195A Network/Spectrum analyser in the frequency range 10 Hz - 100 kHz. Electrochemical impedance techniques are described in detail elsewhere<sup>205</sup>. All impedance measurements were performed in an electrolyte solution containing 154 mM NaCl, 10 mM HEPES, 100 mM potassiumferrocyanide and 100 mM potassiumferricyanide, buffered to a pH-value of 7.00 (HFC-buffer). This electrolyte solution produced a very low electrochemical impedance in the low-frequency region. A two-electrode set-up with a 100 mm<sup>2</sup> gold counter electrode was used.

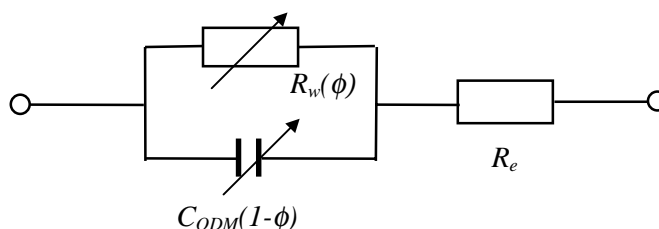
Cyclic voltammetry (CV) was used to evaluate the DC conductivity of the electrodes. The voltammograms were recorded with an EG&G PARC Potentiostat/Galvanostat Model 263, using EG&G PARC Model 270 electrochemical software. The buffer for CV measurements consisted of 5 mM potassiumferrocyanide in PBS buffer (154 mM NaCl, 10 mM phosphate, pH=7.5). The gold electrodes were mounted in an EG&G Model K0264 MicroCell together with a platinum counter electrode and an Ag/AgCl reference electrode. The buffer was purged with nitrogen for 0.5 hours to reduce interference from oxygen. Cyclic voltammetry was also performed on copper electrodes. Common transformer wire (0.75 mm diameter) was fused in Teflon FEP tubing (DuPont) and cleaned by cutting with a sharp knife.



## 2.8 Results and discussion

### 2.8.1 Film formation

The formation of intrinsically conductive layers of thienoviologens was investigated with both impedance and cyclic voltammetry methods<sup>II,VIII</sup>. The impedance spectra of untreated electrodes in HFC-buffer showed impedance values of about 40  $\Omega$  or lower over the measured frequency range (10 Hz - 100 kHz), while the capacitance steadily dropped from around 20  $\mu\text{F}$  at 10 Hz till around 1.5 nF at 100 kHz. After plasma treatment and subsequent coating with ODM the modulus of the impedance increased till a level of 50 k $\Omega$  at low frequencies, which indicates blocking of the electrochemical reaction of the ferri/ferrocyanide couple. This passivation of the gold electrode was used to assess the conductivity of the thienoviologens via the restoration of electrochemistry of the ferri/ferrocyanide couple. A decrease of the impedance modulus of the gold electrodes was observed with increasing thienoviologen concentration with the largest decrease occurring at around 50  $\mu\text{M}$  (Paper II, Fig.1). A more gradual change appeared in the cyclic voltammograms, starting from a near-baseline response at low concentration (<50  $\mu\text{M}$ ) to a reversible electrochemical peak of ferrocyanide at higher concentrations (Paper II, Fig. 4). Thus, both AC and DC measurements indicate the concentration-dependent formation of a conductive layer. The thienoviologen concentration needed to reach full DC conductivity was much higher as that needed for attaining AC conductivity: around 100  $\mu\text{M}$ . The change in impedance could be modelled with a simple equivalent circuit, via a variable parameter  $\theta$ , representing the fraction of conductivity in the membrane<sup>II</sup>:



$$Z(\phi) = \frac{R_w}{\left[ \phi + (1 - \phi)(j\omega C_{ODM} \cdot R_w) \right]} + R_e \quad (2.1)$$

The constant parameters found for  $R_w$  and  $R_e$  were  $0.02 \Omega$  and  $31 \Omega$  respectively, while the capacity of the ODM layer ( $C_{ODM}$ ) was  $0.5 \mu\text{F}$ . The parameter  $\phi$  varied between  $10^{-6}$  and  $10^{-3}$  depending on thienoviologen concentration (Paper II, Fig.3). The increase of  $\phi$  with thienoviologen concentration shows that the electrochemical response of the ferri/ferrocyanide couple was effectively restored.

Layers of ODM and PT2 could also be produced on copper electrodes with the same procedure as followed for gold. Figure 2.10 (trace 1) shows the cyclic voltammogram of an uncoated electrode in PBS buffer (at pH 7.5). The copper stripping wave can be seen at 105 mV vs. Ag/AgCl. Trace 2 displays the CV of the ODM-blocked electrode after 1 (trace 2.) and after 9 scan cycles (trace 3.). Figure 2.11. gives the cyclic voltammograms of the same electrode upon scanning to a larger oxidation potential. Trace 1 is the same as trace 3 from Figure 2.10, trace 2 shows the stripping of the ODM (and Cu) between 400 and 500 mV vs. Ag/AgCl and trace 3 is the cyclic voltammogram after stripping, which is nearly identical to trace 1 of Figure 2.10. It can be thus observed that a large overpotential (300-400 mV) is needed to strip the ODM layer from the copper surface.

Figure 2.12 shows three voltammograms illustrating the effect of PT2 adsorption on the electrochemistry of the copper electrode. Trace 1 is the CV of a copper electrode freshly coated with ODM, trace 2 the same electrode after 3 cycles and trace 3 the same electrode after immersion overnight in a  $200 \mu\text{M}$  solution of PT2.

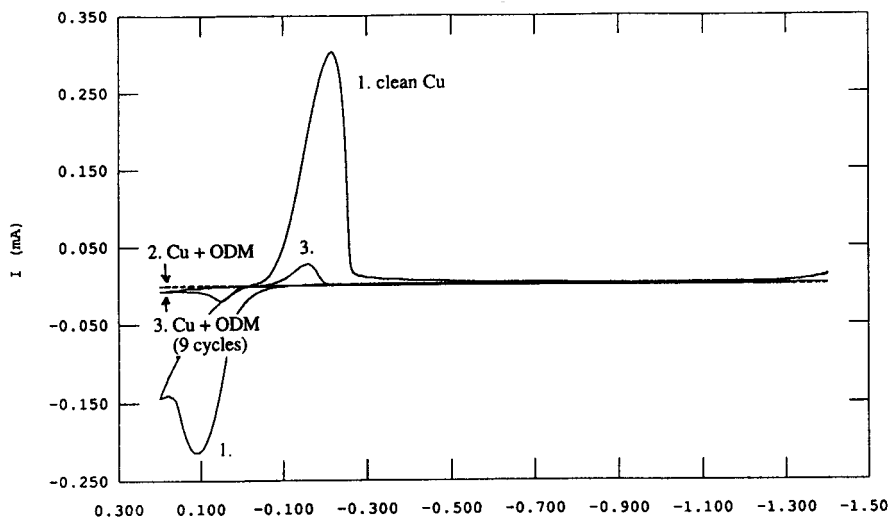


**Figure 2.10** Electrochemical response of copper electrodes towards ODM. 1. blank electrode, 2. electrode coated with ODM and 3. same after 9 CV cycles.

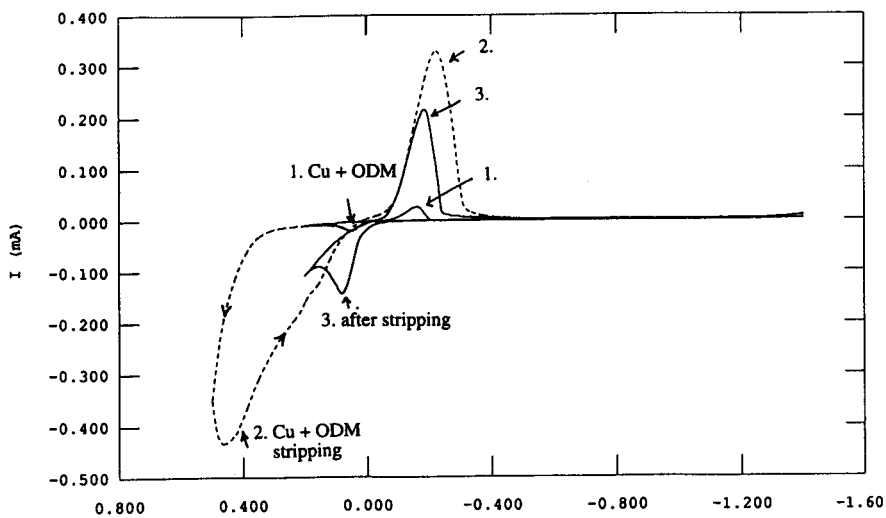


**Figure 2.11** Stripping of ODM from copper electrodes. 1. electrode coated with ODM, 2. stripping of ODM (vertex potential 500 mV), 3. after stripping (vertex potential 200 mV).

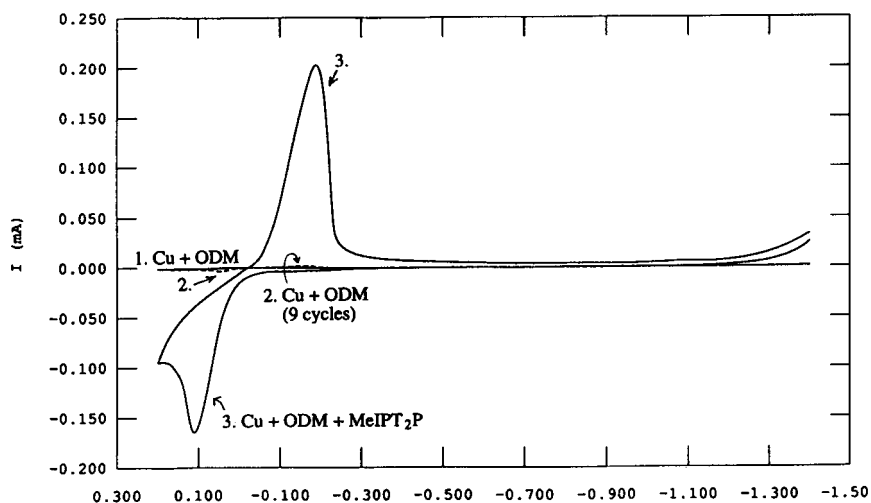


**Figure 2.12** *Electrochemical response of copper electrodes towards PT2. 1. ODM-coated electrode, 2. same after 3 cycles, 3. same after coating with PT2.*

In the last trace the electrochemistry is completely restored to that of an uncoated copper electrode. A much cheaper material can thus also be used for effective self-assembly of thienoviologen layers. With copper, however, the stripping of copper at 105 mV also removes the ODM and PT2 layers.

The adsorption of ODM and PT2 or PT3 on gold was also investigated with secondary ion mass spectroscopy (SIMS) and atomic force microscopy (AFM)<sup>X</sup>. In SIMS measurements it was observed that PT2 and PT3 adsorb to the ODM layer without displacing the ODM (characteristic peaks for ODM were not vanishing, Ref. X, Fig. 3). Also 2-thienyl-4-{N-methyl}pyridinium iodide (PT) was adsorbed irreversibly to the ODM layer. The adsorption was most pronounced for PT2 (Ref. X, Fig. 4). Other similar, but more soluble compounds, however, did not form stable self-assembled layers. AFM measurements clearly showed that ODM and PT2 layers are built up which gradually obscure the nanophase features of the sputtered gold surface (Ref. X, Fig.5).

Semiempirical quantum chemical methods, such as AM1 from the MOPAC package, were found to be useful to assess the different types of binding interactions (van-der-Waals, electrostatic and different forms of charge transfer interaction), although the method is likely not parametrised well for calculations of  $\pi$ -stacking interactions<sup>IX-X</sup>. These interactions should be calculated at a sufficiently high *ab initio* level. The calculated dipole moments and polarizabilities, as calculated with MOPAC/AM1, however, enabled the assessment of a number of physicochemical properties, which might play a role in the relatively strong adsorption of PT2 over other similar compounds (see Ref. X, Table 3). A high dipole moment and polarizability combined with a small degree of amphiphilicity (a result from the monomethylation), a lower solubility in the solvent and an interaction between the thiophene sulphurs are probable driving forces for self-assembly of the thienoviologens to gold/ODM. As these factors increase with the length of the molecule the formation of stable self-assembled layers of thienoviologens on Au/ODM may thus be attained with monomethylated viologens which also exceed PT2 in length<sup>X</sup>.

## 2.8.2 Enzyme immobilisation

### *Adsorption isotherms*

The adsorption isotherms of GOx and choline oxidase (ChOx) were measured to both PT2 and PT3-modified gold electrodes (Paper II, Figures 5-6). The isotherms were characteristically "kinked" at low-concentration point where approximately a monolayer was formed. This was 17 mg/l for GOx and about 33 mg/l for ChOx (with both PT2 or PT3 modified surfaces). The kink could be an indication of the formation of a layer which shows some repulsion to the next layers. Quite small adsorption concentrations are required for the attainment of a monolayer. It was also observed that the desorption in buffer is most prominent during the first two days at high adsorption concentrations. ChOx desorbed during 7 days in saline buffer progressively till about the same surface density as GOx (1.9  $\mu\text{g}/\text{cm}^2$ ). The stability of binding upon preservation in buffer was quite sufficient, but at high adsorption concentrations the amount of enzyme remained, also after long periods of desorption, larger than a monolayer.

The adsorption of GOx onto gold electrodes, which were directly modified with 5,5'-dipyridyl-2,2'-bithiophene (DPBT) and PT2 has also been studied (Fig. 2.13). The adsorption curves of <sup>125</sup>I-labelled GOx onto these self-assembled

layers does not seem to be much different from those with an intermediate ODM layer.

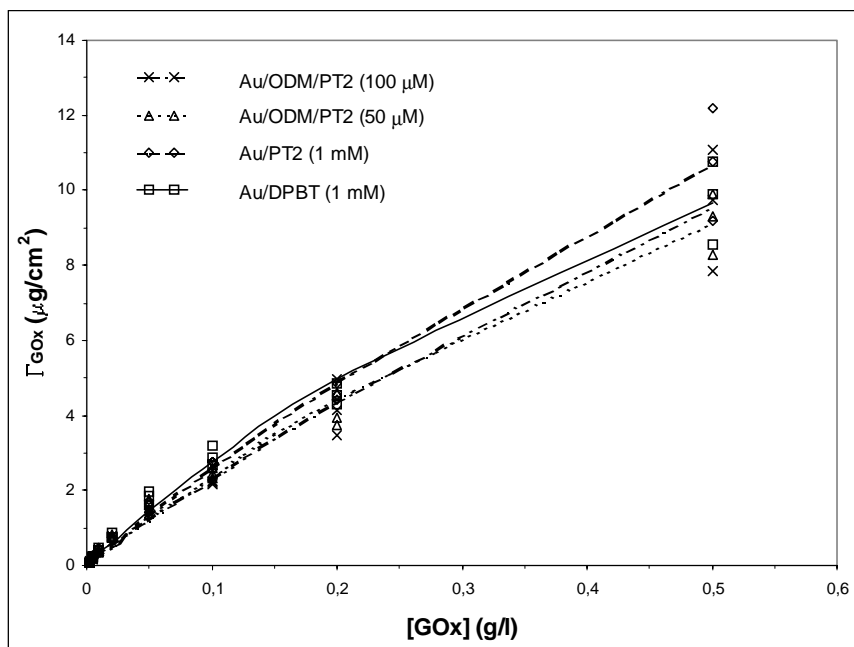


**Figure 2.13** Adsorption isotherms of GOx on Au/DPBT, Au/PT2 and Au/ODM/PT2. The concentrations at which the compounds (PT2 or DPBT) were self-assembled onto the substrate (doping concentration) are indicated in the legend.

The characteristic changes of conductivity of PT2 and PT3 layers occurred at around 50 μM, as observed from the impedance measurements, while full DC conductivity was reached at 100 μM and higher concentrations, as could be seen from the cyclic voltammetry measurements. There are thus large changes in the region 10–50 μM and some gradual changes in the film structure at progressively higher concentrations of the molecular wires. These changes are also reflected in the adsorption behaviour of the two enzymes (Paper II, Figures 7–8). The increase in surface density of the molecular wire gave a measurable enhancement of binding of both GOx and ChOx. With PT2 the amount of GOx (adsorbed from a low 33 mg/l concentration) increased most strongly above 50

$\mu\text{M}$ . This is likely due to the more pronounced adsorption of PT2 at concentrations above  $50 \mu\text{M}$ , giving a much higher positive charge density, which causes a much stronger electrostatic binding of the negatively charged GOx. The adsorption of GOx onto PT3 layers also increased with PT3 concentration, but was more gradual, due to the less pronounced adsorption of PT3 relative to PT2. These adsorption features are further discussed in reference X.

#### *Enzymatic activity*

GOx displayed enzymatic activity, particularly on the slides coated with PT2, while ChOx showed no enzymatic activity. In comparison, ChOx also didn't show activity when adsorbed onto polystyrene (Nunc Maxisorb type), while GOx was active on this surface. The deactivation of choline oxidase may thus be due to residual hydrophobicity of the alkylated gold surface.

The activity of GOx on PT2 layers, prepared at either  $50$  or  $100 \mu\text{M}$  concentration of PT2, vs. GOx adsorption concentration is depicted in Figure 2.14. The effect of ionic strength on the adsorption curves was also measured. As can be observed from the figure, enzymatic activity is increased both by a higher ionic strength during the adsorption step and by using a higher PT2 concentration. The higher ionic strength during immobilisation will decrease the interaction range of the protein with the surface if the adsorption is predominantly of an electrostatic nature. In this case, the enzyme activity is better preserved by using the more mild immobilisation in a higher ionic strength buffer. The maximum activity was  $0,17 \text{ mU}$ .

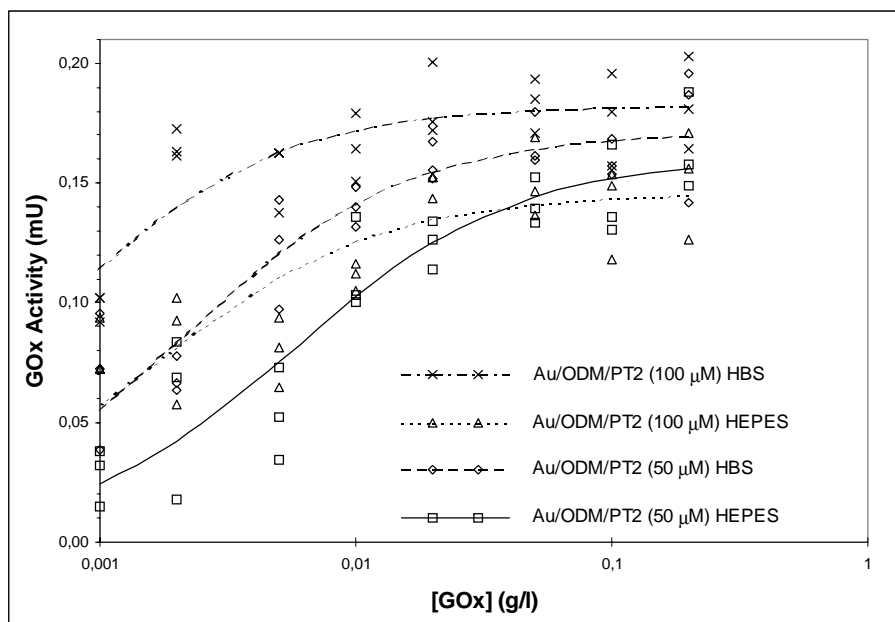


**Figure 2.14** Enzymatic activity of GOx on Au/ODM/PT2. The enzymatic activity was measured at different PT2 doping concentrations (indicated in the legend) and in two buffers: 10 mM HEPES (HEPES) or 150 mM NaCl + 20 mM HEPES (HBS).



## 2.9 Conclusions

The data clearly shows that thienoviologens form a conductive layer on top of the ODM layer and highly effectively reconstitute the electrochemistry of the ferri/ferrocyanide redox couple (both on gold and on copper). Probably highly  $\pi$ -stacked intrinsically conductive layers of thienoviologens are formed onto the ODM. According to SIMS and AFM measurements the PT2 molecule forms multilayers, while PT3 and smaller compounds form monolayers and submonolayers. Gold electrode surfaces could also be directly modified with DPBT and PT2.

The present measurements also clearly illustrate that predominantly electrostatic forces between a positively charged molecular wire and glucose oxidase can be used to stably attach enzymes to an electrode surface. The influence of wire density on GOx and ChOx binding has been clearly observed to increase the binding. Additionally, GOx displayed a moderate enzymatic activity which could be increased by using a higher wire density and a higher ionic strength. From the structure of GOx it can be inferred that the protein probably will not be immobilised in a preferred orientation, e.g. suitable for direct electron transfer. The electrochemical response of thienoviologen- and GOx-modified gold electrodes has been assessed in a few preliminary trials. Unfortunately, no significant response could be observed and a more searching study would be required.

Further work, however, should also assess the means to immobilise GOx onto the electrode surface in an orientation favourable for direct electron transfer. In earlier work of Alvarez-Icaza, however, it became apparent that linking GOx via a suitable disulphide, using SPDP, could not be readily obtained<sup>198</sup>. In own experiments, with polystyrene modified with the slightly more reactive EMCS, it was found that native GOx and DTT-reduced GOx gave exactly the same enzymatic activity. Thus, the covalent link with EMCS was very likely not established, the response being due to adsorbed enzyme. The disulphide is likely too inaccessible for external binding, although the sulphurs are quite close to the surface of the GOx monomer.

Despite the fact that there are a number of practical stumbling blocks that have not been well addressed, the conceptual idea of linking a redox enzyme to electrodes via a single molecular wire may be best approached by further engineering of the wire, e.g. to increase its specificity to bind to a favourable site on the enzyme surface (the disulphide Cys164-Cys206). For further modification the thienoviologens are very suitable, because the pyridine nitrogens can be easily modified with linking groups, as is further discussed in the patent application (Ref. VIII).

## 3. Immobilization of Fab'-fragments on lipid LB-films

### 3.1 Immunoassays

Immunoassays and immunosensors are commonly used to measure the concentration of analytes that are difficult to isolate by normal chemical means, either because no converting enzyme can be found or due to the analyte's extremely low concentrations which requires a ligand with a very high binding affinity. In clinical laboratory tests the important analyte groups for immunoassays are hormones, allergens, viruses and bacteria. Standardised immunoassays, particularly radioimmunoassays, have also been much used for quantifying the amount of binding sites and the affinity constants of immobilised antibodies. The theory for non-linear fitting of antibody titration curves has been elaborated by Feldman<sup>206</sup>. Generally, the method involves the fitting of the bound concentration (B) as a function of the free concentration (F) of antigen, by adjusting the parameters  $Q_a$  (the binding capacity) and  $K_a$  (the affinity constant) of the single-site binding isotherm:

$$B = \frac{Q_a K_a F}{1 + K_a F} \quad (3.1)$$

A Scatchard plot, in which the binding isotherm is linearised by plotting the ratio B/F vs. B, has been used conventionally for the same purpose. Non-linear fitting, however, gives better results than the Scatchard method, because the errors in B are better resolved. In immunoassays there are generally deviations from the ideal single-site binding model. Factors as non-specific binding of the antigen, cooperativity effects and the presence of an affinity distribution may distort the equilibrium binding curves<sup>VII</sup>. Non-specific binding and cooperativity may be introduced into the binding equation as:

$$B = \frac{Q_a (K_a F)^c}{1 + (K_a F)^c} + NF \quad (3.2)$$

where  $N$  is the non-specific binding component and  $c$  the cooperativity factor. Multi-site binding can be described by a multi-phase binding equation:

$$B = \frac{\sum_i Q_{a,i} K_{a,i} F}{1 + \sum_i K_{a,i} F} \quad (3.3)$$

where  $i$  is the  $i$ -th affinity. It is, however, experimentally rather difficult to resolve all the extra parameters, since very precise data and very many data points are needed. Additionally, in multi-site binding, the affinity constants have to be quite different (larger than one order of magnitude) in order to be able to resolve them with non-linear fitting. The single-site binding isotherm has, however, been successfully used for the characterisation of anti-hCG antibodies immobilised on gold and aluminium surfaces<sup>VI,VII</sup>.

### 3.2 Site-directed immobilisation of antibodies

In immunosensors the antibody molecules have to be attached to the transducer surface with optimal preservation of their binding activity and specificity. Methods that were initially widely used for antibody immobilisation were physical adsorption (as in the original ELISA technique, described by Stenvall & Perlman in 1971<sup>207</sup>), covalent coupling or cross-linking to plastic. Neither of these methods can guarantee a proper orientation of the biomolecules, which results in a partial inhibition of the binding to large protein antigens. Furthermore, there are problems with reproducibility and non-homogeneity of the layers with adsorbed antibodies. At Nunc A/S (Roskilde, Denmark) a  $\gamma$ -irradiated type of polystyrene with an enhanced binding capacity and a high accuracy of binding (“Maxisorb”) has been developed. This immobilisation matrix can be used as a reference surface, but has the same drawbacks related to a passive adsorption process<sup>VI,VII</sup>.

A first method for site-directed immobilisation of antibodies was introduced by O’Shannessy & Hoffman in 1987, who bound IgG antibodies via the Fc-domain to amino- or hydrazide-modified surfaces<sup>208</sup>. The method used the selective oxidation of the oligosaccharide moieties by periodate, which makes them

reactive to hydrazide or amines. Protein A or Protein G can also be used for attachment of antibodies to the Fc-domain. These proteins have a specific interaction with the CH2-region of the Fc-domain<sup>209</sup>. Owaku et al. have prepared LB-films of protein A and self-assembled IgG molecules onto these layers<sup>210</sup>.

Protein G appears to increase the reaction stoichiometry of a mouse anti-human antibody with human IgG quite strongly, particularly when the protein G is immobilised onto the gold surface via an epoxysilane layer<sup>211</sup>. The silane layer can be deposited via a chemical vapour deposition process<sup>VI,VII</sup>. Figure 3.1.A depicts the sequential binding, as detected with surface plasmon resonance (SPR), of a mouse anti-human antibody (“Ab”), bovine serum albumin (“BSA”) and the antigen human IgG (“Ag”). The prior injection of salt solutions (“st”) was used as a means of internal standardisation of the refractive index change. The antibody adsorption to epoxylated gold is very fast, but yields a partly denatured layer. The response step of the antigen comprises only 1/6th of that of the antibody after blocking non-specific binding sites with BSA. With the prior adsorption of protein G (“pG”) (Figure 3.1.B) the antibody response decreases and the antigen response increases, such that the reaction stoichiometry is raised to 1:1, which is half of the optimal stoichiometry.

A disadvantage of the use of protein A and Protein G is that these proteins have a relatively low affinity for mouse IgG1, which does not give a very stable attachment of the antibody to the surface and may also provoke displacement of the antibody when working with serum samples.

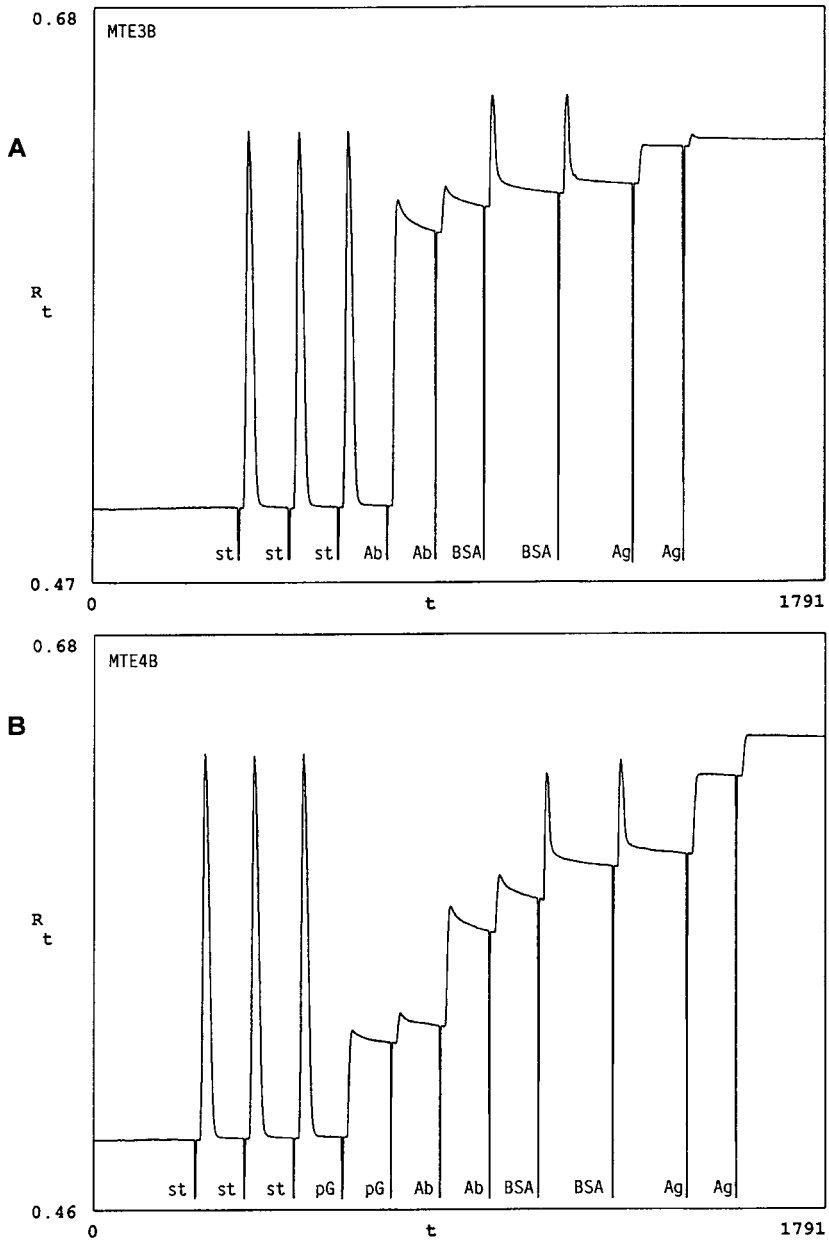


**Figure 3.1** Binding of human IgG to epoxytated gold and the interaction with anti-human IgG, as monitored with SPR. (A) direct binding of the antibody, (B) binding of the antibody via protein G. “s” = 1M NaCl, “pG”=0.2 mg/ml protein G, “Ab”=0.2 mg/ml mouse anti-human IgG, “BSA”=10 mg/ml BSA, “Ag”= 0,05 mg/ml human IgG (+1 mg/ml BSA).

It has been generally recognised, that the use of antibody fragments offers many advantages in immunosensing applications. Firstly, the Fc domain, which normally causes much cross-reactions in immunoassays, can be removed by splitting it off with proteolytic enzymes. Papain cleaves the IgG molecule above the hinge region, which results in an Fc and two Fab fragments. Digestion with pepsin cleaves the IgG molecule below the hinge region, resulting in one Fc and one F(ab')<sub>2</sub> fragment. The F(ab')<sub>2</sub> fragment can be further split into two Fab' fragments, each containing 2 free thiol groups by reduction with a mild reducing agent, such as mercaptoethanol or dithiotreitol (DTT, Cleland's reagent). Since the two thiol groups are situated opposite the antigen binding domain, Fab' fragments are more suitable for site-directed immobilisation. For example, Jimbo and Saito have studied the immobilisation of Fab'-fragments to plasma-polymerised films using maleimide-activation<sup>212</sup>, while Ahluwalia et al. have coupled Fab'-fragments to Langmuir layers of dioctadecyl-N-methyl-N-(2-mercaptoethyl)-ammonium bromide via a disulphide link<sup>213</sup>. Recently, a new amphiphilic polymer, synthesised from a maleimide-containing diamine and pyromellitic dianhydride, has also been reported, especially intended for binding to Fab'-fragments<sup>214</sup>.

A particularly interesting Fab-fragment from the Brookhaven database (without the hinge region) is presented in Figure 3.2., showing a Fab-fragment against a synthetic peptide homologue of the C helix of myohemerythrin<sup>215</sup>. The disulphide groups are depicted in yellow and a surface plot is coloured according to side chain. It can also be observed that the antigen-binding site of the fragment includes a free cysteine residue. Other residues in the protein data bank did not usually show such a residue, but this indicates that for monoclonal antibodies the oriented immobilisation may fail when such a free cysteine is present in the hypervariable region of the antibody.

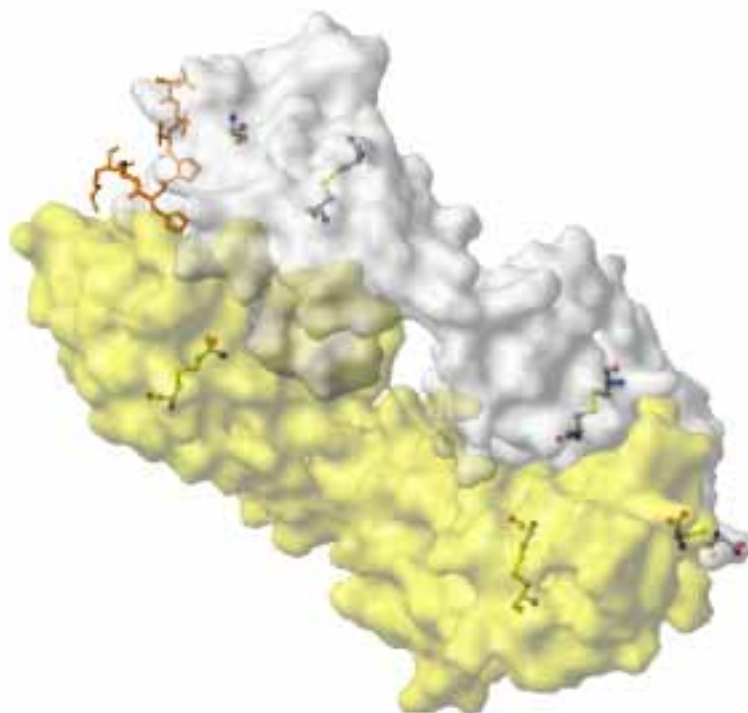


**Figure 3.2** *The Fab-fragment against a synthetic peptide, showing the distribution of the cysteine residues relative to the positions of the light chains (yellow), the heavy chains (grey) and the antigen (orange). (Brookhaven database entry 2IGF, Ref. 215)*

In the present chapter, the LB technique has been employed to more effectively control the orientation and surface density of antibodies. In earlier work, whole IgG molecules were spread directly onto the air-water interface<sup>216</sup> or passively adsorbed onto preformed monolayers<sup>217</sup>. Antibody fragments have also been used in LB films by Egger et al., who bound Fab' fragments first to liposomes and then fused the vesicles onto the air-water interface, a technique that is



experimentally rather tedious<sup>218</sup>. Herron et al. investigated the layer formation of an antibody Fab fragment at the air/water interface via an intermediate layer of streptavidin<sup>219</sup>, although they did not use the thiol chemistry for Fab' fragments, but linked an Fab fragment via an succinimidyl reagent to biotin.

A next step is to use single-chain antibodies, which are quite small and could be useful in immunosensors for the detection of small antigens (haptens). For instance, lipid-tagged single-chain antibodies have been incorporated into various lipid monolayers and the binding has been studied with SPR by Vikholm et al.<sup>220</sup>. In the present work, the direct covalent linking of antibody Fab' fragments to lipid monolayers has been pursued, particularly using maleimide-modified lipids. The motivations are the good reactivity and specificity of the maleimide for thiol groups and possibility for variation of the lipid constitution with the LB-film method.

### 3.3 Linker lipids

Linker lipids have been used extensively for covalent binding of biological compounds to lipids, particularly for conjugation of Fab'-fragments to enzymes or liposomes, for immunoassay and drug targeting applications<sup>221,224</sup>. The most practical linking groups, earlier developed for binding to thiol-groups of proteins, are the maleimide<sup>225</sup> or pyridyldithio<sup>226</sup> moieties, the latter enabling a reversible bond to be formed. Such groups can be easily introduced in phosphatidylethanolamine lipids. Polymerisation of lipids for stabilisation of the layers at interfaces has also been frequently discussed in the literature. Initially, diacetylene derivatives have been used, but such compounds are quite unstable<sup>227</sup>. The polymerised diacetylenes, however, are capable of transducing binding events directly into a colour change, by a "mechanochromic" mechanism<sup>228</sup>. Polymerisable lipids have been reported in which the polymerisation occurs either on the border of the hydrophilic/hydrophobic phase or in the hydrophobic phase<sup>229</sup>. Reversible cross-linking of lipids via thiol groups can also be used in which the reaction occurs either at the hydrophilic/hydrophobic border<sup>230,231</sup> or at the end of the hydrocarbon chain<sup>231</sup>. A particular interesting modification is that with lipoic acid, which introduces two thiol groups upon reduction<sup>232</sup>. The modification with thiol groups also enables self-

assembly on a range of metal surfaces. Here the thiol group is preferentially introduced at the hydrophilic terminus<sup>233,234</sup>.

In the present chapter a number of basic lipid linkers have been applied (Figure 3.3), including a polymerisable lipid linker with two linoleic acid ester chains. Viitala et al. has recently described the photopolymerisation of Langmuir and Langmuir-Blodgett films of linoleic acid<sup>235</sup> and the preparation of the linker lipid DLPE-EMCS and its Langmuir film properties has been recently described<sup>III</sup>. Condensed monolayers of linoleic acid can be formed by inclusion of a  $10^{-4}$  M concentration of  $\text{TbCl}_3$  in the subphase, while the DLPE-EMCS forms condensed layers in the presence of  $10 \mu\text{M}$  uranylacetate.

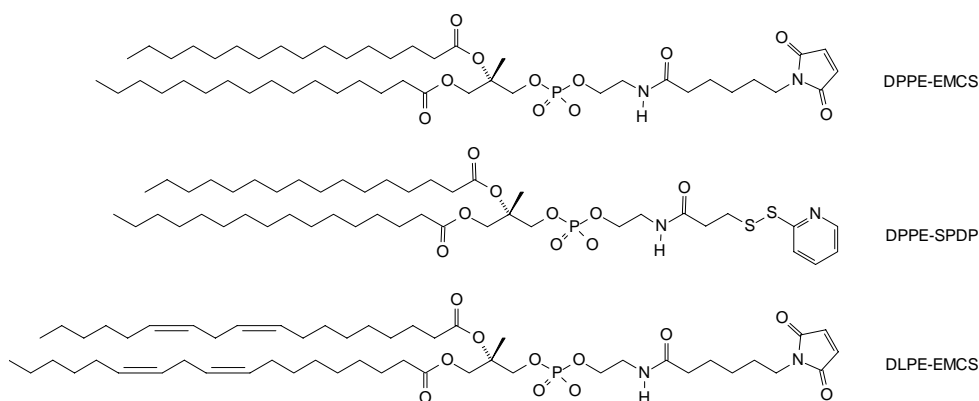


**Figure 3.3** Structures of linker lipids used in this study.

### 3.4 The Quartz Crystal Microbalance

The quartz crystal microbalance (QCM) device is a resonant quartz crystal of which changes in the resonant frequency takes place upon adsorption of material on the surface of the gold electrodes. The QCM has been used for detection of gasses and is presently very much used for the detection of interactions between surface bound receptors and analytes in solution. Recent reports have demonstrated the feasibility of QCM immunosensors for the detection of *Chlamydia Trachomatis*<sup>236</sup> and HIV<sup>240</sup>. The QCM can also be applied to study hydration of lipid layers, DNA hybridisation<sup>237</sup>, drug release and

electrodeposition<sup>238</sup>. For describing the mass-response of a QCM towards mass loading the Sauerbrey equation has been very much used<sup>239</sup>:

$$S = \frac{\delta f}{\delta m} = \frac{-2 \cdot f_0^2}{A \cdot \sqrt{\mu_q \rho_q}} \quad (3.4)$$

where  $S$  is the sensitivity of mass detection,  $\delta m$  is the mass change,  $\delta f$  is the observed shift in the frequency,  $f_0$  is the fundamental oscillation frequency of the crystal,  $\mu_q$  is the shear modulus of AT-cut quartz ( $2.947 \times 10^{10} \text{ kg m}^{-1} \text{ s}^{-2}$ ),  $\rho_q$  is the density of quartz ( $2648 \text{ kg m}^{-3}$ ) and  $A$  is the area of the gold electrode. Originally measurements were performed predominantly in air, because liquid loading causes severe quenching of the QCM oscillation. In aqueous solution the Sauerbrey equation is also not directly valid, because viscosity and elasticity effects of the layer and, moreover, embedded water in protein layers also may play an important role<sup>240,241</sup>. The quenching of the QCM can be circumvented by contacting the QCM only at one side with liquid (which causes less severe damping) and by applying frequency-dependent admittance analysis for determination of the resonant frequency<sup>242,243</sup>. There are different types of liquid load contributions to the measured frequency response, comprising a viscous and a mass-like contribution. In the case of a limited electrode area, which is clamped at the edges, there is also a compressional wave contribution. With adsorbing species the viscous component and the mass component both show their own characteristic changes. Tessier et al. have shown the relatively large contribution of the boundary viscosity change in the binding of erythrocytes to IgM, while the mass contribution dominated for binding of IgG to anti-IgG<sup>244</sup>. Furthermore, also other factors, such as bound water, have to be taken into account, which may give an increase in sensitivity. By comparison with radioassay, Muratsugu et al. have observed experimentally that the frequency change of the QCM is higher than can be expected from theory and that this ratio was higher for albumin than for IgG<sup>245</sup>.

## 3.5 Experimental

### 3.5.1 Materials

The heterobifunctional cross-linking agents N-succinimidyl ( $\epsilon$ -maleimido)-caproate (EMCS, >98%) and N-succinimidyl 3-(2-pyridyldithio)propionate (SPDP, >95%) were obtained from Fluka. Triethylamine (>98%) was obtained from Baker Chemicals. 1,2-dipalmitoyl-sn-glycero-3-phosphoethanolamine (DPPE, >99%) were purchased from Fluka, while 1,2-dilinoleoyl-sn-glycero-3-phosphoethanolamine (DLPE, >98%) was obtained from Avanti Polar Lipids. The host matrix lipid was predominantly 1,2-dipalmitoyl-sn-glycero-3-phosphatidylcholine (DPPC, Sigma >99) Cholesterol was from KSV Chemicals (purity >99.8%) or Fluka (>98%). These materials were all used as received.

Polystyrene tubes of Maxisorb type, were obtained from Nunc (Roskilde, Denmark). Common laboratory glass tubes of 1 cm internal diameter and 6 cm length were also employed for immobilisation on glass. 3-aminopropyltriethoxysilane (APTES, Sigma Prod. Nr. A-3648) and poly(Lysine.HBr, Phenylalanine) 1:1 copolymer (PPL, Sigma Prod. Nr. P-3150) were used as surface pretreatment agents for glass and polystyrene respectively.

The selected antibody model system, polyclonal goat anti-human IgG (anti-hIgG) and the corresponding F(ab')<sub>2</sub> fragment, were purchased from Jackson Immunoresearch (resp. Code Nr. 109-005-098 and 109-006-098) as a chromatographically purified antibody specific for the Fc $\gamma$ -part of human IgG with reduced cross-reactivity for bovine, horse and mouse serum proteins. The antigen, chromatographically purified human IgG (hIgG), was also from Jackson Immunoresearch (Code Nr. 009-000-003). For radiotracer studies a small amount of hIgG and anti-hIgG was labelled with <sup>125</sup>I, using Biobeads (Pierce, Rockford, USA). The F(ab')<sub>2</sub> was split into Fab'-fragments with dithiotreitol (DTT, Merck) prior to use<sup>221</sup>. F(ab')<sub>2</sub> with a concentration of 1.2-1.3 mg/ml (100 $\mu$ l) was mixed with 50  $\mu$ l HEPES/EDTA buffer (150 mM NaCl, 10 mM HEPES, 5 mM EDTA, pH=6.0) and 10  $\mu$ l of 0.1 M DTT solution in HEPES/EDTA buffer in a microdialysis tube. The dialysis tube was immersed in 250 ml argon-purged HEPES/EDTA buffer and dialysed for about 18 hours at

room temperature under argon. The Fab'-fragment preparation was kept under argon and used within a few days.

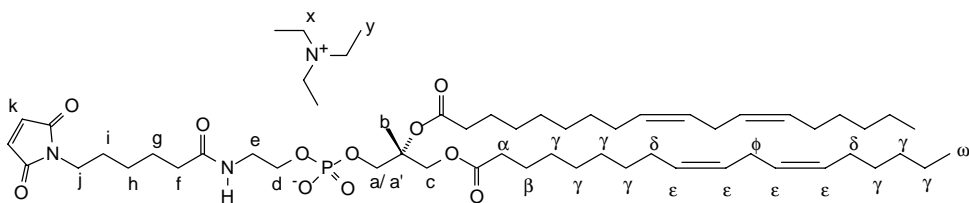
### 3.5.2 Preparation of linker lipids

The linker lipid conjugates DPPE-SPDP and DPPE-EMCS were prepared according to an established procedure<sup>222</sup>. The lipid conjugate was purified by chromatography on silica gel (Si 60) using mixtures of chloroform with increasing amounts of methanol.

The final products were fully characterised with 600 MHz <sup>1</sup>H-NMR spectroscopy. DLPE-EMCS was prepared by similar methods, but the whole procedure, including chromatography was conducted under Argon. The assignments of the protons in DLPE-EMCS, which was produced as a triethylamine salt are given in Table 3.1. The assignments were also made with the help of the <sup>1</sup>H-<sup>1</sup>H COSY spectrum. The electrospray mass spectrum displayed a main peak at 931.55 AU, which corresponded to the exact mass of the compound.

**Table 3.1** Measured NMR parameters (600 MHz, CDCl<sub>3</sub>) for the protons in DLPE-EMCS.

$\delta$ (ppm)	multiplicity	J (Hz)	Amount of protons, assignment
0.90	triplet	6.5	6, $\omega$
1.30	broad multiplet		42, h+y+ $\gamma$
1.60	multiplet		6, g + $\beta$
1.65	broad quartet	7.5	2, i
2.05	broad quartet	7.0	8, $\delta$
2.20	triplet	7.0	2, f
2.30	broad multiplet	7.0	4, $\alpha$
2,77	triplet	7.0	4, $\phi$
3.09	quartet	7.0	6, x
3.45	broad triplet	7.0	2, e
3.50	triplet	7.0	2, j
3.97	broad multiplet		4, c + d
4.16	broad double doublet		1, a'
4.38	broad double doublet		1, a
5.22	broad double doublet		1, b
5.33-5.39	multiplet		8, $\epsilon$
6.69	singlet		2, k
7.23	broad singlet		1, CONH



### 3.5.3 LB-film formation

The lipids were generally dissolved in chloroform at a concentration of 1 mg/ml. DLPE and DLPE-EMCS were kept under argon and stored protected from light at 4°C. Monolayers of lipids were prepared in a home-made Teflon trough with dimensions of 50 x 200 x 10 mm using further a commercial LB-instrument (KSV 2000 LB, Finland). The host matrix lipids 1,2-dipalmitoyl-sn-glycero-3-phosphatidylcholine (DPPC, Sigma >99 %) and cholesterol (KSV Chemicals 99.8%) were mixed in various ratios with linker lipid and spread onto an aqueous subphase of 10 mM HEPES, 150 mM NaCl at pH=6.8 for DPPE-EMCS and pH=7.2 for DPPE-SPDP. DLPE-EMCS was spread in a matrix with DLPE, using a 10% molar density in the monolayer. Isotherms of DLPE and DLPE-EMCS were recorded on three different subphases: (1) pure water, (2) 0.9% NaCl, 20 mM HEPES, pH=6.8 and (3) 0.9% NaCl, 20 mM HEPES, 10 µM Uranylacetate, pH=6.8.

UV-irradiation of the monolayers of DLPE/DLPE-EMCS was carried out with a low-pressure mercury lamp with a power of 30 W. The maximum emission of the lamp was at 254 nm. The UV-radiation was performed at a constant surface pressure of 25 mN/m

### 3.5.4 Quartz Crystal Microbalance measurements

The resonators used in this study were 10 MHz AT-cut quartz crystals with gold electrodes (Universal Sensors, Inc., New Orleans). The quartz plate diameter was 14 mm and the gold electrode diameter 8 mm. The edges of the resonators were covered with a ring of silicone rubber (Dow Corning Corporation). The silicone rubber prevented corrosion of the wires and degradation of the electrical contacts when submersed in solution<sup>IV</sup>. Furthermore, the silicone rubber improved the stability of the device threefold to a noise level of 0.45 Hz in one-sided contact with water. The gold electrode was generally cleaned with chromosulphuric acid, rinsed with water and air dried before measurement. With this procedure the same crystal could be used many times. The precision of the measuring set-up was very high. Surface mass densities of the deposited film could be determined with an error less than 1 ng/cm<sup>2</sup> using the Sauerbrey equation. A Hewlett-Packard 4195A spectrum/network analyser connected to a computer was used to gather the near resonance admittance phase spectra with a

sample time of one minute. The system automatically traced the approximate resonant frequency and adjusted a frequency range to 200 Hz around this frequency. Hereafter the spectrum was rapidly sampled ten times. A mean value of the samples was taken and a linear regression estimate for the resonant frequency was calculated.

For *in situ* measurements with the QCM, the monolayer containing the linker lipid was compressed to a surface pressure of 40 mN/m and one side of the QCM was lowered to make horizontal contact with the monolayer as depicted in Figure 3.4.

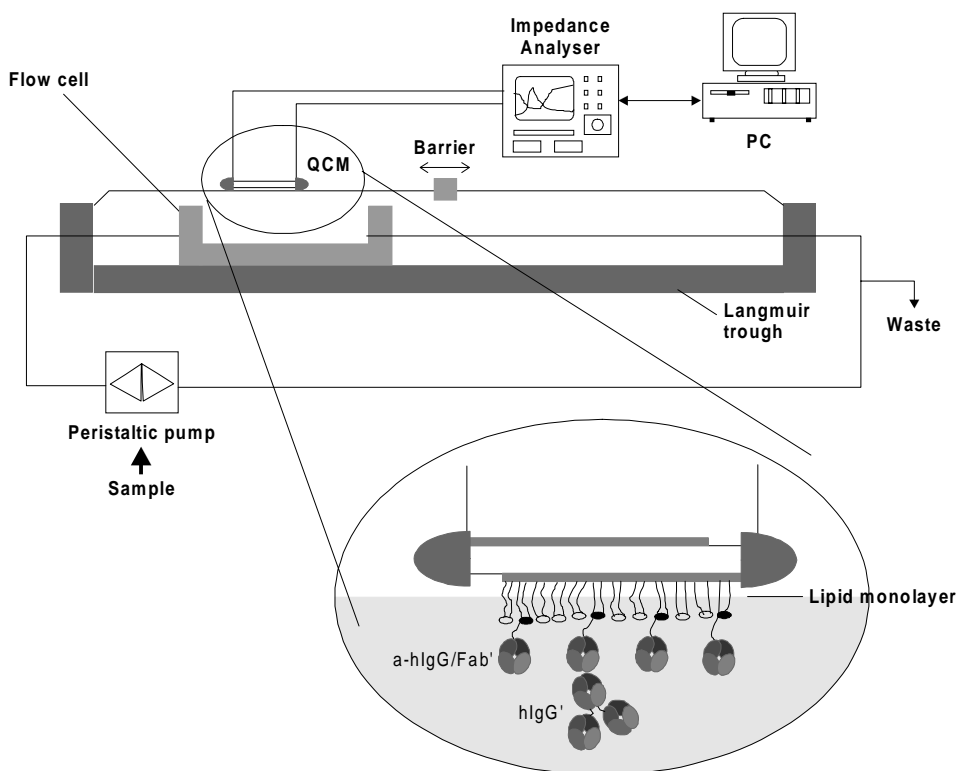


**Figure 3.4** The measuring set-up for performing *in situ* measurements with the QCM of a Langmuir film.



HEPES/EDTA was flushed through a teflon cell placed beneath the monolayer for about three minutes by the means of a peristaltic pump. This allowed a homogeneous and reproducible mixing of the solution. The phase angle shift was recorded until a steady value was obtained. An initial increase in frequency was noticed due to disturbances caused by the peristaltic pump. The antibody stock solution was hereafter introduced beneath the monolayer, followed by 100 µg/ml BSA to block non-specific binding sites and by various concentrations of human IgG. The frequency changes due to the binding of protein were monitored as a function of time for half an hour. At the end of each measuring series the QCM was raised from the air-water interface, rinsed with water and air dried. These  $\Delta F$  values were compared with those obtained in liquid.

### **3.5.5 Surface Plasmon Resonance measurements**

SPR measurements (such as depicted in Fig. 3.1) were performed with equipment as described by Lekkala & Sadowski (Fig. 3.5)<sup>211</sup>. The set-up is based on the Kretschmann configuration, which uses p-polarised light (here from a He-Ne laser at 632.8 nm) in conjunction with a glass prism ( $n= 1.5151$ ) to couple light into a thin gold film<sup>246</sup>. The intensity of the light is measured as a function of time at the particular angle where light is partly in resonance. Very small changes in light levels can be measured by using two lock-in amplifiers to monitor (at two different chopping frequencies) light from the laser (reference beam) and from the prism (sample beam). Although in this case the dynamic range of SPR detection is limited, the method is particularly suited for measurements in liquid, where the resonance peak (vs. incidence angle) is rather broad.

Glass slides with a gold layer of 36.6 nm thickness and an intermediate layer of titanium of 4 nm thickness were used for the SPR measurements. The slides were coated with ODM from a 1 mM solution in ethanol as described in the previous chapter. The LB-film was usually deposited onto the ODM-coated gold surface by horizontal transfer (Langmuir-Schäfer method) and the slide was hereafter contacted with the prism using index-matching oil (Merck). A liquid cell was then placed over the measurement area and filled with buffer solution. The different protein solutions were then injected in FIA mode, which enabled the relative amounts of protein to be measured (not absolute amounts). The

immobilisation efficiency was then deduced from the relative responses of Fab' and h-IgG antigen.

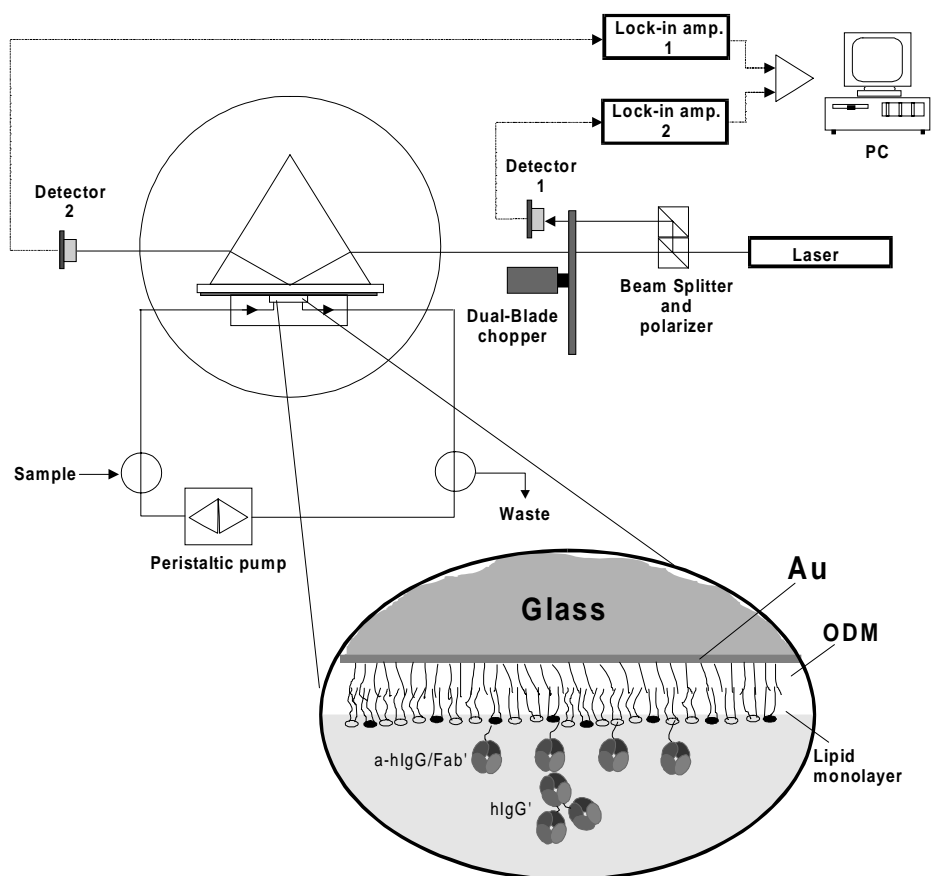


**Figure 3.5** *The SPR set-up used in the present study.*

### 3.5.6 Radiometric assay

Silicon substrates with dimensions of  $6 \times 9 \text{ mm}^2$  were peroxide treated to generate a maximum amount of silanol groups on the surface. The slides were first immersed in a solution containing 30%  $\text{H}_2\text{O}_2$ , 25% ammonia and water in the volumetric ratio 1:1:5 and heated to  $80^\circ\text{C}$  for 1-2 hours. The slides were then

rinsed with water and immersed in a solution containing 30% H<sub>2</sub>O<sub>2</sub>, concentrated hydrochloric acid and water in the volumetric ratio 1:1:5. The slides were heated again to 70-80 °C for 1-2 hours, rinsed with water and subsequently coated with octadecyltrichlorosilane (ODTCS, Aldrich 95%) from toluene solution. The slides were finally rinsed with toluene and air dried.

The Langmuir layers of lipids were then transferred onto these supports with the Langmuir-Schäfer method<sup>IV</sup>. Anti-human Fab' (50 µg/ml of Fab' in HEPES buffer pH=6.8) was subsequently bound to the layers in 2 hours at room temperature using a thin film reaction chamber with a volume of 30 µl. The slides were hereafter transferred to PBS buffer (0.15 M NaCl, 10 mM KH<sub>2</sub>PO<sub>4</sub> pH=7.5) containing 0.5 g/l BSA (bovine serum albumin, Sigma RIA grade) and left in this solution at 4 °C for 18 hours. Series of silicon slides were then incubated in a microtiter plate with increasing standardised amounts of human IgG in the presence of a constant amount of <sup>125</sup>I-labelled human IgG and BSA (3.3-5.0 g/l). The bound amount of Fab' was assessed by a standardised radiotracer method, using <sup>125</sup>I-labelled Fab'. The radiolabelled Fab' had gone simultaneously through all other process steps (dilution and F(ab')<sub>2</sub> splitting) in the same way as the unlabelled Fab', to insure that the label was similar in chemical reactivity.

Antibodies were also bound to polystyrene (Nunc Maxisorb) by two methods: by passive adsorption and by covalent linking via the amphiphilic polyaminoacid Poly(phenylalanine, Lysine.HCl) (PPL), the latter as described by Wood & Gadow<sup>247</sup>. The amino groups were then activated with EMCS before binding to Fab'. Fab' was also bound to glass tubes activated with APTES. The aminosilane was deposited from toluene as described in the literature<sup>248</sup>.

### 3.5.7 Atomic Force Microscopy

A Nanoscope II (Digital instruments, Inc., Santa Barbara, CA) AFM was used for imaging the sample surfaces in air in contact mode. Usually an area of  $1.012 \times 1.012 \mu\text{m}^2$  was scanned with standard Nanoprobe silicon nitride cantilevers with a force constant of 0.06 N/m. The samples were prepared by horizontal transfer of the monolayers of linker lipids onto ODTCS-modified silicon slides. Part of the slides was kept in a solution of Fab'-fragments for two hours, followed by 18 hours in BSA and human IgG for 2 hours. Slides were gathered from every coating step, rinsed with high-purity water and air dried. The slides were kept dry until the AFM imaging was performed.

## 3.6 Results and discussion

### 3.6.1 Film formation

DPPC displays a surface pressure - area ( $\pi$ -A) curve characteristic for saturated phospholipids transforming from the liquid expanded to the condensed phase below 5 mN/m. The phase transition, however, became less pronounced when 10 mol% of the linker lipids were included in the layer, indicating that the linking groups were oriented in a different way in the DPPC monolayer matrix. DPPC/DPPE-SPDP displayed a much higher surface area than DPPC/DPPE-EMCS. The mean molecular area of DPPE-EMCS was about 103 Å<sup>2</sup> at a surface pressure of 40 mN/m, whereas that of DPPE-SPDP is twice this value, 211 Å<sup>2</sup>. The linking groups thus have a different orientation in the DPPC monolayer matrix<sup>V</sup>.

The condensing effect of Cholesterol on the monolayers of DPPC with lipid linkers was also investigated<sup>V</sup>, as this has been demonstrated with vesicles<sup>249</sup>, black lipid membranes<sup>28,36,250</sup> and self-assembled monolayers<sup>251</sup> of DPPC. The mean molecular area of cholesterol was measured to be 35.6 Å<sup>2</sup>. Maximal condensation occurs usually at about 15 mol% cholesterol. DPPC/DPPE-EMCS exhibits a phase transition around 35 mN/m if only 10 mol% cholesterol was included in the layer. DPPE-EMCS is probably squeezed out of the layer at this surface pressure as the collapse pressure of the pure linker occurs around 35 mN/m. At about 30 mol% the mean molecular area of the two linker molecules became equal. The DPPE-EMCS and DPPE-SPDP displayed similar  $\pi$  - A curves when 50 mole percent cholesterol was included in the monolayer. The stability of the DPPC/linker/cholesterol monolayers was assessed by compressing the monolayers to a surface pressure of 40 mN/m and measuring the molecular area versus time. Concave relaxation curves were observed, due to a reorganisation of molecules and a partial dissolution into the subphase. The relaxation was minor after 40 minutes and was dependent on the linker molecule. The relaxation decreased in the order of DPPC/DPPE-SPDP < DPPC/DPPE-EMCS < DPPC.

DLPE-EMCS films could be formed at pure water and buffer subphases<sup>III</sup>. DLPE-EMCS showed a larger molecular area at moderate (30 mN/m) surface

pressure as DLPE, possibly due to the increased electrostatic interactions between the phosphate groups. The introduction of 10 mM Uranyl acetate in the subphase gave a relatively higher degree of condensation for DLPE-EMCS as for DLPE. The final molecular area's in the condensed layers were  $76 \text{ \AA}^2$  for DLPE-EMCS and  $58 \text{ \AA}^2$  for DLPE. A mixed monolayer of DLPE-EMCS and DLPE in a molar ratio of 1:9 was used in the polymerisation experiments. The layer could be polymerised best in the presence of Uranyl acetate. At the constant surface pressure of 25 mN/m the monolayer first showed a quick, but small expansion followed by a contraction during 2.5 minutes. The layer then expanded again, attaining a stable value after 30 minutes.

### **3.6.2 Fab' binding and activity.**

The QCM frequency changes, during the immobilisation of antibody fragments onto a monolayer of DPPC/DPPE-EMCS from 10  $\mu\text{g/ml}$  and 25  $\mu\text{g/ml}$  Fab'-fragment solutions and a 25  $\mu\text{g/ml}$  F(ab')<sub>2</sub> solution, are shown in Fig. 3.6. No change in frequency was observed when F(ab')<sub>2</sub>-fragments were pumped into the cell beneath the monolayer, but with the Fab' fragments a binding reaction occurred. This indicates that the basic chemistry for Fab'-attachment to maleimide works as expected. The initial increase in frequency was caused by pumping of the buffer. Binding equilibrium was achieved within about 15-30 min.

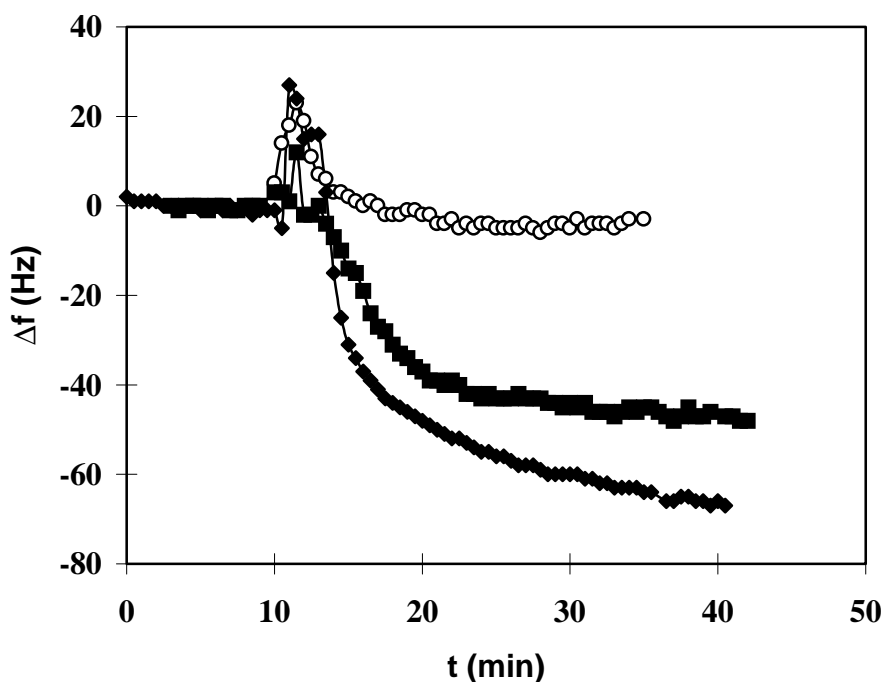


**Figure 3.6** The change in resonant frequency upon binding of  $F(ab')_2$  and  $Fab'$ . 25  $\mu\text{g/ml}$  (O)  $F(ab)_2$ , 10  $\mu\text{g/ml}$  (■) and 25  $\mu\text{g/ml}$  (◆)  $Fab'$ -fragments to a monolayer of DPPC/DPPE-EMCS (molar ratio 9:1).

The subsequent non-specific binding of BSA and specific binding of hIgG as a function of  $Fab'$ -fragment concentration is shown in Figure 3.7. A frequency response of 25 Hz was observed for BSA when no  $Fab'$ -fragments were attached to the layer. The amount of non-specific BSA adsorption then first decreased with  $Fab'$ -fragment concentration, reaching a minimum at about 15  $\mu\text{g/ml}$ , and then increased as the  $Fab'$ -concentration exceeded the 25  $\mu\text{g/ml}$  saturation value. At 50  $\mu\text{g/ml}$  a maximum of BSA adsorption was reached, after which the non-specific binding again dropped. The minimum in BSA binding is probably caused by the formation of a sufficiently dense monolayer of  $Fab'$ , which prevents BSA adsorption.

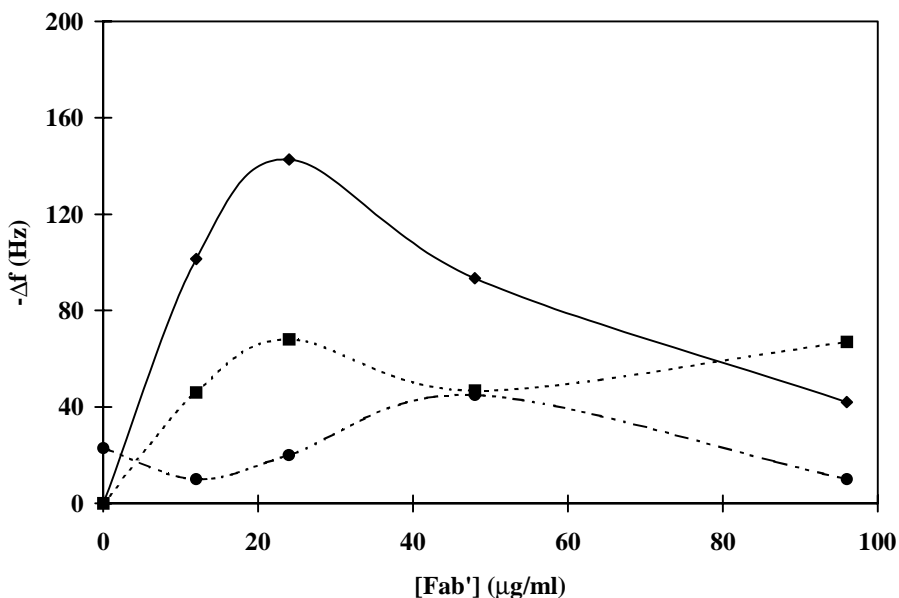


**Figure 3.7** The total change in frequency upon binding of Fab'-fragments. (■), 0.1 mg/ml BSA (●) and 0.1 mg/ml human IgG (◆) to a monolayer of DPPC/DPPE-EMCS (ratio 9:1) vs. Fab'-fragment concentration. (data points are averages,  $n=2-3$ ,  $CV=16,5\%$ )

The maximum of BSA adsorption at higher Fab'-concentration is likely the result of adsorption to an imperfect multilayer of Fab' in which BSA can yet again fill up space between the Fab' molecules. The binding of antigen, h-IgG, was also a function of Fab'-concentration, as can be observed from Figure 3.7 and Figure 3.8. A maximum binding of IgG was obtained at a Fab' concentration of 24 μg/ml, at which the non-specific binding of BSA represented about 10% of the specific binding. Fab'-fragment concentrations exceeding 24 μg/ml lead to a lower binding of h-IgG, indicating the existence of steric hindrance.



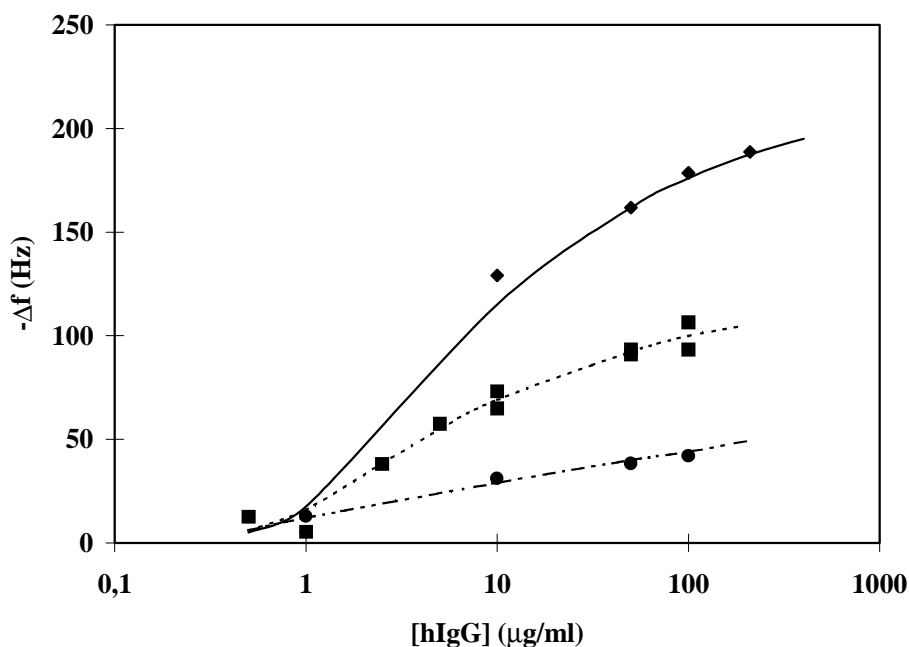


**Figure 3.8.** The change in frequency upon binding of human IgG to Fab'-fragments bound to a monolayer of DPPC/DPPE-EMCS using a 12 μg/ml (■), 24 μg/ml (◆), and 96 μg/ml (●) concentration of Fab'-fragments. (n=1-2, CV=15%).

The efficiency of the Fab'-fragment to bind h-IgG could be calculated from the frequency response of the QCM as a function of the Fab'-fragment concentration (Fig. 3.9). A maximum efficiency of 67% IgG binding to Fab' could be attained at low Fab' concentration, but the efficiency decreased with higher Fab' concentration. This indicates that Fab'-fragments may become too closely packed for effective binding to IgG when bound from too high concentrations. Steric hindrance is a plausible effect when considering that the Fab' is much smaller than IgG.

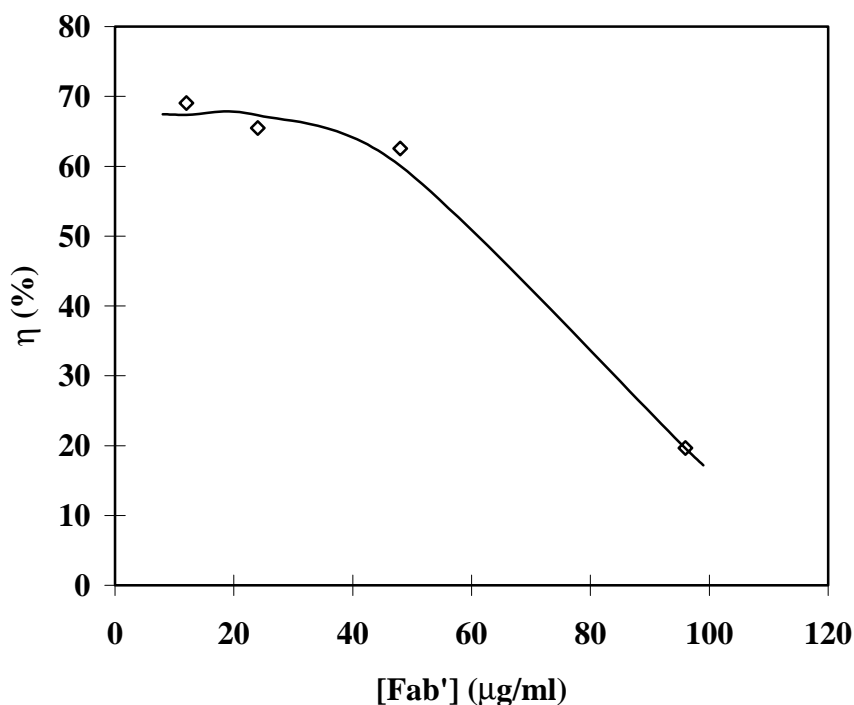


**Figure 3.9.** The binding efficiency of Fab'-fragments attached to a monolayer of DPPC/DPPE-EMCS in binding to human IgG. ( $n=2-3$ ,  $CV=5\%$ ).

BSA and human IgG could be washed off from the Fab' monolayer with a cleaning solution of glycine/HCl at  $pH=2.5$ . Only the Fab'-layer remained, indicating that a covalent bond between the lipid and the Fab' had been formed. The antibodies, however, lost their IgG binding activity, when treated with this regeneration solution.

### 3.6.3 Monolayer matrix effects

The composition of the monolayer matrix and the influence on the Fab' immobilisation efficiency was also studied. A first important modifier was cholesterol (CHOL), since the response appeared to be very dependent on the amount of cholesterol in the lipid film and it is known that cholesterol stabilises lipid bilayers, as discussed earlier.

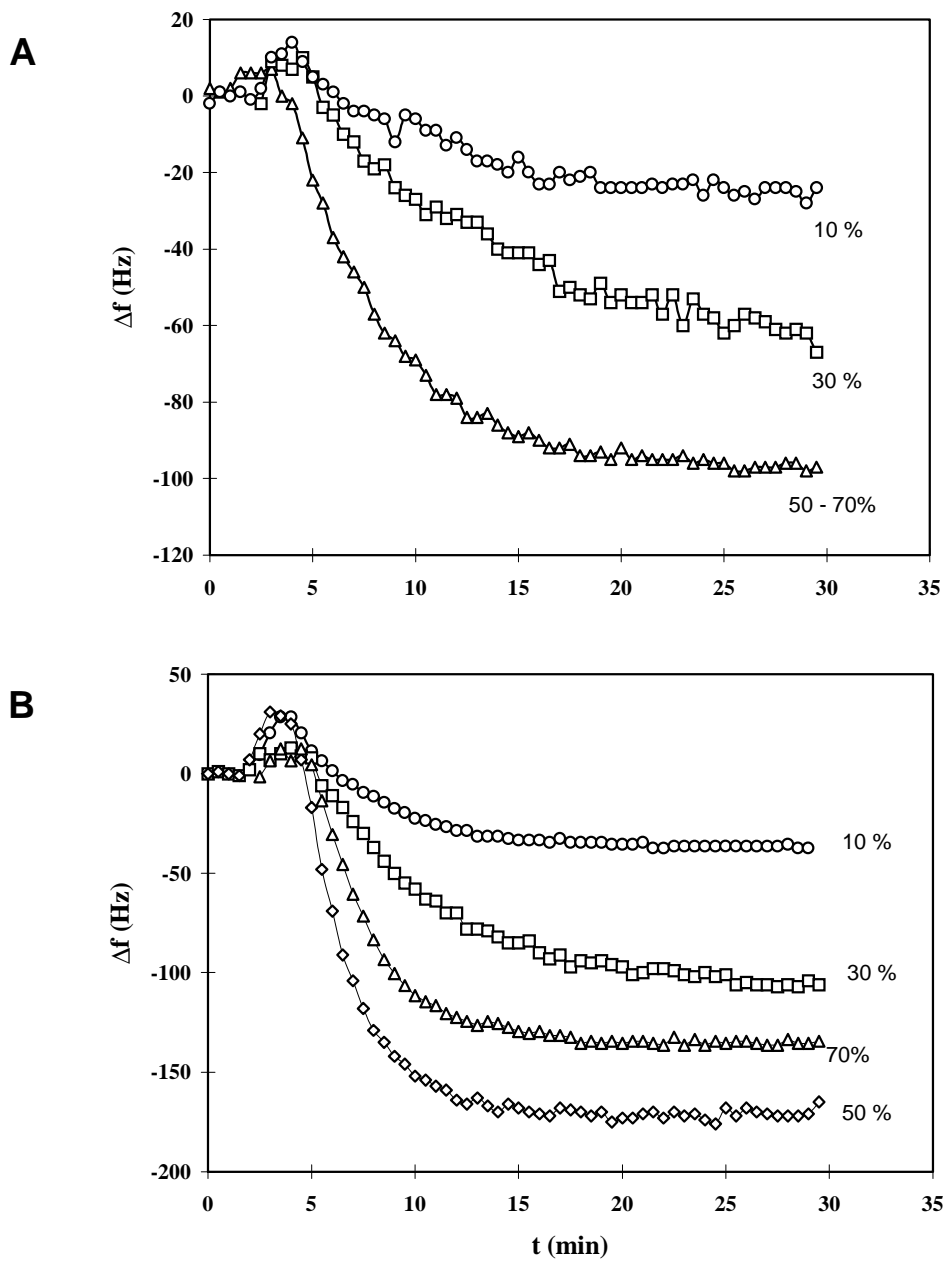


**Figure 3.10** The change in frequency upon binding of (A) Fab'-fragments and (B) the subsequent binding of human IgG to a monolayer of DPPC/Chol/DPPE-EMCS.

Figure 3.10.A shows the change in resonant frequency upon binding of Fab' (form 25  $\mu\text{g/ml}$ ) onto monolayers of DPPC/DPPE-EMCS with cholesterol added at different concentrations in the film. Binding equilibrium was obtained within about 10–15 minutes, which is slightly faster compared to the DPPC/DPPE-EMCS monolayer. There was a low binding of Fab'-fragments to the layer containing 10 mol% cholesterol. In this case, the non-specific binding of BSA to the layer gave a frequency change of 15 Hz and the subsequent interaction with IgG was very low (Fig. 3.10.B). An increase in the binding of Fab'-fragments was observed for cholesterol concentrations exceeding 10 mol% (Fig. 3.10.A). A saturation value of 95 Hz was reached at 50 mol% cholesterol. The highest binding efficiency for h-IgG was observed at this molar ratio (Fig. 3.11).

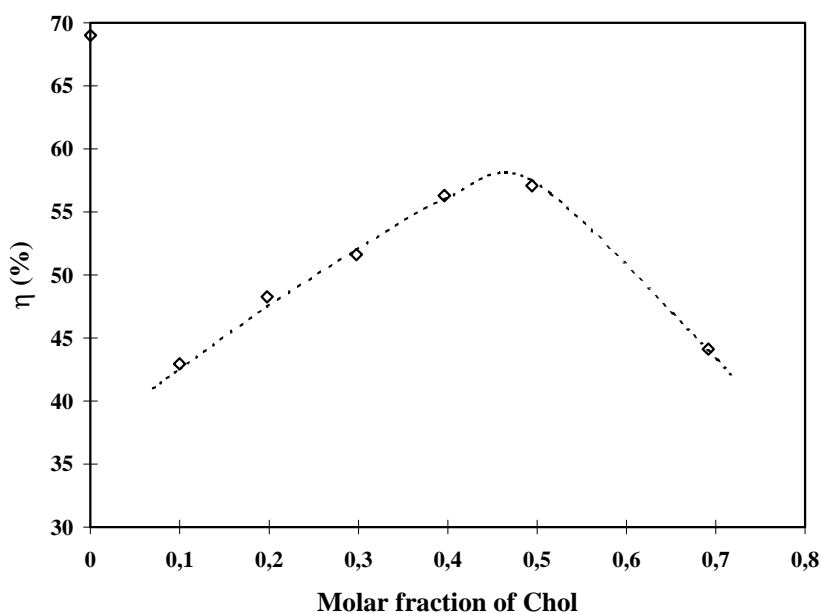


**Figure 3.11.** *The binding efficiency of the Fab'-fragments bound to a monolayer of DPPC/Chol/DPPE-EMCS to human IgG. (n=1)*

The binding of Fab'-fragments to DPPE-SPDP was also investigated. The frequency response associated with Fab'-binding to a DPPE-SPDP-containing lipid layer with 50% cholesterol was much smaller as that of a lipid layer with DPPE-EMCS. In the QCM measurements, the efficiency of the Fab'-fragments to bind IgG was still quite high: about 51 %. If cholesterol was not included in

the layer, the attachment of Fab'-fragments was very low and the binding efficiency for antigen was below 5%. It could be observed from the film-formation isotherm that the molecular area of DPPE-SPDP is about twice as that for DPPE-EMCS. It is quite probable that the SPDP-group had an unfavourable orientation, e.g. with the disulphide directly attached to the gold surface.

### 3.6.4 Operation of the QCM

As discussed in the introductory paragraph, the operation of the QCM in liquid still remains poorly understood in the cases where direct measurements in liquid are involved, although the theory has been well-reviewed<sup>240</sup>. Sauerbrey's equation cannot necessarily be directly applied in this case. The difference between liquid and air measurements appears to be dependent on the type of protein. Geddes et al. obtained a liquid to air ratio of about 2.5 and 3.6 for monolayers of IgG and antibodies, respectively<sup>252</sup>. This amplification of the QCM response might be due to viscoelasticity changes occurring in the layer, slipping or entrapped water molecules. In order to evaluate the difference between liquid and air measurements, the total change in frequency after binding of Fab'-fragments, BSA and human IgG to monolayers of DPPC/DPPE-EMCS was monitored in air and in liquid. (The mass change of the lipid layer was here reduced from the responses in air, because the frequency shift caused by the lipid layer was not measured in the liquid experiments.) The QCM response in air attained a saturation value of 88 Hz at a Fab'-fragment concentration of 25 µg/ml, whereas that in liquid had a maximum at this concentration and then decreased (Fig. 3.12.A). The frequency shift in air corresponded to a surface density of 192 ng/cm<sup>2</sup>.

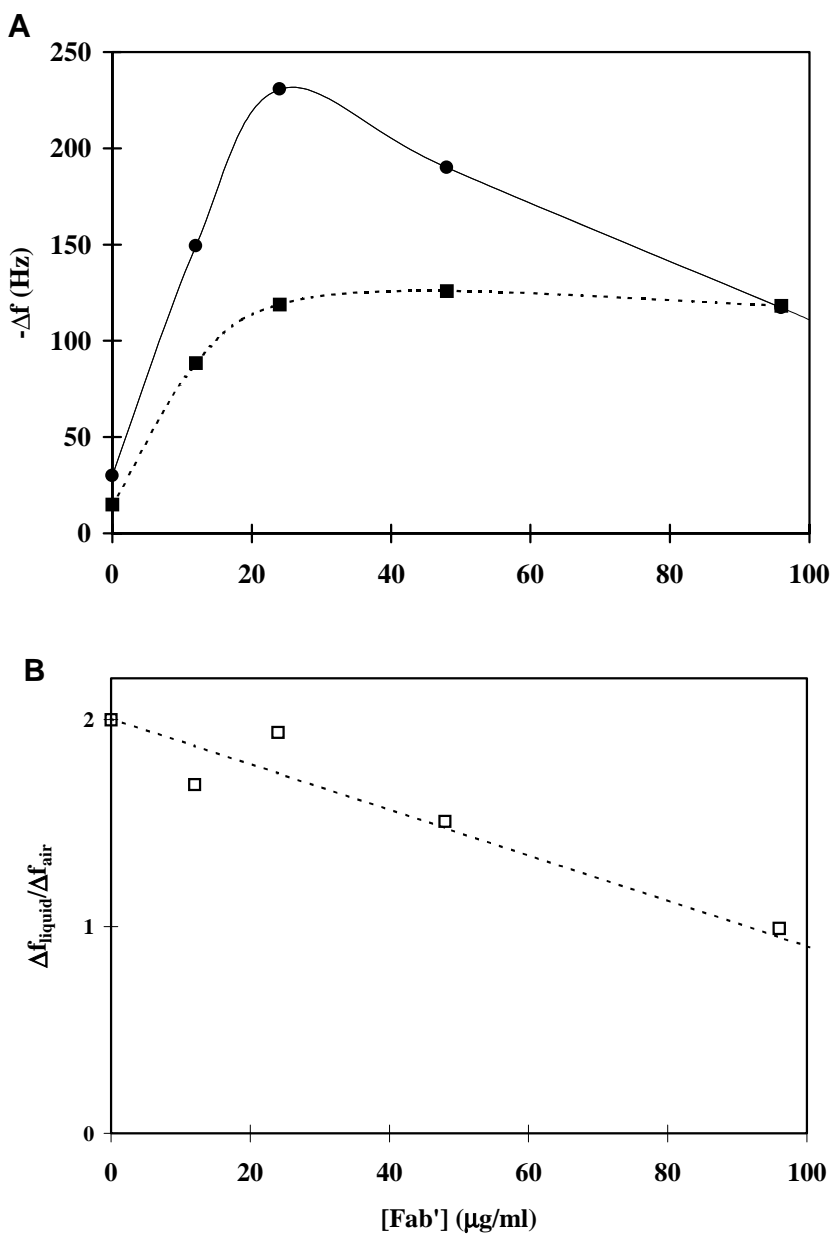


**Figure 3.12** (A) The total change in frequency in liquid (-●-) and air (·■·) after binding of Fab'-fragments, 0.1 mg/ml BSA and 0.1 mg/ml human IgG to a monolayer of DPPC/DPPE-EMCS vs. Fab'-fragment concentration ( $n=2-3$ ,  $CV=16.5\%$ ) and (B) the ratio between liquid and air measurements. ( $n=2-3$ ,  $CV=25\%$ ).

The ratio between liquid and air measurements decreased linearly with Fab'-fragment concentration and approached unity at higher concentrations (Fig. 3.12.B). The frequency shift in liquid was probably due to an increased contribution from changes in viscoelasticity and/or surface bound water quite close to the QCM surface in the first Fab' monolayer.

Additionally, the difference in response from the QCM and radioassay measurements was investigated, while radioassay was also used to compare the present immobilisation system with a number of more conventional coupling methods. As an example, some radioassay binding curves for the PPL method are given in Figure 3.13. Here the Fab' gives a much higher response as the F(ab')<sub>2</sub>, although the binding of F(ab')<sub>2</sub> is still quite high, indicating that some degree of non-specific adsorptive attachment to the polystyrene surface still occurred. It was also observed that a higher concentration increases the binding capacity. Figure 3.14 gives the binding curves of the lipid layers with different matrices. The radioassay results for the lipid matrices have, unfortunately, a lower reproducibility as those of the PPL method. These differences are likely caused by the multiple washing steps involved in the radioassay method.

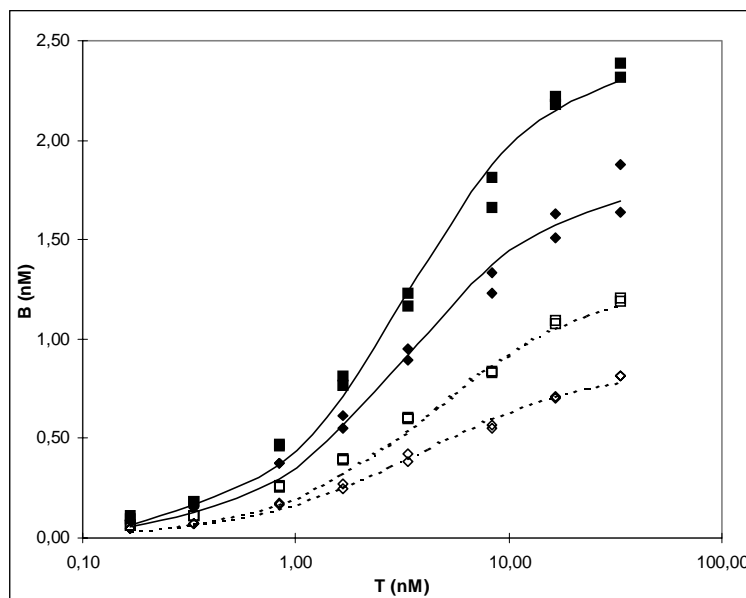


**Figure 3.13.** Binding curves of Fab' and F(ab')<sub>2</sub> to derivatised polystyrene via PPL and EMCS. Antibody concentration 5 µg/ml (◆) and 20 µg/ml (■), using either F(ab')<sub>2</sub> (----) or Fab' (——).

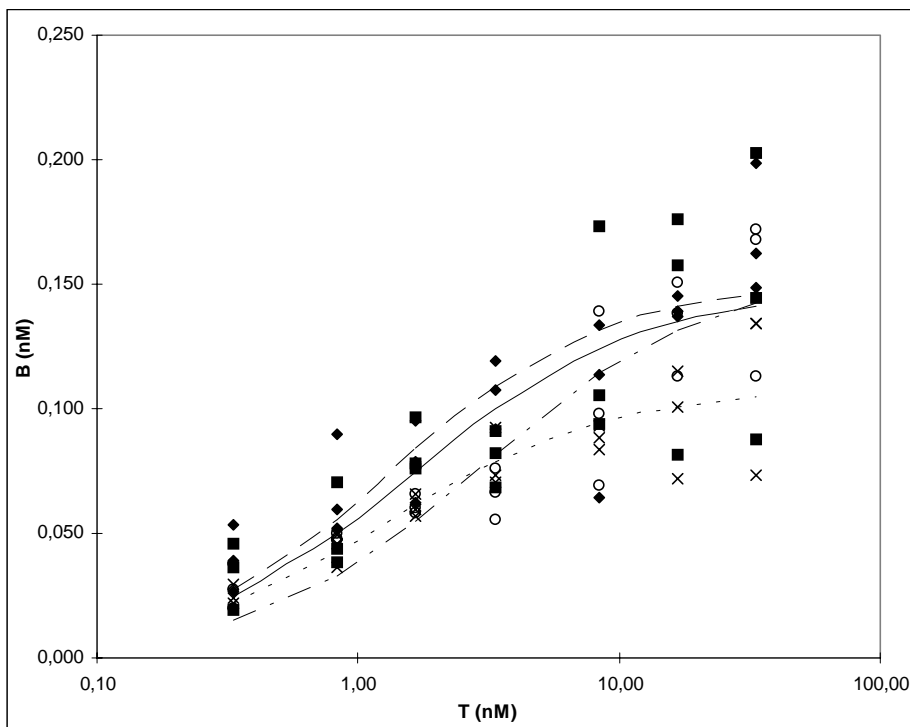


**Figure 3.14.** Binding curves of Fab' to various linker lipid films. (—■—) DPPE-EMCS/DPPC (1:9), (----◆----)DPPE-EMCS/DPPC/CHOL (1:4:5), (···x···) DPPE-SPDP/DPPC (1:9) (—·O·—), DPPE-SPDP/DPPC/CHOL (1:4:5)

In the RIA data (Table 3.2) it was observed that adsorption of  $F(ab')_2$  to polystyrene gave improved recovery of binding sites and a higher affinity in comparison to adsorption of the whole antibody. In fact, the binding affinity ( $K_a$ ) was in general highest for adsorption of  $F(ab')_2$  to polystyrene. The affinity constant for the whole antibody, adsorbed to polystyrene was lowest, while the lipid matrices gave values intermediate to these. The immobilisation efficiency of the antibodies in terms of recovered binding sites was, however, much higher with the lipid films. The highest recoveries were observed for films without cholesterol (60–70%), while these with cholesterol were already much lower (20–25%). The efficiency with adsorption to polystyrene was lowest (3–10%). The incorporation of cholesterol seems to lead to much higher densities of binding sites, but increases the total density of Fab' relatively more, such that the efficiency drops from a 70% to a 23% level. The Fab's are probably more non-



specifically adsorbed to monolayers with CHOL. A surface density of 47 ng.cm<sup>-2</sup> has been reported Fab' attached to maleimide linkers on a plasma polymerised surface<sup>212</sup>, which agrees with the RIA measurements. The total density of bound Fab'-fragments ( $\Gamma_{\text{tot}} = \Theta_{\text{tot}}/A$ , with  $A = 0.45 \text{ cm}^2$ ) and antigen from RIA correlate with those obtained from the QCM measurements, if it is taken into account that the QCM measurements were performed in the aqueous phase, while RIA measurements are based on gravimetric and spectroscopic assessments of the protein concentration, which only reflect the dry weight of the protein. If the liquid to air ratio of the QCM measurements are taken into account, the density of Fab'-fragments attached to the DPPE-EMCS layers with and without cholesterol as measured with RIA are still a factor of 2 lower than those obtained from QCM. The QCM and RIA measurements differ much for DPPC/DPPE-SPDP but agree for DPPC/DPPE-SPDP/CHOL. This may be due to a difference in binding efficiency of Fab'-fragments to transferred DPPC/DPPE-SPDP layers compared to the binding at the monolayer-air interface. In this case the SPDP moiety likely rearranged to bind to the gold surface directly, since the gold surface in the QCM measurements was not alkyl-silane coated and the DPPC/DPPE-SPDP film had a much less condensed state as the DPPC/CHOL/DPPE-SPDP film at the used pressure during transfer.

With respect to the other systems in Table 3.2, it could be observed that the direct attachment to glass via maleimide-activated APTES gave reasonably high binding capacities, but a relatively low affinity constant. In the preliminary measurements with the mixed monolayer of DLPE/DLPE-EMCS a very low affinity and capacity was observed and polymerisation of the mixed monolayer even further deteriorated the results. This is probably due to the matrix lipid DLPE, which could be replaced by the phosphatidylcholine derivative (DLPC), or due to an unfavourable degree of polymerization.

**Table 3.2** Comparison of immobilisation system performance with radioassay (RIA), QCM and SPR.

	RIA					QCM			SPR
	$K_a$	$Q_a$	$\Theta_a$	$\Theta_{tot}$	$\eta_a$	$\Gamma_a$	$\Gamma_{tot}$	$\eta_a$	$\eta_a$
PS/IgG	0.24	0.20	4.5	145	3.1				
PS/F(ab') <sub>2</sub>	0.87	0.44	6.3	65	9.6				
PS/PPL-EMCS-Fab'	0.25	2.67	36.7	468	7.8				
PS/PPL-EMCS/F(ab') <sub>2</sub>	0.25	1.33	18.3	292	6.3				
Glass/APTES-EMCS	0.32	1.56	21.5						
DPPC+DPPE-EMCS	0.65	0.15	6.6	11.1	60	99	148	67	66
DPPC+DPPE-EMCS+Chol	0.78	0.15	6.8	28.3	24	118	219	57	36
DPPC+DPPE-SPDP	0.81	0.11	4.9	6.8	71	2	42	4	
DPPC+DPPE-SPDP+Chol	0.34	0.16	7.0	31.8	22	31	61	50	
DLPE+DLPE-EMCS	0.27	0.095	1.32	85.6	1.5				
DLPE+DLPE-EMCS polym.	0.17	0.072	0.99	85.8	1.2				

### 3.6.5 Detection limits for QCM response of hIgG

The sensitivity of detection (initial slope of the response curves) and the detection limits were assessed from a number of measurements, determining the effect of the Fab-concentration with the DPPC/DPPE-EMCS (9:1) films and the effect of increasing the cholesterol in the film (Table 3.3). The highest sensitivity and lowest detection limit could be obtained with 24  $\mu\text{g/ml}$  Fab'-concentration, lowering the detection limit below 1 nM. Thus, the film with a good orientation (Table 3.2) also gives the best assay performance.

**Table 3.3** Effective noise ( $N$ ), sensitivity ( $S$ ) and detection limits ( $DL$ ) for hIgG detection at different immobilisation matrices.

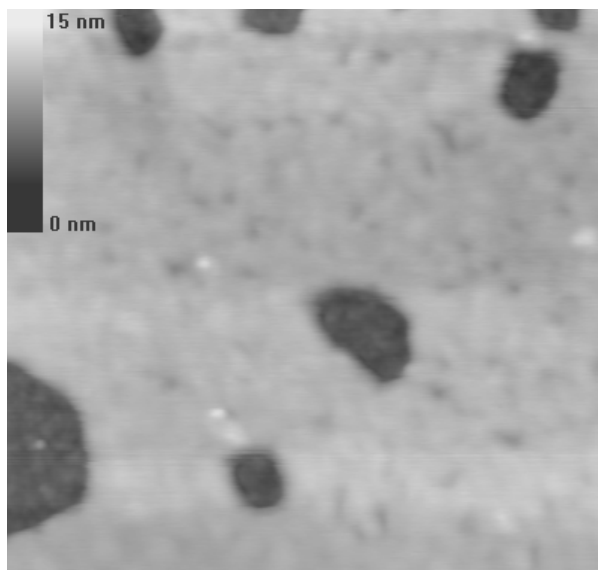
Matrix	$C_{\text{Fab}}$ ( $\text{mg.l}^{-1}$ )	$S$ ( $\text{Hz.l.mg}^{-1}$ )	$N$ (Hz)	$DL$ ( $\text{mg.l}^{-1}$ )	$DL$ (nM)
DPPC/DPPE-EMCS (9:1)	12,0	8,2	0,75	0,18	1,2
	24,0	12,3	0,75	0,12	0,8
	45,0	10,2	0,75	0,15	1,0
	96,0	1,7	0,75	0,87	5,8
DPPC/CHOL/DPPE-EMCS					
molar ratio: 8:1:1	25,0	0,4	1,20	6,38	42,5
7:2:1	25,0	1,2	1,50	2,56	17,0
6:3:1	25,0	1,0	2,50	4,77	31,8
5:4:1	25,0	1,3	1,80	2,78	18,5
4:5:1	25,0	1,4	4,00	5,62	37,4
2:7:1	25,0	1,4	1,00	1,48	9,8

Cholesterol produced an overall decrease of assay sensitivity and increasing cholesterol ratio in the film produced a relative increase in sensitivity, reaching a maximum at about 50% cholesterol, a point where the Langmuir monolayer is already well-condensed. The detection limits were lowered extra by an increased noise in the QCM detector, which was caused by the reuse of the quartz crystals in the particular experiments.

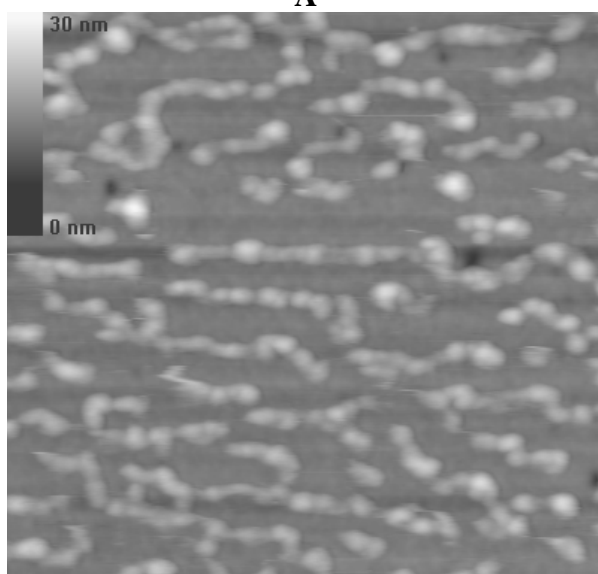
### 3.6.6 Film structure

In preliminary investigations with AFM, the surfaces of the monolayer matrices DPPC/DPPE-EMCS (9:1) and DPPC/CHOL/DPPE-SPDP (5:4:1) were imaged in air in contact mode (Fig. 3.15.A and Fig. 3.16.A). The non-condensed DPPC/DPPE-EMCS matrix appeared to be less homogeneous as the condensed DPPC/CHOL/ DPPE-SPDP matrix: the DPPC/DPPE-EMCS layer displayed bilayer holes in the film, while the DPPC/CHOL/DPPE-SPDP was quite smooth in air.

The surfaces were imaged after sequential binding of Fab' (Figures 3.15 and 3.16 Pictures B), BSA (pictures C) and human IgG (pictures D). After Fab' -binding (pictures B) globular structures could be observed, which may correspond to aggregates of Fab-fragments (2–10 molecules) with a predominantly straight to slightly slanted orientation.

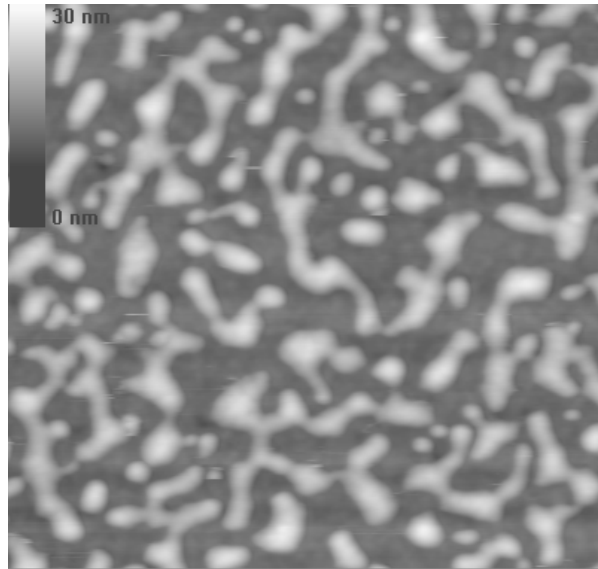


**A**

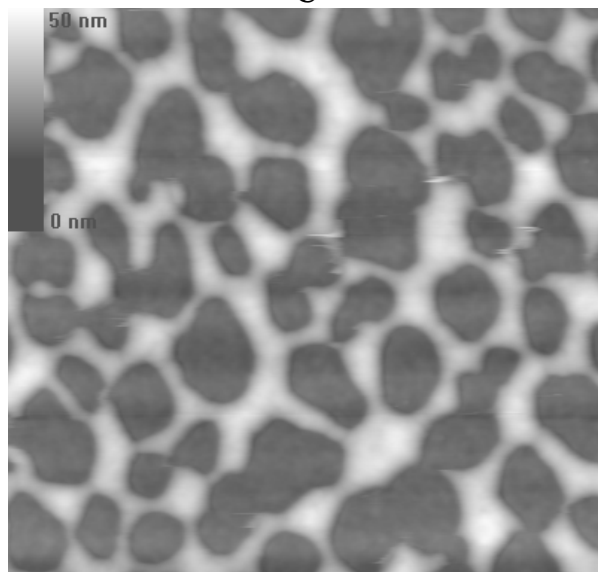


**B**

**Figure 3.15 (A-B)** AFM images (area: 1024 x 1024 nm) of anti-hIgG Fab', BSA and hIgG on DPPC/DPPE-EMCS (9:1). (A) the monolayer matrix DPPC/DPPE-EMCS, (B) after Fab'-attachment.

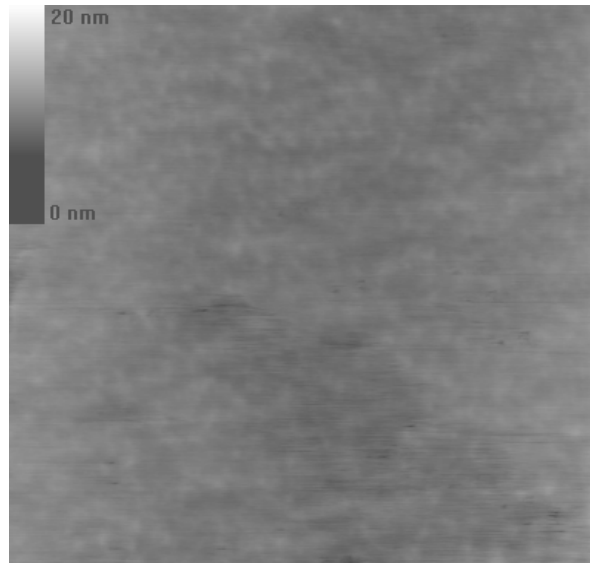


C

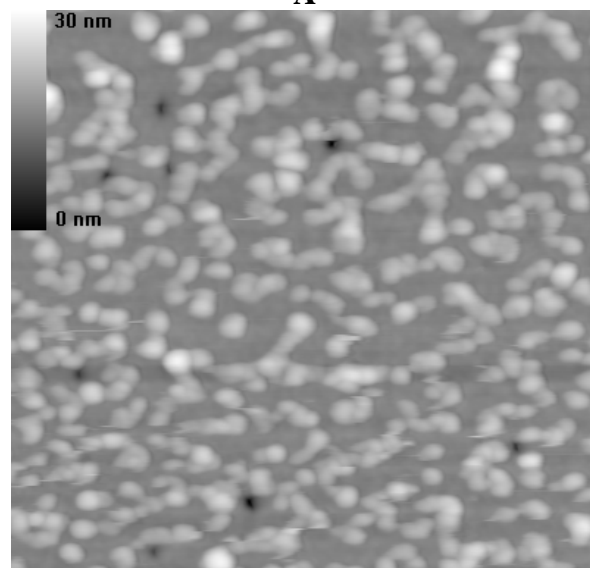


D

**Figure 3.15 (C-D)** AFM images (area: 1024 x 1024 nm) of anti-hIgG Fab', BSA and hIgG on DPPC/DPPE-EMCS (9:1). (C) after BSA adsorption (blocking) (D) after reaction with the antigen human IgG.

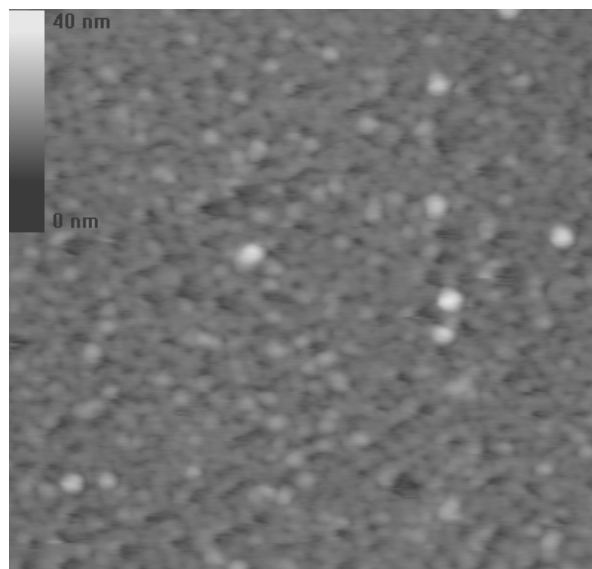


**A**

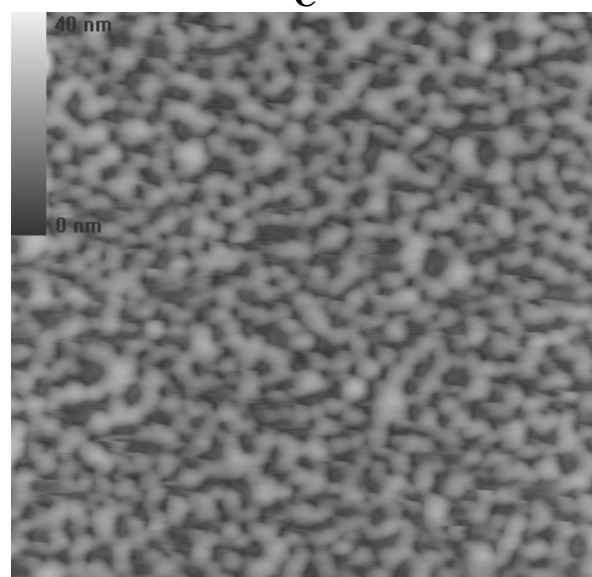


**B**

**Figure 3.16 (A-B)** AFM images (area: 1024 x 1024 nm) of anti-hIgG Fab', BSA and hIgG on DPPC/CHOL/DPPE-SPDP (4:5:1). (A) the monolayer matrix (B) after Fab'-attachment.



**C**



**D**

**Figure 3.16 (C-D)** AFM images (area: 1024 x 1024 nm) of anti-hIgG Fab', BSA and hIgG on DPPC/CHOL/DPPE-SPDP (4:5:1). (C) after BSA adsorption (blocking) (D) after reaction with the antigen human IgG.



With the DPPC/DPPE-EMCS monolayer the Fab-fragment aggregates were arranged in strings (Fig. 3.15.B). Since the strings are oriented parallel to the scanning direction, they are likely produced by the scanning process. The images of the condensed matrix show more evenly distributed aggregates with (on average) less height. In this case, with a more condensed layer, the modification by the tip was much less noticed, but the orientation of the Fab'-fragments is likely more tilted.

The adsorption of bovine serum albumin to the condensed film (picture 3.16.C) gives a more equal surface with less height features, suggesting that the spaces between Fab'-fragments are filled up by the BSA. In the non-condensed matrix, however, not all the space is filled up. Instead the molecules cling together in even larger aggregates. Upon interaction with h-IgG a network is formed with the DPPC/DPPE-EMCS matrix (Fig. 3.16.D).

### 3.7 Conclusions

It has been reported by Buijs et al. that IgG and F(ab')<sub>2</sub> have a similar adsorption behaviour onto polystyrene surfaces, although in their work the orientation of antibodies (IgG and F(ab')<sub>2</sub>) had not been assessed via immunological activity measurements<sup>253</sup>. In the present work the amounts of antibody adsorbed onto polystyrene at high pH appeared to be higher for IgG than for F(ab')<sub>2</sub>, which according to the results of Buijs et al., are in concordance with the behaviour of positively charged polystyrene. The difference in immunological activity, however, with the model system anti-h-IgG, as observed in the present study with radioassay, was quite pronounced. Both affinity constant and orientation (from an immunological point of view) were much higher for the F(ab')<sub>2</sub> fragment. Thus orientation in an end-on fashion, as observed from measurement of the surface density only, still doesn't clarify the proper orientation for immunological measurements and use in a sensor.

The present studies show that it is possible to control the density and orientation of antibody fragments by attaching them covalently to linker lipids in a monolayer matrix via the thiol groups in the hinge region. The orientation of the coupled Fab' appears to be rather dependent on the linking group (EMCS vs. SPDP) and non-specific binding levels depend critically on the monolayer

matrix. The overall highest density of specific binding sites was obtained by including cholesterol in the monolayer matrix, which may be utilised in immunosensors. The highest overall binding efficiency, however, was obtained for monolayers without cholesterol, reaching to 70% activity of the monolayer. The latter monolayer matrix may thus be useful for highly efficient immunoassays that additionally require a minimum amount of Fab'. It was observed that the structure of the antibody/BSA/antigen layers was quite dependent on the degree of condensation of the layer.

For attaining high efficiency of binding a possibility for lateral movement and the formation of aggregates seems to be important, as seen in the more fluid layers of DPPC/DPPE-EMCS. Although methods for probing lipid monolayer films with AFM (e.g. comparing contact mode versus tapping mode and measurements in air and in liquid) and the interpretation of the images are still quite incomplete at the present stage, it can be clearly observed that in the case of a condensed film the results were quite in concordance with the conventional concept of antibody attachment and "blocking" with BSA. The immunochemical reaction is also clearly visible. A non-condensed film (DPPC/DPPE-EMCS 9:1) gives aggregated complexes, which are easily modified by the AFM tip in contact mode, but which at the same time have proven to give the best assay performance both in immunosensing and radioassay. An important observation was that the QCM detection gave on the average a much larger response in comparison with radiotracer methods, a feature that can be explained by factors as protein hydration and increased rigidity in the protein layer. The amplification of the the QCM response is highest at a particular Fab'-concentration. A detection limit of slightly below 1 nM could be attained, which is more than 1 order of magnitude lower than the detection limits reported in a recent article on detection of h-IgG with SPR using self-assembled films on silver<sup>254</sup>.

## 4. General conclusions

In the design of biosensors it appears that strict control over the immobilisation conditions and the possibility to control the surface properties is a key factor. At the same time the activity of the biological component is not a mere ‘macroscopic’ constant (affinity and capacity constants) which can be investigated with simple means. In order to get more insight in what really happens on the surface, very many different techniques, both microscopic and macroscopic, are needed. Performing these measurements simultaneously and/or *in situ* gives additional advantages.

In the first part of the present thesis, electrostatic binding appears to be a good way to immobilise glucose oxidase onto a intrinsically conductive layer. The activity could be optimised by control of the wire concentration prior to enzyme binding and the ionic strength during enzyme binding. A bioelectrochemical response could not yet be attained at his stage of the work. In the case of GOx a more oriented immobilisation is an interesting option. However, it appeared to be quite difficult to attain a linkage via maleimide to the appropriate disulphide. This is probably caused by inaccessibility of the disulphide on the surface of the dimeric GOx molecule.

As demonstrated in the second subject of the present thesis, QCM detection, radioassay methods, SPR and AFM form a very good set of characterisation methods for a more intricate study of structure and function of biomolecular films, as demonstrated for the model system anti-human IgG. It not only appears that interfacial aspects, when well-controlled, can be used in a positive way for optimisation of orientation and functionality of antibodies, but that the detection sensitivity and detection limits in biosensing configurations are also clearly improved. Detection limits are attained close to or slightly below the theoretical limit of 1 nM<sup>12</sup>.

According to preliminary AFM-investigations, the structure with more fluidity appears to act more optimally in immunological tests and in immunosensing (with QCM). Presently there are still complications with the AFM-measurements concerning the causes of formation of aggregates and the layer stability. Also convolution effects (size-scaling due to a larger tip diameter) have

to be taken into account to estimate the real size of the domains that are observed and these issues are still under investigation.

The way biomolecules can be attached to lipid monolayers (either produced by self-assembly of LB-film methods) may prove to be also a good alternative for the attachment of enzymes or redox enzymes to electrodes. The monolayer nature of the films, however, does limit the maximum amount of current that can be obtained. The attachment of a genetically modified azurin to a free pyridine of a bis(pyridyl)thiophene oligomer is a more interesting and also more 'designed' approach to attaining intricate contact of a biomolecule with an electrode, as has been discussed in reference II. The azurin, however, seems to interact better with a 3-pyridine moiety as with a 4-pyridine moiety.

There are still no diagnostic products or sensors based on Langmuir-Blodgett films, which is surprising when considering the high quality of the films produced and the low amounts of molecular preparations that are consumed in the coating process. Automation of the coating procedure for commercial production, preferentially using the Langmuir-Schäfer technique, is also quite feasible. Taking also into account the results of the present thesis, it can be expected that LB-films will be entering the biosensor market in the near future.

## References

1. Turner, A. P. F., Karube, I. & Wilson, G. (Eds.) (1987). *Biosensors. Fundamentals and Applications*. Oxford Univ. Press, Oxford.
2. Göpel, W., Hesse, J. & Zemel, J. N. (eds.) (1991). *Sensors, a Comprehensive Survey*. VCH, Weinheim.
3. Beckles, D. L., Maioriello, J., Santora, V. J., Bell, T. W., Chapoteau, E., Czech, B. P. & Kumar, A. (1995). Complexation of creatinine by synthetic receptors. *Tetrahedron* **51**, 363-376.
4. Blaedel, W. J. & Bugoslaski, R. C. (1978). Chemical amplification in analysis: A review. *Anal. Chem.* **50**, 1026-1032.
5. Köhler, G. (1981). The technique of hybridoma production. *Immunol. Meth.* **2**, 285-98.
6. Hock, B. (1997). Antibodies for immunosensors. A Review. *Anal. Chim. Acta* **347**, 177-186.
7. de Alwis, W. U. & Wilson, G. S. (1985) Rapid sub-picomole electrochemical enzyme immunoassay for Immunoglobulin G. *Anal. Chem.* **57**, 2754-2756.
8. Blackburn, G. F., Shah, H. P., Kenten, J. H., Leland, J., Kamin, R. A., Link, J., Peterman, J., Powell, M. J., Shah, A., Talley, D. B., Tyagi, S. K., Wilkins, E., Wu, T.-G. & Massey R. J. (1991). Electrochemiluminescence detection for development of immunoassays and DNA probe assays for clinical diagnostics. *Clin. Chem.* **37**, 1534-1539.
9. Kricka, L. J. (1993). Ultrasensitive immunoassay techniques. *Clin. Biochem.* **26**, 325-31.
10. Gibbons, I., Armenta, R., DiNello, R. K. & Ullman, E. F. (1987). Nonseparation enzyme channeling immunometric assays. *Meth. Enzymol.* **136**, 93-103.
11. Ullman, E. F., Schwarzberg, M. & Rubenstein, K. E. (1976). Fluorescent excitation transfer immunoassay. *J. Biol. Chem.* **251**, 4172-4178.
12. Eddowes, M. (1987/88). Direct immunochemical sensing: basic chemical principles and fundamental limitations. *Biosensors* **3**, 211-225.
13. Bataillard, P., Gardies, F., Jaffrezic-Renault, N., Martelet, C., Colin, B., Mandrand, B. (1988). Direct detection of immunospecies by capacitance measurements. *Anal. Chem.* **60**, 2374-2379.
14. Pace, S. J. (1981). Surface modification and commercial application. *Sens. & Act.* **1**, 475-527.
15. Merz, A. (1990). Chemically modified electrodes. *Top. Curr. Chem.* **152**, 49-90.
16. Kamau, G. N. (1988). Surface preparation of glassy carbon electrodes. *Anal. Chim. Acta* **207**, 1-16.
17. Murray, R. W., Ewing, A. G. & Durst R. A. (1987). Chemically modified electrodes. Molecular design for electrocatalysis. *Anal. Chem.* **59**, 379A-390A.
18. Baldwin, R. P. & Thomsen, K. N. (1991). Chemically modified electrodes in liquid chromatography detection: a review. *Talanta* **38**, 1-16.
19. Espenscheid, M. W., Ghatak-Roy, A. R., Moore, R. B., Penner, R. M., Szentirmay, M. N. & Martin C. R. (1986). Sensors from polymer modified electrodes. *J. Am. Chem. Soc., Faraday Trans. 1* **82**, 1051-1070.
20. Barraud, A. (1990). Chemical sensors based on LB films. *Vacuum* **41**, 1624-1628.

21. Ulman, A. (1996). Formation and structure of self-assembled monolayers. *Chem. Rev.* **96**, 1533-1554.
22. Bain, C. D., Troughton, E. B., Tao, Y.-T., Evall, J., Whitesides, G. M. & Nuzzo, R. G. (1989). Formation of monolayer films by the spontaneous assembly of organic thiols on gold. *J. Am. Chem. Soc.* **111**, 321-335.
23. Pan, J., Tao, N. & Lindsay, S. M. (1993). An atomic force microscopy study of a self-assembled octadecyl mercaptan monolayer adsorbed on gold(111) under potential control. *Langmuir* **9**, 1556-1560.
24. Malem, F. & Mandler, D. (1993). Self-assembled monolayers in electroanalytical chemistry: application of  $\omega$ -mercapto carboxylic acid in monolayers for the electrochemical detection of dopamine in the presence of a high concentration of ascorbic acid. *Anal. Chem.* **65**, 37-41.
25. Kinnear, K. T. & Monbouquette, H. G. (1993). Direct electron transfer to Escheria coli fumarate reductase in self-assembled alkanethiol monolayers on gold electrodes. *Langmuir* **9**, 2255-2257.
26. Willner, I., Riklin, A., Shoham, B., Rivenson, D. & Katz, E. (1993). Development of novel biosensor enzyme electrodes: glucose oxidase multilayer arrays immobilized onto self-assembled monolayers on electrodes. *Adv. Mat.* **5**, 912-915.
27. Miller, I. R., Doll, L. & Lester, D. S. (1992). Interaction of alamethicin, mellitin and protein kinase C with pure and phospholipid monolayer covered mercury electrode surfaces. *Bioelectrochem. & Bioenerg.* **28**, 85-103.
28. Tien, H. T. (1974). *Bilayer Lipid Membranes (BLM), theory and practice*. Marcel Dekker Inc, New York.
29. Koryta, J. & Dvorak, J. (1987). *Principles of Electrochemistry. Chapter 6: Membrane Electrochemistry and Bioelectrochemistry*. John Wiley & Sons, Chichester.
30. Wonderlin, W. F., Finkel, A. & French, R. J. (1990). Optimizing planar lipid bilayer single-channel recordings for high resolution with rapid voltage steps. *Biophys. J.* **58**, 289-297.
31. Hanke, W., Methfessel, C., Wilmsen, U. & Boheim, G. (1984). Ion channel reconstitution into lipid bilayer membranes on glass patch pipettes. *Bioelectrochem. & Bioenerg.* **12**, 329-339.
32. Hamill, O. P., Marty, A., Neher, E., Sakmann, B. & Sigworth, R. J. (1981). Improved patch-clamp techniques for high-resolution current recording from cells and cell-free membrane patches. *Pfluegers Arch., Eur. J. Physiol.* **391**, 85-100.
33. Albrecht, O., Gruler, H. & Sackmann, E. (1981). Pressure-composition phase diagrams of cholesterol/lecitin, cholesterol/phosphatidic acid and lecitin/phosphatidic acid mixed monolayers: a Langmuir film balance study. *J. Coll. & interf. Sci.* **79**, 319-339.
34. Sellström, Å., Gustafson, I., Ohlsson, P.-Å., Olofson, G. & Puu, G. (1992). On the deposition of phospholipids onto planar supports with the Langmuir-Blodgett technique using factorial experimental design. *Colloids & Surfaces* **64**, 275-298.
35. Chapman, D. (1993). Biomembranes and new hemocompatible materials. *Langmuir* **9**, 39-45.

36. Weis, R. & McConnel. H. M. (1985). Cholesterol stabilizes the liquid crystal interface in phospholipid monolayers. *J. Phys. Chem.*, **1985**, 89, 4453.
37. Ohki, S. (1980). Membrane potential and ion permeability of lipid bilayer membranes. *Bioelectrochem. & Bioenerg.* **7**, 487-501.
38. Barnett, A. (1990). The current-voltage relation of an aqueous pore in a lipid bilayer membrane. *Biochim. Biophys. Acta* **1025**, 10-14.
39. Pastor, R. W., Venable, R. M. & Karplus, M. (1991). Model for the structure of the lipid layer. *Proc. Natl. Acad. Sci. USA* **88**, 892-896.
40. Sugawara, M., Kataoka, M., Odashima, K. & Umezawa, Y. (1989). Biomimetic ion-channel sensors based on host-guest molecular recognition in Langmuir-Blodgett membrane assemblies. *Thin Solid Films* **180**, 129-133.
41. Tien, H. T. (1984). Cyclic voltammetry of bilayer lipid membranes. *J. Phys. Chem.* **88**, 3172-3174.
42. Kutnik, J. & Tien, H. T. (1986). Cyclic voltammetry of dye-modified BLM's. *Bioelectrochem. & Bioenerg.* **16**, 435-447.
43. Salamon, Z. & Tien, H. T. (1988). Light-induced electrical effects in a liquid crystal BLM containing TCNQ. *Photochem. & Photobiol.* **48**, 281-287.
44. Janas, T., Kotowski, J. & Tien H. T. (1988). Polymer-modified bilayer lipid membranes: the polypyrrole-lecithin system. *Bioelectrochem. & Bioenerg.* **19**, 405-412.
45. Tien, H. T. & Salamon, Z. (1989). Formation of self-assembled lipid bilayers on solid substrates. *Bioelectrochem. & Bioenerg.* **22**, 211-218.
46. Zviman, M. & Tien, H. T. (1991). Formation of a bilayer lipid membrane on rigid supports: an approach to BLM-based biosensors. *Biosens. & Bioelectron.* **6**, 37-42.
47. Ottova-Leitmannova, A. & Tien, H.T. (1992). Bilayer Lipid Membranes: An experimental system for biomolecular electronic devices development. *Prog. Surf. Sci.* **41**, 337-445.
48. Stenger, D. A., Fare, T. L. Cribbs, D. H. & Rusin, K. M. (1992). Voltage modulation of a gated ion channel admittance in platinum-supported lipid bilayers. *Biosens. & Bioelectron.* **7**, 11-20.
49. Paltauf, F. & Hermetter, A. (1994). Strategies for the synthesis of glycerophospholipids. *Prog. Lipid Res.* **33**, 239-328.
50. Tien, H. T., Salamon, Z., Kutnik, J., Kryszinski, P., Kotowski, J., Ledermann, D. & Janas, T. (1988). Bilayer Lipid Membranes: an experimental system for biomolecular device development. *J. Mol. Electron.* **4**, S1-S30.
51. Thompson, M. & Krull U. J. (1991). Biosensors and the transduction of molecular recognition. *Anal. Chem.* **63**, 393A-405A.
52. Valleton, J.-M. (1990). Information processing in biomolecule-based biomimetic systems. From macroscopic to nanoscopic scale. *React. Polym.* **12**, 109-131.
53. Tedesco, J. L., Krull, U. J. & Thompson, M. (1989). Molecular receptors and their potential for artificial transduction. *Biosensors* **4**, 135-167.
54. Stelzle, M., Weissmüller, G. & Sackmann, E. (1989). On the application of supported bilayers as receptive layers for biosensors with electrical detection. *J. Phys. Chem.* **97**, 2974-2981.

55. Plant, A. (1993). Self-assembled phospholipid/alkanethiol biomimetic bilayers on gold. *Langmuir* **9**, 2764-2767.
56. de Gier, J. (1992). Permeability barriers formed by membrane lipids. *Bioelectrochem. & Bioenerg.* **27**, 1-10.
57. Ligler, F. S., Fare, T. L., Seib, K. D., Smuda, J. W., Singh, A., Ayers M. E., Dalziel, A. & Yager, P. (1988). Fabrication of key components of a receptor-based biosensor. *Med. Instr.* **22**, 247-256.
58. Thompson, M., Krull, U. J. & Worsfold, P. J. (1980). The structure and electrochemical properties of a polymer-supported lipid biosensor. *Anal. Chim. Acta* **117**, 133-145.
59. Arya, A., Krull, U. J., Thompson, M. & Wong, H. E. (1985). Langmuir-Blodgett deposition of lipid films on hydrogel as a basis for biosensor development. *Anal. Chim. Acta* **173**, 331-336.
60. Kotowski, J., Janas, T. & Tien H. T. (1988). Immobilization of glucose oxidase on a polypyrrole-lecithin bilayer lipid membrane. *Bioelectrochem. & Bioenerg.* **19**, 277-282.
61. Martynski, T. & Tien, H. T. (1991). Spontaneous assembly of bilayer membranes on a solid surface. *Bioelectrochem. & Bioenerg.* **25**, 317-324.
62. Salamon, Z. & Tollin G. (1991). Interfacial electrochemistry of cytochrome c at a lipid bilayer modified electrode: effect of incorporation of negative charges in to the bilayer on cyclic voltammetric parameters. *Bioelectrochem. & Bioenerg.* **26**, 321-334.
63. Passechnik, V. I., Hianik, T., Ivanov, S. A., Sivak, B., Šnejdárková, M. & Reháč, M. (1998) Current fluctuations of bilayer lipid membranes modified by glucose oxidase. *Bioelectrochem. & Bioenerg.* **45**, 233-237.
64. Clark, L. C. Jr. & Lyons, C. (1962). Electrode systems for continuous monitoring in cardiovascular surgery. *Ann. NY Acad. Sci.* **102**, 29-45.
65. Guilbault, G. G. & Kauffmann J.-M. (1987). Enzyme-based electrodes as analytical tools. *Biotechnol. & Appl. Biochem.* **9**, 95-113.
66. Frew, J.E. & Hill, H. A. O. (1987). Electrochemical biosensors. *Anal. Chem.* **59**, 933A-944A.
67. Nagy, G. & Pungor, E. (1988). Bioelectrochemical sensors and analytical problems in their application. *Bioelectrochem. & Bioenerg.* **20**, 1-19.
68. Mascini, M. & Palleschi, G. (1989). Design and applications of enzyme electrode probes. *Selective Electrode Rev.* **11**, 191-264.
69. Gorton, L., Csöregi, E., Dom'nguez, E., Emnéus, J., Jönsson-Petterson, G., Marko-Varga, G. & Persson, B. (1991). Selective detection in flow analysis based on the combination of immobilized enzymes and chemically modified electrodes. *Anal. Chim. Acta* **250**, 203-248.
70. Campanella, L. & Tomassetti, M. (1992). The State-of-the-Art of electrochemical sensors. *Bull. Electrochem.* **8**, 229-238.
71. Bartlett, P. N. & Cooper, J. M. (1993). A review of the immobilization of enzymes in electropolymerized films. *J. Electroanal. Chem.* **362**, 1-12.
72. Wang, J. (1993). Organic-phase biosensors - new tools for flow analysis: a short review. *Talanta* **40**, 1905-9.



73. Ikeda, T. (1995). Enzyme-modified electrodes with bioelectrocatalytic function (review). *Bunseki Kagaku* **44**, 333-54.
74. Wilson, R. & Turner, A. P. F. (1992). Glucose oxidase: an ideal enzyme. *Biosens. & Bioelectron.* **7**, 165-185.
75. Kerner, W., Kiwit, M., Linke, B., Keck, F. S., Zier, H. & Pfeiffer, D. (1993). The function of a hydrogenperoxide-detecting electroenzymatic glucose electrode is markedly impaired in human subcutaneous tissue and plasma. *Biosens. & Bioelectron.* **8**, 473-482.
76. D'Costa, E. J., Higgins, I. J. & Turner, A. P. F. (1986). Quinoprotein glucose dehydrogenase and its application in an amperometric glucose sensor. *Biosensors* **2**, 71-87.
77. Bourdillon, C., Bourgeois, J. P. & Thomas, D. (1980). Covalent linkage of glucose oxidase on modified glassy carbon electrodes. *J. Am. Chem. Soc.* **102**, 4231-4235.
78. Ianniello, R. M. & Yacynych, A. M. (1981). Immobilized enzyme chemically modified electrode as an amperometric sensor. *Anal. Chem.* **53**, 2090-2095.
79. Cass, A. E. G., Davis, G., Francis, G. D., Hill, H. A. O., Aston, W. J., Higgins, I. J., Plotkin, E. V., Scott, L. D. L. & Turner, A. P. F. (1984). Ferrocene-mediated enzyme electrode for amperometric determination of glucose. *Anal. Chem.* **56**, 667-671.
80. Marko-Varga, G., Appelqvist, R. & Gorton, L. (1986). A glucose sensor based on glucose dehydrogenase adsorbed on a modified carbon electrode. *Anal. Chim. Acta* **179**, 371-379.
81. Smolander, M., Livio H.-L. & Räsänen, L. (1992). Mediated amperometric determination of xylose and glucose with an immobilized aldose dehydrogenase electrode. *Biosens. & Bioelectron.* **7**, 637-643.
82. Leung, H. W., Hallesy, D. W., Shott, L. D. Murray, F. J. & Paustenbach D. J. (1987). Toxicological evaluation of substituted dicyclopentadienyliron (ferrocene) compounds. *Toxicol. Lett.* **38**, 103-108.
83. Zakeeruddin, S. M. Fraser, D. M. & Nazeeruddin, M.-K. & Grätzel, M. (1992). Towards mediator design: characterization of tris-(4,4'-substituted-2,2'-bipyridine) complexes of Iron(II), Ruthenium(II) and Osmium(II) as mediators for glucose oxidase of *Aspergillus niger* and other redox proteins. *J. Electroanal. Chem.* **337**, 253-283.
84. Abu Nader, P., Sagardo Vives, S. & Mottola, H. A. (1990). Studies with a sulphite oxidase-modified carbon paste electrode for detection/determination of sulphite ion and SO<sub>2</sub>(g) in continuous flow systems. *J. Electroanal. Chem.* **266**, 47-55.
85. Durliat, H., Barry, M. B. & Comtat, M. (1988). FAD used as a mediator in the electron transfer between platinum and several biomolecules. *Bioelectrochem. & Bioenerg.* **19**, 413-423.
86. Harak, D. W. & Mottola, H. A. (1993). Electrostatically immobilized hexacyanoferrate ions as redox mediators in biochemical sensing: controlled release and cyclic voltammetric behavior. *Biosens. & Bioelectron.* **6**, 589-594.
87. Wang, J. & Varughese, K. (1990). Polishable and robust biological electrode surfaces. *Anal. Chem.* **62**, 318-320.

88. Marcus, R. A. & Sutin, N. (1985). Electron transfers in chemistry and biology. *Biochim. Biophys. Acta* **811**, 265-322.
89. Foulds, N. C & Lowe, C. R. (1988). Immobilization of glucose oxidase in ferrocene-modified pyrrole polymers. *Anal. Chem.* **60**, 2473-2478.
90. Skotheim, T. A., Lee, H. S., Hale, P. D., Karan, H. I., Okamoto, I., Samuelson, L & Tripathy, S. (1991). Derivatized poly-pyrrole Langmuir-Blodgett films. Applications to bioelectronics. *Synth. Met.* **41-43**, 1433-1437.
91. Hendry, S. P., Cardosi, M. F., Turner, A. P. F. & Neuse, E. W. (1993). Polyferrocenes as mediators in amperometric biosensors for glucose. *Anal. Chim. Acta* **281**, 453-459.
92. Lee, H. S., Liu L.-F., Hale, P. D. & Okamoto, Y. (1992). Amperometric enzyme-modified electrodes based on tetrathiafulvalene derivatives for the determination of glucose. *Heteroatom Chem.* **3**, 303-310.
93. Gregg, B. A. & Heller, A. (1990). Cross-linked redox gels containing glucose oxidase for amperometric biosensor applications. *Anal. Chem.* **62**, 258-263.
94. Ohara, T. J., Rajagopalan, R. & Heller, A. (1993). Glucose electrodes based on cross-linked Os(bpy)<sub>2</sub>Cl<sup>+2+</sup> complexed with poly(1-vinylimidazole) films. *Anal. Chem.* **65**, 3512-3517.
95. Ye, L., Hämmerle, M., Olsthoorn, A., Shuhmann, W., Schmidt, H.-L. Duine J. & Heller, A. (1993). High current density "wired" quinoprotein glucose dehydrogenase electrode. *Anal. Chem.* **65**, 238-41.
96. Smolander, M., Cooper, J., Schuhmann, W., Hämmerle, M. & Schmidt, H.-L. (1993). Determination of xylose and glucose in a flow-injection system with PQQ-dependent aldose dehydrogenase. *Anal. Chim. Acta* **280**, 119-127.
97. Bartlett, P. N., Booth, S., Caruana, D. J., Kilburn J. D., & Santamaria C. (1997). Modification of glucose oxidase by the covalent attachment of a tatrathiafulvalene derivative. *Anal. Chem.* **69**, 734-742.
98. Willner, I., Katz, E., Willner, B., Blonder, R., Heleg-Shabtai, V. & Bückmann, A. F. (1997). Assembly of functionalized monolayers of redox proteins on electrodes surfaces: Novel bioelectronic and optobioelectronic systems. *Biosens. & Bioelectron.* **12**, 337-356.
99. Kinnear, K. T. & Monbouquette, H. G. (1997). An amperometric fructose biosensor based on fructose dehydrogenase immobilized in a membrane mimetic layer on gold. *Anal. Chem.* **69**, 1771-1775.
100. Alvarez-Icaza, M. & Schmidt, R. D. (1994). Observation of direct electron transfer from the active centre of glucose oxidase to a graphite electrode achieved through the use of mild immobilization. *Bioelectrochem. & Bioenerg.* **33**, 191-199.
101. Bidan, G. (1992). Electroconducting conjugated polymers: new sensitive matrices to build up chemical or electrochemical sensors. *Sens. & Act. B* **6**, 45-56.
102. Roncali, J. (1992). Conjugated poly(thiophenes): Synthesis, functionalization, and applications. *Chem. Rev.* **92**, 711-738.
103. Bartlett, P. N. & Birkin, P. R. (1993). The application of conductive polymers in biosensors. *Synth. Met.* **61**, 15-21.

104. Atta, N. F., Galal, A., Karagözler, A. E., Russell, G. C., Zimmer, H. & Mark, H. B. Jr. (1991). Electrochemistry and detection of some organic and biological molecules at conducting poly(3-methylthiophene) electrodes. *Biosens. & Bioelectron.* **6**, 333-41.
105. Foulds, N. C. & Lowe, C. R. (1986). Enzyme entrapment in electrically conducting polymers. Immobilization of glucose oxidase in polypyrrole and its application in amperometric glucose sensors. *J. Chem. Soc., Faraday Trans. Trans. 1* **82**, 1259-64.
106. Umana, M. & Waller, J. (1986). Protein-modified electrodes. Glucose oxidase/polypyrrole system. *Anal. Chem.* **58**, 2979-83.
107. Bartlett, P. N. & Whitaker R. G. (1987). Electrochemical immobilisation of enzymes. Part 1. Theory. *J. Electroanal. Chem.* **224**, 27-35.
108. Bartlett, P. N. & Whitaker R. G. (1987). Electrochemical immobilisation of enzymes. Part 2. Glucose oxidase immobilised in poly-N-methyl-pyrrole. *J. Electroanal. Chem.* **224**, 37-48.
109. Fortier, G., Brassard, E. & Bélanger, D. (1990). Optimization of a polypyrrole glucose oxidase biosensor. *Biosens. & Bioelectron.* **5**, 473-490.
110. Kitani, A., Kasyu, N. & Sasaki, K. (1994). Effect of flavin coenzymes on current response for glucose at glucose oxidase/polypyrrole modified electrodes. *Electrochim. Acta* **39**, 7-8.
111. Cooper, J. A. & Bloor, D. (1993). Evidence for the functional mechanism of a polypyrrole glucose oxidase electrode. *Electroanal.* **5**, 883-86.
112. Bélanger, D., Nadreau, J. & Fortier, G. (1989). Electrochemistry of the polypyrrole glucose oxidase electrode. *J. Electroanal. Chem.* **274**, 143-155.
113. Almeida, N. F., Beckman, E. J. & Ataai, M. M. (1993). Immobilization of glucose oxidase in thin polypyrrole films: Influence of polymerization conditions and film thickness on the activity and stability of the immobilized enzyme. *Biotechnol. & Bioeng.* **42**, 1037-1045.
114. de Taxis du Poet, P., Miyamoto, S., Murakami, J., Kimura, J. & Karube, I (1990). Direct electron transfer with glucose oxidase immobilized in an electropolymerized poly(N-methylpyrrole) film on a gold microelectrode. *Anal. Chim. Acta* **235**, 255-263.
115. Koopal, C. G. J., de Ruiter, B. & Nolte, R. J. M. (1991). Amperometric biosensor based on direct communication between Glucose Oxidase and a conducting polymer inside the pores of a filtration membrane. *J. Chem. Soc., Chem. Commun.* **1991**, 1691-1692.
116. Cai, Z. & Martin, C. R. (1989). Electronically conductive polymer fibers with mesoscopic diameters show enhanced electronic conductivities. *J. Am. Chem. Soc.* **111**, 4138-4139.
117. Koopal, C. G. J., Feiters, M. C., Nolte, R. J. M., de Ruiter, B & Schasfoort, R. B. M. (1992). Glucose sensor utilizing polypyrrole incorporated in track-etch membranes as the mediator. *Biosens. & Bioelectron.* **7**, 461-471.
118. Koopal, C. G. J. (1992). *Third generation amperometric biosensors. PhD Thesis.* Catholic University of Nijmegen.

119. Koopal, C. G. J. & Nolte, R. J. M. (1994). Kinetic study of the performance of third-generation biosensors. *Bioelectrochem. & Bioenerg.* **33**, 45-53.
120. Weibel, M. K. & Bright, H. J. (1971). The glucose oxidase mechanism: interpretation of the pH dependence. *J. Biol. Chem.* **246**, 2734-2744.
121. Kuwabata, S & Martin, C. R. (1994). Mechanism of the amperometric response of a proposed glucose sensor based on a polypyrrole-tubule-impregnated membrane. *Anal. Chem.* **66**, 2757-2762.
122. Deshpande, M. V. & Hall, E. A. H. (1990). An electrochemically grown polymer as an immobilisation matrix for whole cells: application in an amperometric dopamine sensor. *Biosens. & Bioelectron.* **5**, 431-448.
123. Cosnier, S. & Innocent, C. (1992). A novel biosensor elaboration by electropolymerization of an adsorbed amphiphilic pyrrole-tyrosinase enzyme layer. *J. Electroanal. Chem.* **328**, 361-366.
124. Cosnier, S., Innocent, C., Allien, L., Poitry, S. & Tsacopoulos, M. (1997). An electrochemical method for making enzyme microsensors. Application to the detection of dopamine and glutamate. *Anal. Chem.* **69**, 968-971.
125. Kajiya, Y. K., Tsuda, R. & Yoneyama, J. (1991). Conferment of cholesterol sensitivity on polypyrrole films by immobilization of cholesterol oxidase and ferrocenecarboxylate ions. *J. Electroanal. Chem.* **301**, 155-164.
126. Cooper, J. C. & Hall E. A. H. (1992). Electrochemical response of an enzyme-loaded polyaniline film. *Biosens. & Bioelectron.* **7**, 473-485.
127. Bartlett, P. N. & Whitaker, R. G. (1987/88). Strategies for the development of amperometric enzyme electrodes. *Biosensors* **3**, 359-379.
128. Nalwa, H. S. (Ed.) (1997). *Handbook of organic conductive molecules and polymers, Vol. 2: Conductive Polymers: Synthesis and electrical properties*. John Wiley & Sons, Chichester 1997.
129. Edelman, P. G. & Wang, J. (Eds.) (1992). Biosensors & Chemical sensors. Optimizing performance through polymeric materials. *ACS Symp. Ser.* **487**. American Chemical Society, Washington.
130. Röckel, H., Huber, J., Gleiter, R & Schuhmann W. (1994). Synthesis of functionalized poly(dithienylpyrrole) derivatives and their application in amperometric biosensors. *Adv. Mater.* **6**, 568-571.
131. Higgins, S. & Crayston J. A. (1993). Metal-containing conducting polymers. *Synth. Met.* **55-57**, 879-883.
132. Ochmanska, J. & Pickup, P. G. (1991). Synthesis, electrochemistry, and ligand substitution reactions of conducting copolymer films of ruthenium polypyridine complexes and aromatic heterocycles. *Can. J. Chem.* **69**, 653-660
133. Bevierre, M.-O., Mercier, F., Ricard, L. & Mathey, F. (1990). A first step toward the phosphorus analogues of polythiophenes. *Angew. Chem., Int. Ed. Engl.* **29**, 655-657.
134. Tamao, K., Yamaguchi, S., Shiozaki, M., Nakagawa, Y. & Ito, Y. (1992). Thiophene-silole co-oligomers and copolymers. *J. Am. Chem. Soc.* **114**, 5867-5869.
135. Agrawal, A. & Jenekhe, S. A. (1991). New conjugated polyantrazolines containing thiophene moieties in the main chain. *Macromolecules* **24**, 6806-6808;

136. Tanaka, S., Sato, M.-A. & Kaeriyama, K. (1987). Electrochemical polymerization of dithienylbenzene and dithienylpyridine. *J. Macromol. Sci.- Chem.* **A24**, 749-761.
137. Amrani, M. E. H., Ibrahim, M. S. & Persaud, K. C. (1993). Synthesis, chemical characterization and multifrequency measurements of poly(N-(2-pyridyl) pyrrole for sensing volatile chemicals. *Mater. Sci. & Eng.* **C1**, 17-22.
138. Yamamoto, T., Miyazaki, Y., Fukuda, T., Zhou, Z., Maruyama, T., Kanbara, T. & Osakada, K. (1993). Properties and structure of substituted poly(thiophene-2,5-diyl), poly(pyridine-2,5-diyl) and their analogs prepared by organometallic processes. *Synth. Met.* **55-57**, 1214-1220.
139. Sariciftci, N. S., Mehring, M., Gaudl, K. U., Bäuerle, P., Neugebauer, H. & Neckel, A. (1992). Third generation of conducting polymers: spectroelectrochemical investigations on viologen-functionalized poly(3-alkylthiophenes). *J. Chem. Phys.* **96**, 7164-7170.
140. Bäuerle, P. & Gaudl, K.-U. (1990). Synthesis and properties of viologen functionalized poly(3-alkylthienylenes). *Adv. Mater.* **2**, 185-188.
141. Saika, T. Iyoda, T. & Shimidzu, T. (1993). Electropolymerization of bis(4-cyano-1-pyridinio) derivatives for the preparation of polyviologen films on electrodes. *Bull. Chem. Soc. Jpn.* **66**, 2054-2060.
142. Thanos, I. C. G & Simon H. (1987). Electro-enzymic viologen-mediated stereospecific reduction of 2-enoates with free and immobilized enoate reductase on cellulose filters of modified carbon electrodes. *J. Biotechnol.* **6**, 13-29.
143. Cosnier, S., Innocent, C. & Jouanneau, Y. (1994). Amperometric detection of nitrate via a nitrate reductase immobilized and electrically wired at the electrode surface. *Anal. Chem.* **66**, 3198-3201.
144. Cosnier, S., Galland, B. & Innocent, C. (1997). New electropolymerizable amphiphilic viologens for the immobilization and electrocal wiring of a nitrate reductase. *J. Electroanal. Chem.* **433**, 113-119.
145. Eng, L. H., Elmgren, M., Komlos, P., Nordling, M., Lindquist, S.-E. & Neujahr, H. Y. (1994). Viologen-based redox polymer for contacting the low-potential redox enzyme hydrogenase at an electrode surface. *J. Phys. Chem.* **98**, 7068-7072.
146. Kulys, J. J. (1981). Development of new analytical systems based on biocatalyzers. *Enz. & Microb. Technol* **3**, 342-352.
147. Khan, G. F., Ohwa, M. & Wernet, W. (1996). Design of a stable charge transfer complex electrode for a third-generation amperometric glucose sensor. *Anal. Chem.* **68**, 2939-2945.
148. Anzai, J., Hoshi, T., Lee, S. & Osa, T. (1993). Use of the avidin-biotin system for the immobilization of an enzyme on the electrode surface. *Sens. & Act. B* **13-14**, 73-75.
149. Lee, S., Anzai, J. & Osa, T. (1993). Enzyme Langmuir-Blodgett membranes in glucose electrodes based on avidin-biotin interaction. *Sens. & Act. B* **12**, 153-158.
150. Samuelson, L. A., Wiley, B., Kaplan, D. L., Sengupta, S., Kamath, M., Lim, J. O., Cazeca, M., Kumar, J., Marx, K. A. & Tripathy, S. K. (1994). Intelligent systems based on ordered arrays of biological molecules using the LB technique. *J. Intell. Mater. Syst. & Struct.* **5**, 305-310.

151. Moriizumi, T. (1985). Langmuir-Blodgett films as chemical sensors. *Thin Solid Films* **160**, 413-429.
152. Nakagawa, T., Kakimoto, M., Miwa, T. & Aizawa, M. (1991). New method for fabricating Langmuir-Blodgett films of water-soluble proteins with retained enzyme activity. *Thin Solid Films* **202**, 151-156.
153. Arisawa, S., Arise, T. & Yamamoto, R. (1992). Concentration of enzymes adsorbed onto Langmuir films and characteristics of a urea sensor. *Thin Solid Films* **209**, 259-263.
154. Lee, S., Anzai, J. & Osa, T. (1993). Enzyme-modified Langmuir-Blodgett membranes in glucose electrodes based on avidin-biotin interaction. *Sens. & Act. B* **12**, 153-158.
155. Taylor, D. M., Gupta, S. K., Underhill, A. E. & Dhindsa, A. S. (1994). Formation and electrical characterization of Langmuir-Blodgett films of metal-(dmit)<sub>2</sub> charge transfer salts. *Thin Solid Films* **243**, 530-535.
156. Nichogi, K., Taomoto, A., Nambu, T. & Murakami, M. (1995). Mixed stack charge-transfer films prepared by Langmuir-Blodgett technique and donor doping. *Thin Solid Films* **254**, 240-245.
157. Aviram, A. & Ratner, M. A. (1974). Molecular rectifiers. *Chem. Phys. Lett.* **29**, 277-283.
158. Arrhenius, T. S., Blanchard-Desce, M., Dvolaitzky, M., Lehn, J.-M. & Malthete, J. (1986). Molecular devices: carviologens as an approach to molecular wires-synthesis and incorporation into vesicle membranes. *Proc. Natl. Acad. Sci. USA* **83**, 5355.
159. Tour, J. M. (1996). Conjugated macromolecules of precise length and constitution. Organic synthesis for the construction of nanoarchitectures. *Chem. Rev.* **96**, 537-553.
160. Fujii, M., Aso, Y., Otsubo, T. & Ogura, F. (1993). Synthesis and properties of ethanediylidene-2,2'-bis(5-dicyano-methylene-3-thiolene). and its dibromoderivatives as new extensively conjugated electron donors. *Synth. Met.* **55-57**, 2136-2139.
161. Duhamel, L., Duhamel, P., Plé, G. & Ramondenc, Y. (1993). Terminally substituted linear conjugated polyenes: precursors of molecular wires. *Tetrahedron Lett.* **34**, 7399-7400.
162. Bitoh, A., Kohchi, Y., Otsubo, T., Ogura, F. & Ikeda, K. (1995). Synthesis and properties of 2,5-bis((2-tetrathiafulvalen-2-yl)ethenyl)thiophene and related compounds as novel dumbbell-type electron donors. *Synth. Met.* **70**, 1123-1124.
163. Elandaloussi, E. H., Frère, P., Roncali, J., Richomme, P., Jubault, M. & Gorgues, A. (1995). extended hybrid tetrathiafulvalene  $\pi$ -donors with oligothiophenylenevinylene conjugated spacer groups. *Adv. Mater.* **7**, 390-394.
164. Pearson, D. L., Schumm, J. S. & Tour, J. M. Iterative divergent/convergent approach to conjugated oligomers by a doubling of molecular length at each iteration. A rapid route to potential molecular wires. *Macromol.* **27**, 2348-2350.
165. Adam, M. & Müllen, K. (1994). Oligomeric tetrathiafulvalenes: extended donors for increasing the dimensionality of electrical conduction. *Adv. Mat.* **6**, 439-459.

166. Ikeda, K., Kwabata, K., Tanaka, k., & Mizutani, M. (1993). Synthesis of novel donor, BETE-DMB, and its properties. *Synth. Met.* **55-57**, 2007-2012.
167. Hansen, T. K., Lakshmikantham, M. V., Cava, M. P., Metzger, R. M. & Becher, J. (1991). *J. Org. Chem.* **56**, 2720-2722.
168. Bryce, M. R., Fleckenstein, E. & Hünig, S. (1990). Synthesis and redox behaviour of highly conjugated bis(benzo-1,3-dithiole) and bis(benzothiazole) systems containing aromatic linking groups: model systems for organic metals. *J. Chem. Soc., Perkin Trans. 2*, 1777-1783.
169. Barzoukas, M., Blanchard-Desce, M., Josse, D., Lehn, J.-M. & Zyss, J. (1989). Very large quadratic optical non-linearities in solution of two push-pull polyene series: effect of the conjugation length and of the end groups. *Chem. Phys.* **133**, 323-329.
170. Bubeck, C., Effenberger, F., Häussling, L., Neher, D., Niesert, C.-P. & Ringsdorf, H. (1992). Donor-acceptor substituted polyenes: orientation in mono- and multilayers. *Adv. Mat.* **4**, 4113-4115.
171. J.P. Launey, S. Woitellier, M. Sowinska, and M. Turrel. (1988). Control of intramolecular electron transfer. II: Experimental approaches. In: F. L. Carter, R. E. Siatkowski and H. Wohltjen (Eds.), *Molecular electronic devices*. Elsevier Science Publishers, Amsterdam. pp. 171-185.
172. Beley, M., Chodorowski-Kimmes, S., Collin, J.-P., Lainé, P., Launey, J.-P. & Sauvage, J.-P. (1994). Pronounced electronic coupling in rigidly connected N,C,N-coordinated diruthenium complexes over a distance of up to 20 Å. *Angew. Chem., Int. Ed. Engl.* **33**, 1775-1778.
173. Tolbert, L. M., Zhao, X., Ding, Y., Bottomley, L. A. (1995). Bis(ferrocenyl)polymethine cations. A prototype molecular wire with redox-active end groups. *J. Am. Chem. Soc.* **117**, 12891-12892.
174. Coat, F. & Lapinte, C. (1996). Molecular wire consisting of a C8 chain of elemental carbon bridging two metal centres: synthesis and characterization of  $[\{Fe(\eta^5-C_5Me_5)(dppe)\}_2(\mu-C_8)]$ . *Organomet.* **15**, 477-479.
175. Takahashi, K., Nihira, T., Akiyama, K., Ikegami, Y. & Fukuyo, E. (1992). Synthesis and characterization of new conjugation-extended viologens involving a central aromatic linking group. *J. Chem. Soc., Chem. Commun.* **92**, 620-622.
176. Nakajima, R., Iida, H., & Hara, T. (1990). Synthesis and spectral properties of 5,5'-di-(4-pyridyl)-2,2'-bithienyl as a new fluorescent compound. *Bull. Chem. Soc. Jpn.* **63**, 636- 637.
177. Nakajima, R., Ise, T., Takahashi, Y., Yoneda, H., Tanaka, K. & Hara, T. (1994). Synthesis and properties of new laser dyes containing 4-(2-thienyl)pyridine skeleton. *Phosphorus, Sulfur and Silicon* **95-96**, 535-536.
178. Takahashi, K. (1993). Bipyridinium salt extended with 5-membered heterocyclic ring and its production. *J. Pat. 0507045* (Sony Corp.).
179. Befort, O. & Möbius, D. (1994). Molecular organization in mixed monomolecular films and Langmuir-Blodgett layers of alkylaminostyryl-pyridinium dyes and stearic acid. *Thin Solid Films* **143**, 553-558.

180. Goldenberg, L. M., Becker, J. Y., Levi, O. P.-T., Khodorkovsky, V. Y., Bryce, M. R. & Petty, M. C. (1995). Semiconducting Langmuir-Blodgett films of non-amphiphilic ethylenedithio-tetrathiafulvalene derivatives bearing pyridine and pyridinium substituents. *J. Chem. Soc. Chem. Commun.* **95**, 475-476.
181. Eddowes, M. J. & Hill, H. A. O. (1977). A novel method for the investigation of the electrochemistry of metalloproteins: cytochrome c. *J. Chem. Soc. Chem. Commun.* **1977**, 71.
182. Allen, P. M., Hill, H. A. O. & Walton, N. J. (1984). Surface modifiers for the promotion of direct electrochemistry of cytochrome c. *J. Electroanal. Chem.* **178**, 69-86.
183. Sagara, T., Niwa, K., Sone, A., Hinnen, C. & Niki, K., (1990). Redox Mechanism of cytochrome c at modified gold electrodes. *Langmuir* **6**, 254-262.
184. Sagara, T., Murakami, H., Igarashi, S., Sato, H. & Niki, K. (1991). Spectroelectrochemical study of the redox reaction mechanism of cytochrome c at a gold electrode in a neutral solution in the presence of 4,4'-bipyridyl as a surface modifier. *Langmuir* **7**, 3190-3196.
185. Jiang, L., McNeil, C. J. & Cooper J. M. (1995). Direct electron transfer reactions of glucose oxidase immobilized at a self-assembled monolayer. *J. Chem. Soc., Chem. Comm.* **1995**, 1293-1295.
186. Dong, X.-D., Lu, J. & Cha, C. (1997). Characteristics of the glucose oxidase at different surfaces. *Bioelectrochem. & Bioenerg.* **42**, 63-69.
187. Murthy, A. S. N. & Sharma, J. (1998). Glucose oxidase bound to self-assembled monolayers of bis(4-pyridyl)disulfide at a gold electrode: Amperometric determination of glucose. *Anal. Chim. Acta* **363**, 215-220.
188. Willner, I., Doron, A., Katz, E. and Levi, S. (1996). Reversible associative and dissociative interactions of glucose oxidase with nitrospyrans monolayers assembled onto gold electrodes: amperometric transduction of recorded optical signals. *Langmuir* **12**, 946-954.
189. Schmidt, H.-L., Gutberlet, F. & Schuhmann, W. (1993). New principles of amperometric enzyme electrodes and of reagentless oxidoreductase biosensors. *Sens. & Act.* **13-14**, 366-371.
190. Aizawa, M., Yabuki, S. & Shinohara, H. (1988). Potential controlled enzymic activity of conducting enzyme membrane. In: Dryhurst, G. & Niki, K. (eds) *Redox Chemistry & Interfacial Behavior of Biological Molecules*. Plenum Press, New York.
191. Wingard, L. B. & Narasimhan, K. (1988). Immobilized flavin coenzyme electrodes for analytical applications. *Meth. Enzymol.* **137**, 103-111.
192. Phadke, R. S., Sonawat, H. M. & Govil, G. (1988). Biomolecular electronics using coenzymes immobilized on solid supports." *J. Mol. Electron.* **4**, 67-74.
193. Komplin, G. C. & Pietro, W. J. (1996). Redox coenzyme functionalization of electrochemically grown prussian blue films. *Sens. & Act. B*, **30**, 173-178.
194. Katz, E., Schlereth, D. D., Schmidt, H.-L. & Osthoorn, A. J. J. (1994). Reconstitution of the quinoprotein glucose dehydrogenase from its apoenzyme on a



- gold electrode surface modified with a monolayer of pyrroloquinoline quinone. *J. Electroanal. Chem.* **368**, 165-171.
195. Schlereth, D. D. & Kooyman, R. P. H. (1997). Self-assembled monolayers with biospecific affinity for lactate dehydrogenase for the electroenzymatic oxidation of lactate. *J. Electroanal. Chem.* **431**, 285-295.
  196. Betts, J. N., Beratan, D. N. & Onuchic, J. N. (1992). A search algorithm for mapping tunneling pathways in proteins. *J. Am. Chem. Soc.* **114**, 4043-4046.
  197. Hecht, H. J., Kalisz, H. M., Hendle, J., Schmid, R. D. & Schomburg, D. (1993). Crystal structure of glucose oxidase from *Aspergillus niger* refined at 2.3 Å resolution. *J. Mol. Biol.* **229**, 153-172.
  198. Alvarez-Icaza, M., Kalisz, H. M., Hecht, H. J., Aumann, K.-D., Schomburg, D & R. D. Schmid. (1995). The design of enzyme sensors based on the enzyme structure. *Biosens. & Bioelectron.* **10**, 735-742.
  199. Onuchic, J. N., Beratan, D. N., Winkler, J. R. & Gray, H. B. (1992). Pathway analysis of protein electron-transfer reactions. *Ann. Rev. Biophys. Biomol. Struct.* **21**, 349-77.
  200. Friesner, R. A. (1994). Comparison of theory and experiment for electron transfers in proteins: where's the beef? *Structure* **2**, 339-343.
  201. Steward, J. J. P. (1998). Personal communication.
  202. Tamao, K., Kodama, S., Nakajima, I., Kumada, M., Minato, A., & Suzuki, K. (1982). Nickel-phosphine complex-catalyzed Grignard coupling. II. Grignard coupling of heterocyclic compounds. *Tetrahedron* **38**, 3347-3354.
  203. Minato, A., Suzuki, K., Tamao, K., Kumada, M. (1984). Mixed heteroarene oligomers. *J. Chem. Soc., Chem. Commun.* **1984**, 511-513.
  204. Bergmeyer H. U. (ed.) (1984). *Methods of enzymatic analysis*. 3rd ed. VCH, Weinheim.
  205. MacDonald, J. R. (1987). *Impedance Spectroscopy*. John Wiley & Sons, New York.
  206. Feldman, H. A. (1972). Mathematical theory of complex ligand-binding systems at equilibrium: some methods for parameter fitting. *Anal. Biochem.* **48**, 317-338.
  207. Engvall, E. & Perlmann, P. (1971). Enzyme-linked immunosorbent assay (ELISA). Quantitative assay of immunoglobulin G. *Immunochem.* **8**, 871-4.
  208. O'Shannessy, D. J. & Hoffman, W. L. (1987). Site-directed immobilization of glycoproteins on hydrazide-containing solid supports. *Biotechnol. & Appl. Biochem.* **9**, 488-496.
  209. Deisenhofer, J. (1981). Crystallographic refinement and atomic models of a human Fc fragment and its complex with fragment B of protein A from *Staphylococcus aureus* at 2.9 and 2.8-Å resolution. *Biochem.* **20**, 2361-2370.
  210. Owaku, K., Goto M., Ikariyama, Y. & Aizawa, M. (1995). Protein A Langmuir-Blodgett film for antibody immobilization and its use in optical immunosensing. *Anal. Chem.* **67**, 1613-1616.
  211. Lekkala, J. O. & Sadowski, J. W. (1994). Surface Plasmon Immunosensors. In: Aizawa, M. (Ed.) *Chemical Sensor Technology* **5**, Kodansha Ltd., Tokyo.

212. Jimbo, Y. & Saito, M. (1988). Orientation-controlled immobilization of protein molecules on thin organic films deposited by the plasma technique. *J. Mol. Electron.* **4**, 111-118.
213. Ahluwalia, A., Carra, M., De Rossi, D., Ristori, C., Tundo, P. & Bomben, A. (1994). Improvement of antibody surface density by orientation of reduced fragments. *Thin Solid Films* **247**, 244-247.
214. Watson, H. & Peltonen, J. (1997). Synthesis of a surface-active polyamic acid with pendant biological linker molecule for specific immobilization of antibodies. *Sens. & Act. B* **38-39**, 261-265.
215. Stanfield, R. L., Fieser, T. M., Lerner, R. A., Wilson, I. A. (1992). Crystal structures of an antibody to a peptide and its complex with peptide antigen at 2.8 Å. *Science* **248**, 712-719.
216. Tronin, A., Dubrovsky, T., De Niitti, C., Gussoni, A., Erokhin, V. & Nicolini, C. (1994). Langmuir-Blodgett films of immunoglobulins IgG. Ellipsometric study of the deposition process and of immunological activity. *Thin Solid Films* **238**, 127-132.
217. Vikholm, I. & Teleman, O. (1994). Adsorption of antibodies to a Langmuir layer of octadecylamine and the interaction with antigen. *J. Colloid & Interf. Sci.* **168**, 125-129.
218. Egger, M., Heyn, S.P., & Gaub, H.E. (1992). Two-dimensional recognition pattern of lipid-anchored Fab'-fragments. *Biophys. J.* **57**, 669-673.
219. Herron, J. N., Mueller, W., Paudler, M., Riegler, H., Ringsdorf, H. & Suci, P. A. (1992). Specific recognition-induced self-assembly of a biotin lipid/streptavidin/Fab fragment triple layer at the air/water interface: ellipsometric and fluorescence microscopy investigations. *Langmuir* **8**, 1413-16.
220. Vikholm, I.; Györvary, E. & Peltonen, J. (1996). Incorporation of lipid-tagged single-chain antibodies into lipid monolayers and the interaction with antigen. *Langmuir* **12**, 3276-3281.
221. Ishikawa, E. (1983). Enzyme-labeling of antibodies. *J. Immunoassay* **4**, 209.
222. Heath, T. D. (1987). Covalent attachment of proteins to liposomes. *Meth. Enzymol.* **149**, 111-123.
223. Rongen, H. A. H., Bult, A. & van Bennekom, W. P. (1997). Liposomes and immunoassays. *J. Immunol. Meth.* **204**, 105-133.
224. Heath, T. D., Fraley, R. T. & Papahadjopoulos, D. (1980). Antibody targeting of liposomes: cell specificity obtained by conjugation of F(ab')<sub>2</sub> to vesicle surface. *Science* **210**, 539-541.
225. Kitagawa, T., Shimozone, T., Aikawa, T., Yoshida, T. & Nishimura, H. (1981). Preparation and characterization of hetero-bifunctional cross-linking reagents for protein modifications. *Chem. Pharm. Bull.* **29**, 1130-1135.
226. Carlsson, J., Drevin, H. & Axén, R. (1978). Protein thiolation and reversible protein-protein conjugation. *Biochem. J.* **173**, 723-737.
227. Markowitz, M. & Singh, A. (1991). Self-assembling properties of 1,2-diacyl-sn-glycero-3-phosphodihydroxyethanol: A headgroup-modified diacetylene phospholipid. *Langmuir* **7**, 16-18.

228. Spevak, W., Nagy, J. O. & Charych, D. H. (1995). Molecular assemblies of functionalized polydiacetylenes. *Adv. Mater.* **7**, 85-89.
229. Tyminski, P. N., Ponticello, I. S. & O'Brien, D. F. (1987). Polymerizable dienoyl lipids as spectroscopic bilayer membrane probes. *J. Am. Chem. Soc.* **109**, 6541-6542.
230. Weber, B. A., Dodrer, N. & Regen, S. L. (1987). Phospholipid membranes from a polymeric phosphatidyl choline. *J. Am. Chem. Soc.* **109**, 4419-4421.
231. Samuel, N. K. P., Singh, M., Yamaguchi, K. & Regen, S. L. (1985). Polymerized-depolymerized vesicles. Reversible thiol-disulfide-based phosphatidylcholine membranes. *J. Am. Chem. Soc.* **107**, 42-47.
232. Stefely, J., Markowitz, M. A. & Regen, S. L. (1988). Permeability characteristics of lipid bilayers from lipoic acid derived phosphatidylcholines: Comparison of monomeric, crosslinked and non-crosslinked polymerized membranes. *J. Am. Chem. Soc.* **110**, 7463-7469.
233. King, L. G., Raguse, B., Cornell, B. A. & Pace, R. J. (1992). Ionic reservoir at electrode surface. *Int. Pat. WO 92/17788*.
234. Lang, H., Duschl, C. & Vogel, H. (1994). A new class of thiolipids for the attachment of lipid bilayers on gold surfaces. *Langmuir* **10**, 197-210.
235. Viitala, T. J. S., Peltonen, J., Lindén, M. & Rosenholm, J. B. (1997). Spectroscopy, polymerization kinetics and topography of linoleic acid Langmuir and Langmuir-Blodgett films. *J. Chem. Soc., Faraday Trans.* **93**, 3185-3190.
236. Ben-Dov, I., Willner, I. & Zisman, E. (1997). Piezoelectric immunosensors for urine specimens of *Chlamydia trachomatis* employing quartz crystal microbalance microgravimetric analysis. *Anal. Chem.* **69**, 3506-3512.
237. Caruso, F., Rodda, E., Furlong, D. N., Niikura, K. & Okahata, Y. (1997). Quartz crystal microbalance study of DNA immobilization and hybridization for nucleic acid sensor development. *Anal. Chem.* **69**, 2043-2049.
238. Hepel, M. & Mahdavi, F. (1997). Application of the electrochemical quartz crystal microbalance for the electrochemically controlled binding and release of chlorpromazine from conductive polymer matrix. *Microchem. J.* **56**, 54-64.
239. Sauerbrey, G. (1959). Verwendung von Schwingquarzen zur Wägung dünner Schichten und der Mikrowag. *Z. Phys.* **155**, 206-222.
240. Meccea, V.M. (1994). Loaded vibrating quartz sensors. *Sens. and Act. A* **40**, 1-27.
241. Kösslinger, C., Drost, S., Aberl, F & Wolf, H. (1994). Quartz crystal microbalance for immunosensing. *Fresenius' J. Anal. Chem.* **349**, 349-354.
242. Rickert, J., Brecht, A. & Göpel, W. (1997). QCM operation in liquids: constant sensitivity during formation of extended protein multilayers by affinity. *Anal. Chem.* **69**, 1441-1448.
243. Välimäki, H., Lekkala, J., Helle, H. (1997). Prediction ability of a lumped-element equivalent-circuit model for thickness-shear mode resonators in liquids. *Sens. & Act. A* **60**, 80-85.
244. Tessier, L., Schmitt, N., Watier, H., Brumas, V. & Patat, F. (1997). Potential of the thickness shear mode acoustic immunosensors for biological analysis. *Anal. Chim. Acta* **347**, 207-217.

245. Muratsugu, M., Ohta, F., Miya, Y., Hosokawa, t., Kurosawa, S., Kamo, N. & Ikeda, H. (1993). Quartz crystal microbalance for the detection of microgram quantities of human serum albumin: relationship between the frequency change and the mass of protein adsorbed. *Anal. Chem.* **65**, 2933-2937.
246. Kretschmann, E. (1971). Die Bestimmung optischer Konstanten von Metallen durch Anregung von Oberflächenplasmaschwingungen. *Z. Physik* **216**, 313.
247. Wood, W. G. & Gadow, A (1983). Immobilization of antibodies and antigens on macro solid phases - a comparison between adsorptive and covalent binding. *J. Clin. Chem. & Clin. Biochem.* **21**, 789-797.
248. Weetal, H. A. (1976). Covalent coupling methods for inorganic support materials. *Meth. Enzymol.* **44**, 134-148.
249. Needham, D. & Nunn, R.S. (1990). Elastic deformation and failure of lipid bilayer membranes containing cholesterol. *Biophys. J.* **58**, 997-1009.
250. Yamauchi, H., Takao, Y., Abe, M. & Ogino, K. (1993). Molecular interactions between lipid and some steroids in a monolayer and a bilayer. *Langmuir* **9**, 300-304.
251. Snejdàrková, M., Reháková, M. & Otto, M. (1997). Stability of bilayer lipid membranes on different solid supports. *Biosens. & Bioelectron.* **12**, 145-153.
252. Geddes, N. J., Paschinger, E. M., Furlong, D. N., Ebara, Y., Okahata, Y., Than, K. A. & Edgar, J. A. (1994). Piezoelectric crystal for the detection of immunoreactions in buffer solutions. *Sens. & Act. B* **17**, 125-131.
253. Buijs, J., Lichtenbelt, J. W. Th., Norde, W. & Lyklema, J. (1995). Adsorption of monoclonal IgG's and their F(ab')<sub>2</sub> fragments onto polymeric surfaces. *Coll. & Surf. B: Biointerfaces* **5**, 11-23.
254. Disley, D. M., Cullen, D. C., You, H.-X. & Lowe, C. R. (1998). Covalent coupling of immunoglobulin G to self-assembled monolayers as a method for immobilizing the interfacial-recognition layer of a surface plasmon resonance immunosensor. *Biosens. & Bioelectron.* **13**, 1213-1225.

***Appendices of this publication are not included in the PDF version.  
Please order the printed version to get the complete publication  
(<http://www.inf.vtt.fi/pdf/publications/1999/>)***